THE EFFECT OF PLY THICKNESS ON THE FREE EDGE DELAMINATION OF GRAPHITE/EPOXY LAMINATES

by

JOHN CHARLES BREWER

S.B. Massachusetts Institute of Technology
(1983)

SUBMITTED IN PARTIAL FULFILLMENT
OF THE REQUIREMENTS OF THE
DEGREE OF

MASTER OF SCIENCE IN
AERONAUTICS AND ASTRONAUTICS

at the

MASSACHUSETTS INSTITUTE OF TECHNOLOGY

May 1985

Signature of Author_____
Department of Aeronautics and Astronautics
May 23, 1985

Certified by_____
Professor Paul A. Lagace
Thesis Supervisor

Accepted by_____
Professor Harold Y. Wachman
Chairman, Departmental Graduate Committee

THE EFFECT OF PLY THICKNESS ON THE FREE EDGE DELAMINATION OF GRAPHITE/EPOXY LAMINATES

by

JOHN CHARLES BREWER

Submitted to the Department of Aeronautics and Astronautics
on May 23, 1985 in partial fulfillment of the
requirements for the Degree of Master of Science

ABSTRACT

The initiation of delamination in graphite/epoxy laminates was investigated both analytically and experimentally and the effect of effective ply thickness on this phenomenon assessed. Three different laminate families were investigated: $[\pm 15_n]_s$, $[\pm 15_n/0_n]_s$, and $[0_n/\pm 15_n]_s$ with the normalized effective ply thickness, n, varying from 1 to 5. Delamination initiation was detected using the load drop technique in conjunction with edge replication. Initiation was determined to have occurred when a load drop was detected and a delamination initiation was confirmed on the replication of the specimen edge. Two different analytical techniques were used to correlate the measured delamination initiation stresses: the previously proposed strain energy release rate approach and the Quadratic Delamination Criterion which is introduced herein. The strain energy release rate approach was unable to accurately correlate the data for two of the three laminate families as the data clearly showed that the critical value of strain energy release rate is significantly dependent on the effective ply thickness. The Quadratic Delamination Criterion, an average stress criterion which involves the comparison of the calculated interlaminar normal stress and interlaminar shear stress (σ_{1z}) to their related strength parameters, is proposed and shows excellent correlation with the delamination initiation stress data.

Thesis Supervisor: Paul A. Lagace

Title: Charles Stark Draper Assistant Professor
of Aeronautics and Astronautics

ACKNOWLEDGEMENTS

It would be virtually impossible for me to thank all the people who have helped to get where I am today. The number of coworkers in the Technology Laboratory for Advanced Composites (TELAC) alone is well over one hundred. With that in mind and knowing that I will inadvertently forget someone, I will do my best:

First, I would like to thank all my teachers and professors over the last 18 years. Without them to educate and inspire me, I would not be pursuing a Ph.D. today. I would especially like to thank professor James W. Mar, founder and director of TELAC, for hiring me as an inexperienced freshman five and a half years ago.

The staff of the Department of Aeronautics and Astronautics have been very helpful. Al Shaw has lived up to his reputation as the quintessential jack-of-all-trades and answerman. Within the laboratory, I must thank Carl Varnerin for relieving me of the duties of chief TELAC ordering officer and summer manufacturing course teacher. Without this relief, I would still be trying to find enough time to manufacture my specimens. (I'd also like to thank all the people who got their material requests in on time during 1982 and 1983, if there were any.) The most important laboratory staff member to the success of this and all my TELAC projects is Al Supple. Besides beign a wiz at finding out what button I have forgotten to push and knowing every machine in the laboratory inside and out, Al has an abundance of that very rare quality, common sense.

All the secretaries and administrators have provided help and friendship. Special thanks are owed to Ping Lee for her aid and her candy and Debra Smith for typing all of those tables.

The other students in the laboratory have made those long hours watching the autoclave or playing with equations bearable. I would like to thank my officemates over the years: Michael, John, Paul, Tony, Dave, Hatem, Mark, Steve, and Doug. It's only by watching people go through the process of finishing a thesis that make it bearable. I'd especially like to thank Tony Vizzini for taking our PDP 11/34 and transforming it from crude data acqusition equipment into a very powerful acquisition, analysis, and graphics system. I would also like to thank Tony and his wife, Patty, for introducing me to the love of my life.

I'd like to thank all of the students who worked in conjunction with me on individual projects. In the delamination

work, this includes Karen Archard, Doug Weems, and John Shrewsbury. The most important student to this project, however, has been Mary Bayalis. Her dedication was well above and beyond what anyone would have any right to expect. She even sacrificed her manicure in the name of science. I only wish that she could have seen more specimens go all the way to failure. Sincerely, Mary, thank you so much.

The life of a graduate student is made richer by his friends. For me, this is mainly composed of a group of alumni of MacGregor House and their friends. MIE has been a very important part of my life here at MIT. It has truly been a second family. I spent my undergraduate years with the likes of Roy and Joelle, Stevie, Veds, Jelly, Swannee, Ducky, Dana, Eric, Gabe, and Ski. The blinking red light has introduced me to such other friends as Oscar, Jiffy, Felsh, Teddy, Charlie, Bobby, Charlie, Kathy, the Sullies, Dave, Waaaayne, and Bully - and who can forget Betty or the Gerbils (other than Don Zimmer).

Despite a brief mention as an officemate, I have been saving a lot of thanks for my good friend Paul Lagace. It was Paul who recruited a shy young freshman into TELAC and MIE. It was Paul who worked closely with me in my first years in the laboratory (through 800 tests - even more than I've done for this thesis). Whether in the laboratory or on the soft-ball field, he has always had confidence in me - often more than I've had in myself. I consider myself very lucky to have such a good friend as a thesis advisor. It's hard to thank someone who has done so much for me enough. Thanks, Galoot.

I would be very remiss if I did not thank my family. I want to thank all my brothers and sisters: Mark, Steve, Sue, Jeff, Mike, and Dawn. If not for their encouragement, I would not be here and I love them very much. I also want to thank my brother- and sisters-in-law: Jim, Molly, Dwbbie, Ann Marie (see, I didn't call you Boobie), and Trish.

One of my greatest pleasures in life is to visit my nieces and nephews. Their innocence, their imagination, their uncomplicated outlook, their never-ending quest for fun make them the best thing for me when I need to get away from it all. I want to especially thank each of them: Tonya, Jeremy, Jessie (Van-hmph-hmph-hmph Brewer), Jennifer (the original goober-nose), Matt the Nut, Andy B., (Atsami) David, Lindsey, and John, Too.

As much as I owe to everyone I've mentioned so far, I owe even more to my parents. They have always been there when I needed them, always prepared to support me in whatever

way I needed, always ready to help, always there to talk to (except maybe on Bingo nights). Throughout my life, they've always told me I could be whatever I wanted to be as long as I worked at it. Well, I've found what I want to be and I've worked at it, but it would all be for naught without them. I've seen many people over the last few years who have had problems with their partnts. All the seven of us have gotten is love. That is very rare and very special. We are very thankful for it and love them for it very much.

I would now like to thank my love, Katy. I could go on about what she has meant to me over the last three and a half years, but I'd rather concentrate on looking forward to our future together. T-44 days, kid.

This work was performed in the Technology Laboratory for Advanced Composites (TELAC) of the Deparrment of Aeronautics and Astronautics at the Massachusetts Institute of Technology. This work was sponsored by the Air Force Office of Scientific Research and the Boeing Military Aircraft Company under contract numbers F49620-83-K-0015 and BMAC AA0045, respectively. Major David Glasgow and Mr. Robert Waner were the contract monitors, respectively.

DEDICATION

To Pops

TABLE OF CONTENTS

TABLE OF CONTENTS (Continued)

LIST OF FIGURES

LIST OF FIGURES (Continued)

LIST OF FIGURES (Continued)

LIST OF FIGURES (Continued)

LIST OF TABLES

NOMENCLATURE

2a	length of test section
A_{cs}	cross-sectional area of the test section
A_{del}	delaminated area
A_{tot}	total area of the test section
AS1/3501-6	graphite/epoxy system used in this investigation
2b	width of the test section
E	modulus
E_{avg}	weighted average modulus of the sublaminates
E_{eff}	longitudinal modulus of partially delaminated specimen
E_{lam}	longitudinal modulus of unerlaminated laminate
f	interlaminar stress constant determined for a specific interace via the Force Balance Method reflecting the magnitude of σ_{zz}
G	strain energy release rate (per unit area)
h	1. interlaminar stress constant determined for a specific interface via the Force Balance Method reflecting the magnitude of σ_{lz} 2. laminate thickness
P	applied load
$\dot{P}$	applied loading rate
P_{del}	load applied to partially delaminated specimen
P_{und}	load applied to undelaminated specimen
t	laminate thickness
TELAC	Technology Laboratory for Advanced Composites

NOMENCLATURE (Continued)

t_i	time at which i^{th} data point is taken
t_{ply}	ply thickness
x	distance from the free edge
x_{avg}	averaging dimension
Z^s	interlaminar shear strength
Z^t	interlaminar normal strength
ΔP_{fr}	fractional load drop as defined by Equation 4.4
ΔT	difference in temperature between the curing temperature and room temperature, taken to be -157°C
ε	strain level
$\dot{\varepsilon}$	strain rate
λ, ϕ	interlaminar stress parameters determined for a laminate via the Force Balance Method
ν	Poisson's ratio
σ	stress
$\dot{\sigma}$	stress rate
$\bar{\sigma}$	component of stress averaged over a distance x_{avg} from the free edge
$[\bar{\sigma}_{zz}]$	a quantity equal to $\bar{\sigma}_{zz}$ if $\bar{\sigma}_{zz}$ is compressive
θ	lamination angle

SUBSCRIPTS

c	critical value for delamination
I	mode I component
L,l	longitudinal or 0° direction
m	mechanical

NOMENCLATURE (Continued)

t	thermal
T,2	transverse or 90° direction
z	through-the-thickness direction

CHAPTER 1

INTRODUCTION

The development and use of advanced composite materials in recent decades has been a significant boon to the aerospace industry. These materials offer high strength and stiffness at less weight than their metallic counterparts and engineers have found many applications for them. The present apparent high cost per pound of the materials are being offset by the fact that they produce less waste than metals and the weight savings they produce translates into a significant savings in life-cycle costs for aerospace structures.

Some unique applications of advanced composites are in the Harrier AV-8B vertical takeoff and landing (VTOL) fighter aircraft and the Grumman-DARPA X-29 forward swept wing aircraft. The AV-8B has a graphite/epoxy wing assembly which enables it to perform as an advanced fighter while still being light enough to have VTOL capability and sufficient range. The forward swept wing configuration of the X-29 is aeroelastically feasible only because clever use is made of the highly orthotropic nature of advanced composites.

The transport and business jet industries are also learning to successfully integrate advanced composites into new generations of aircraft. The new Boeing 757 and 767 aircraft

make extensive use of composites in their secondary structural components. This helps to make these aircraft fuel-efficient and hence, fuel costs decrease over the life of the aircraft. Several new business jets are vying to be the first aircraft to be certified in which all of the primary structure is advanced composite. These aircraft are the Learfan 2000, the Beech Starship 1., and the Avtek 400.

The astronautical industry is also very interested in advanced composites for their high specific strength and stiffness. When the cost of getting a pound of payload to orbit is considered, a premium must be placed on weight. The largest use of composites in a single structure today is in fact in a new solid rocket booster casing for the space shuttle. This new casing is manufactured by Hercules, Inc. It has fewer components and weighs 35 tons as compared to the present 50 ton steel casing. This results in a significant increase in shuttle payload capability or the ability to achieve higher orbits.

Composites, however, have even greater potential. Because engineers lack a total understanding of the materials, they are reluctant to use them to their fullest extent. It is believed, for example, that composites could easily constitute half of the structural weight of future transport aircraft, including a substantial portion of primary structural compo-

nents such as wings and fuselage. At present, designers usually prefer "quasi-isotropic" laminates. Since equal strength and stiffness is generally not needed in all directions of a structure, this is a waste of the unique abilty of highly orthotropic composites to be "tailored" to specific applications.

The various modes of damage in composites (fiber fracture, fiber pullout, ply delamination, fiber debond, matrix cracking, etc.), and how they interact to cause failure are still not completely understood. In part due to this inadequate understanding of failure, the composite structures presently in use are limited to design ultimate strains of 4000 microstrain.

Some progress has been made in the prediction of composite strength and failure modes. Tsai and Wu [1] proposed a method by which failure of component plies could be predicted on the basis of the plane stress state predicted by Classical Laminated Plate Theory. This correlated well with tensile data [2] except in some cases where the strength of the composite laminates was significantly less than that predicted by this method.

In many cases, the failure modes of these laminates showed out-of-plane separation (delamination) of component plies. Delamination is seen to be the result of the failure

of an interlaminar epoxy layer between two plies. It has been known for some time [3] that this failure is caused by a full three-dimensional state of stress that arises near the free edge of multi-directional laminated specimens. This delamination failure mode is not something which is seen in the failure of homogenous materials such as metals. One key issue to the future of the efficient use of composites is the development of criteria which can be used in preliminary and advanced design stages to determine the propensity of various candidate laminates to delaminate.

A review of the literature on the subject of delamination of composite laminates is contained in Chapter 2. The various approaches for studying delamination including the calculation of the interlaminar stresses that arise in a boundary region at the free edges of composite laminates are discussed. The development of methods for incorporating interlaminar stress calculations into criteria for the prediction of delamination initiation are traced in Chapter 3. Details of these analyses as applied to the specific laminates used in the experiments in this thesis are included. The experimental portion of the thesis is described in Chapter 4. In particular, specimen manufacture, testing methods, and edge replication techniques are discussed. The results of the experiments are contained in Chapter 5 where specific data is presented as well as de-

scriptions of the varying degrees of delamination seen in specimens. In Chapter 6 there is a complete discussion of the data and how well the proposed methods of predicting delamination initiation correlate this data. A summary of this work is presented in Chapter 7 in the form of relevant conclusions and recommendations for further research into the subject of the strength of composites prone to delamination.

CHAPTER 2

SUMMARY OF PREVIOUS WORK

2.1 Interlaminar Stresses and Delamination

The problem of free edge delamination of advanced composites has been studied for more than a decade. There is general agreement that the cause of delamination is the interlaminar stresses that arise in a boundary region near the free edge. Since elastic properties (such as Young's modulus, Poisson's ratio, the coefficient of mutual influence, etc.) of the layers (plies) that make up the laminate change when the angular orientation of the fibers in the plies changes with respect to the longitudinal axis of the composite, mismatches of these properties arise between plies. Classical Laminated Plate Theory, which imposes strain continuity through the laminate thickness, therefore predicts differences in the in-plane stresses (σ_{11}, σ_{22}, σ_{12}) in the plies when the laminate is loaded. The Classical Laminated Plate Theory solution cannot hold at stress-free edges of the laminate. For example, consider the case of a laminate under uniaxial loading as illustrated in Figure 2.1. The coordinate system used in this investigation is defined in this figure. Unless Poisson's ratio is identical for all plies, Classical Laminated Plate The-

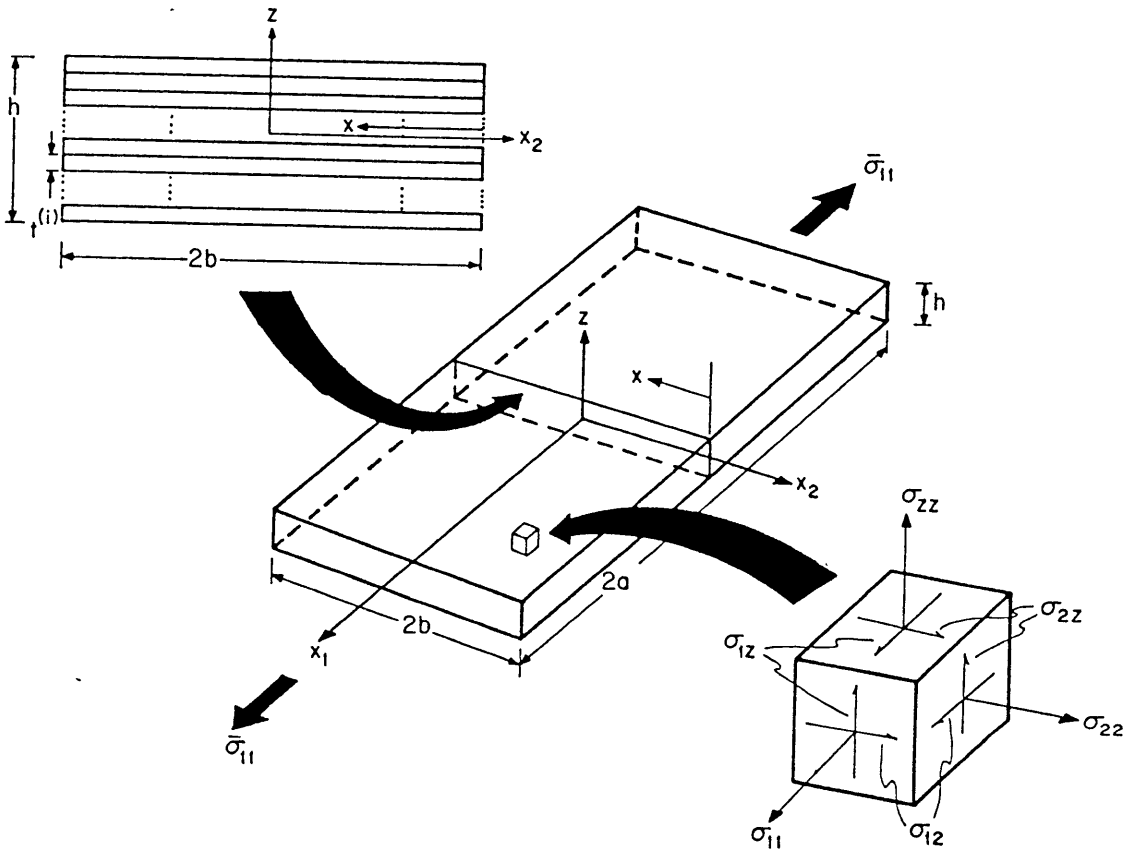

FIGURE 2.1 GEOMETRY FOR THE PROBLEM OF A LAMINATED PLATE UNDER UNIAXIAL LOADING

ory will predict a transverse stress (σ_{22}) which varies from ply to ply. At the free edge, the stress free boundary conditions are therefore only met in an average sense. The boundary conditions thus require that a full three-dimensional state of stress arise in the region of the free edge to preserve force and moment equilibrium. The state of stress at a free edge is illustrated in Figure 2.2.

Much work has been done on the calculation of interlaminar stresses over the past fifteen years. Some attempts used numerical techniques such as finite difference [3] or finite elements [4,5]. Early analytical attempts often only dealt with one component of interlaminar stress. Puppo and Evensen [6] calculated an interlaminar shear stress (σ_{1z}) by modeling the interlaminar resin layers as isotropic shear layers. Pagano and Pipes [7] derived a rough approximation of interlaminar out-of-plane normal stress (σ_{zz}) by assuming a σ_{zz} distribution and satisfying equlibrium of moment and normal force near the free edge. Whitney [8] approximated several of the components of interlaminar stresses by assuming more complicated stress functions which satisfied differential equilibrium and achieved reasonable agreement with some elasticity solutions despite the fact that he had not satisfied compatability. Pipes and Pagano [9] tried a Fourier series approach to the calculation, but found the derivative of

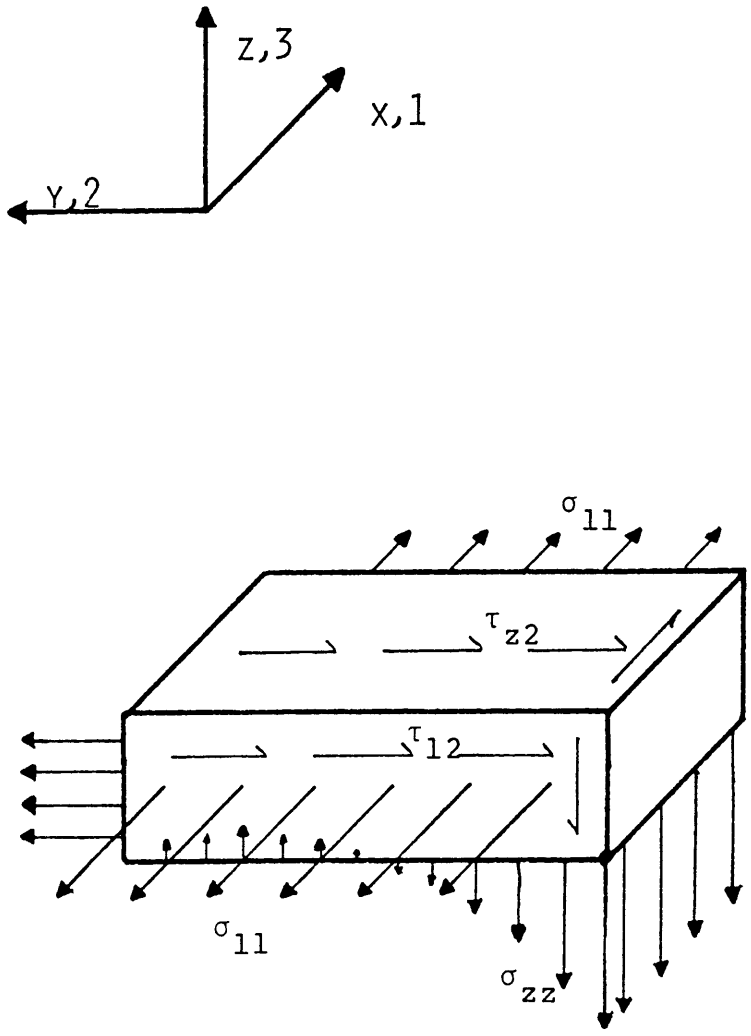

FIGURE 2.2 STATE OF STRESS AT THE FREE EDGE OF A SPECIMEN

displacement with respect to distance through the thickness diverged as more terms were added. Hsu and Herakovich [10] used a perturbation solution. They found fair agreement with finite difference solutions, some instabilities in σ_{zz}, and a dependence of the distribution on specimen width and far-field strain.

Lagace and Kassapoglou [11,12] have recently developed a method for determining the stresses at the free edge by assuming stress functions which satisfy both integral and differential equilibrium. Given these functions, energy is minimized. This "Force Balance Method" requires considerably less computation time than the finite element methods. It has been shown to have the capability of handling laminates of 100 plies or more quite easily. The results of the calculations show excellent agreement with numerical solutions in the literature. This method also has the capability of easily handling interlaminar stresses due to thermal loading.

Interlaminar stresses are the cause of delamination initiation. There are several approaches used to analyze how this happens. Two main methods have been employed in the literature: the mechanics of materials approach, which takes interlaminar stress calculations and material strength parameters directly into account, and fracture mechanics approaches, which need not specifically use values of interlaminar

stresses, but instead use the amount of strain energy available per unit of delaminated area as a delamination parameter.

2.2 Mechanics of Materials Approach

Early mechanics of materials methods were generally qualitative attempts to correlate delamination with the interlaminar stress state. Rough approximations of the stress components were often used in these calculations. In a 1973 paper, Pipes et al. [13] studied the delamination of $[\pm\theta]_s$ laminates. Since these laminates have no mismatch in Poisson's ratio, they have no σ_{zz}. They concluded that σ_{1z} was the primary cause of interfacial delamination in these laminates. Herakovich [14] did similar experiments in which he compared the effect of clustering versus alternating the $+\theta$ and $-\theta$ plies. He found that eight-ply laminates with clustered plies ($[+\theta_2/-\theta_2]_s$) failed at significantly lower stresses than the corresponding laminates with alternated plies ($[(\pm\theta)_2]_s$). He concluded that "the differences are explained analytically through consideration of the influence of layer thickness on the magnitude of the interlaminar shear stress."

Rodini and Eisenmann [15] attempted to correlate delamination to σ_{zz}. Their assumption that only normal stress is

important is based on the fact that several laminates showed a greater propensity to delaminate when their stacking sequence was altered to give higher values of σ_{zz}. They used the approximate approach of Pagano and Pipes [7] to determine the sign and relative magnitude of σ_{zz}. They proposed, as a criterion, that delamination was a function of the integral over the volume of the specimen of the tensile values of σ_{zz}. They believed that delamination initiation fit a Weibull distribution. This approach predicted that delamination was only a function of σ_{zz} and that it was highly dependent on stacking sequence. It also predicted that, for any given laminate type, delamination strength is inversely proportional to both the length of the free edge and the square root of the ply thickness.

Lagace [16] also considered σ_{zz} as a basis on which to predict delamination. Rather than considering the integral over the entire volume, however, he looked at each ply interface separately. He suggested that the propensity for a given interface to delaminate could be qualitatively correlated with the value of the integral of σ_{zz} along the interface from the free edge to the point where it changed signs as illustrated in Figure 2.3. It was believed that positive values of this integral indicated interfaces prone to delamination. Within

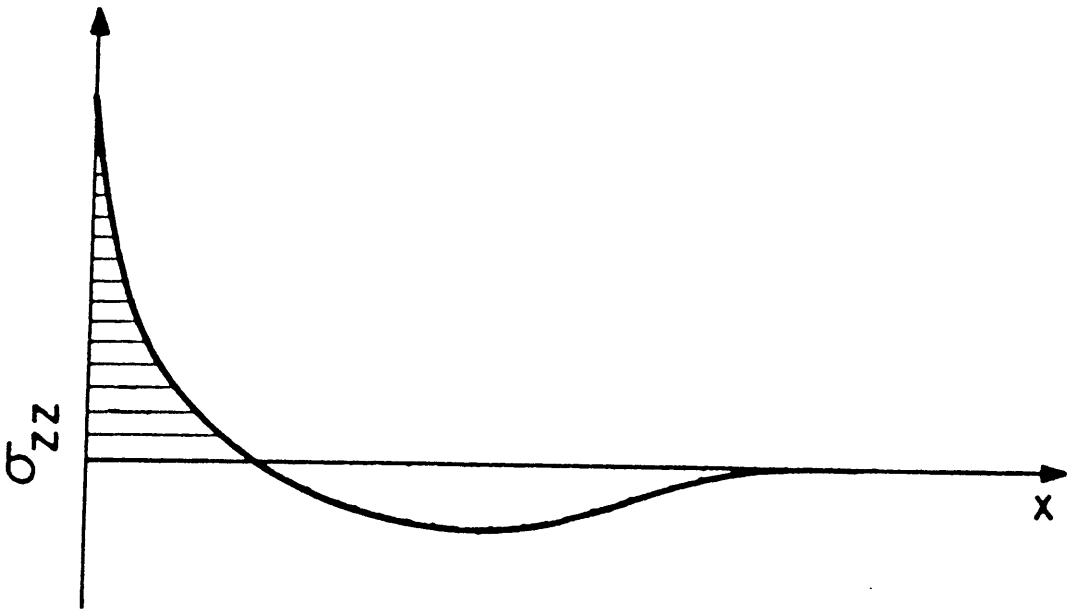

FIGURE 2.3 A REPRESENTATION OF THE INTEGRAL CRITERION FOR DELAMINATION

any given laminate, a larger value indicated a higher probability of delamination.

There are some papers, such as the one by Wang and Choi [17], which suggest stress singularities may exist at the free edge. These singulariies, however may only be important in very small regions near the free edge. This region may be so small that the underlying analytical assumption that all plies can be treated as homogeneous orthotropic layers breaks down.

The region of high stress at the free edge is in some ways similar to the region of high stress near the edge of a hole in the failure process. In the case of a hole, the stresses at the edge far exceed the ultimate stresses of the material as determined by testing an unnotched specimen. It is therefore reasoned failure at the hole is due to an average of over a region rather than the point value at the hole edge. In an investigation of the failure of composites with notches, Whitney and Nuismer [18] introduced this concept of an "average stress" criterion. They averaged the longitudinal stress (σ_{11}) over a certain distance from the free edge of the hole and predicted failure when the average stress reached a critical value.

The interlaminar shear and normal stresses calculated at the free edge of an unnotched specimen far exceed the strength

of the neat matrix. It would thus seem plausible that this average stress concept could be applied to describe delamination initiation. Kim and Soni [19] first attempted to apply this method to delamination initiation. They tried to correlate delamination initiation stress with the averaged value of σ_{zz}. They arbitrarily chose an averaging dimension of one nominal ply thickness and predicted that initiation would occur when the averaged value of σ_{zz} reached an estimated interlaminar normal strength parameter which they approximated as the transverse strength of the unidirectional ply. Reasonable agreement with their data was achieved. The results clearly showed that the approximate value of the σ_{zz} at the free edge is significantly higher than this averaged value. This serves as proof that the calculated value of σ_{zz} at the free edge is considerably higher than this estimated interlaminar strength.

In another set of experiments, Kim and Soni [20] used this average stress approach for the interlaminar shear stress by averaging the σ_{1z} component of interlaminar stress over a distance of one ply thickness from the free edge. Delamination was predicted to occur when this parameter reached the interlaminar shear strength of the laminate, which was estimated as the in-plane shear strength of the composite. Reasonable agreement was again achieved. It is not clear from

these experiments whether or not both the σ_{zz} and σ_{1z} components are important in delamination initiation. It is also not clear that the nominal ply thickness is necessarily the proper dimension over which the stresses should be averaged.

The recent development by Lagace and Kasapoglou [11,12] of the Force Balance Method for the calculation of interlaminar stresses has made it easier to use an average stress approach. The stress distributions assumed for this calculation technique are sums of constant and exponential terms. It is therefore simple to calculate the average stress values.

Brewer et al. [21] conducted a study of delamination failure. A strong correlation was found between an increase in ply thickness and a decrease in failure strength. This correlation applied not only to laminates with tensile values of interlaminar normal stress at the free edge ($[\pm 15_n/0_n]_s$), but also to laminates where this normal stress was compressive at the free edge ($[0_n/\pm 15_n]_s$) or identically equal to zero throughout the laminate ($[\pm 15_n]_s$). Interlaminar stress calculations were made using the Force Balance Method of Lagace and Kassapoglou [11,12].

The study also concluded that delamination failure is a two step process consisting of an initiation point for delamination and a growth stage. Failure is assumed to occur when

the delaminated area reaches a critical size. It is believed that initiation stress shows a similar trend with respect to ply thickness. The initiation stress is thought to be an important parameter in design.

2.3 Strain Energy Release Rate Approach

In recent years, some researchers have attempted other methods for predicting delamination. Since delamination can be modeled as an interlaminar crack, many researchers decided to use a fracture mechanics approach. Rybicki et al. [22] reasoned that delamination could only occur if the strain energy released as the delamination grew was sufficient to provide the energy needed to create the new surface. They believed this could be characterized by a critical value of the strain energy release rate per unit of delaminated area, G_c. They computed the value of strain energy available to be released per unit area, G, as a function of the far field stress. This was done simply by releasing nodes of the finite element model as a representation of delamination growth. The change in strain energy per unit increase in delaminated area was then calculated. Their experiments with boron/epoxy laminates demonstrated that the G_c approach "warranted further investigation."

Wang and Crossman [23] extended this approach. They calculated the strain energy available for release using finite elements and assumed that the resistance curve ("R-curve") of strain energy release rate required to extend the delamination starts at zero at an assumed inherent flaw size and rises rapidly to a constant critical value. These curves are illustrated in Figure 2.4. They proposed that the following sequence of events lead to delamination failure. The initial interlaminar flaw undergoes relatively little growth until the stress level reaches a critical value. Since the available strain energy release rate is proportional to the applied far field stress and it rises to a local maximum and then dips slightly, there can be instantaneous but limited growth when this maximum value of available strain energy release rate reaches the critical value. This is followed by stable delamination growth. At a critical value of delamination size, the curve of available strain energy turns rapidly upward. This causes unstable delamination growth which can trigger laminate failure. These curves were determined for $[\pm 25/90_n]_s$ laminates (n = 1, 2, 3). Their experiments [24] showed good agreement with theory despite the fact that the transverse cracking that occurred in the two thicker laminates before the onset of stable delamination growth was not accounted for in their analysis.

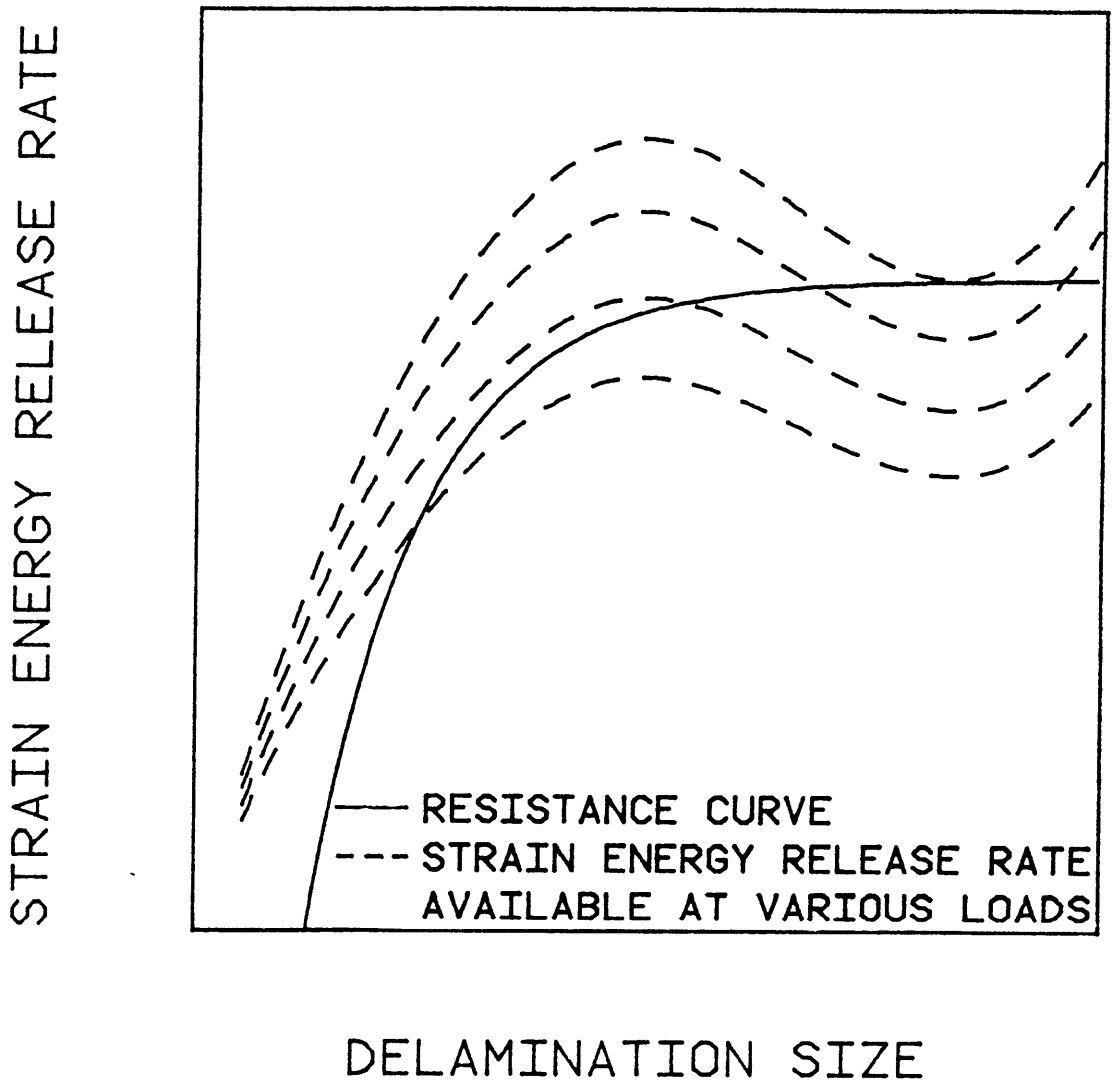

FIGURE 2.4 AVAILABLE STRAIN ENERGY RELEASE RATE AND RESISTANCE CURVE

O'Brien [25] attempted to simplify this approach by developing an easy way to approximate the strain energy release rate. He proposed that the modulus of the delaminated region could be estimated as the weighted average modulus (by thickness) of the sublaminates formed by the delamination. By computing the difference in strain energy between the delaminated and undelaminated cases at a given strain level, he derived a simple formula for calculating the strain energy release rate:

$$G = \frac{\epsilon^2 t}{2} [E_{lam} - E_{avg}] \qquad (2.1)$$

where: E_{avg} = modulus of delaminated region

E_{lam} = modulus of undelaminated laminate

t = laminate thickness

ϵ = strain level

With this equation, he predicted that if a simple G_c approach is used, initiation strain (and therefore, since linear behavior is assumed, initiation stress) is inversely proportional to the square root of the ply thickness. O'Brien also stated that only a numerical method such as finite elements can be used when it is necessary to break the strain energy release rate into its mode I (opening), II (sliding), and III (tear-

ing) components. In his experimental work on quasi-isotropic laminates, a value of G_c for the material system used was determined. He also plotted an experimental R-curve for delamination growth of one of his laminates. He concluded that the G_c approach could give estimations of delamination stresses that may be "sufficient" for early stages of design.

In a further paper [26], this idea was extended by comparing the utility of the width tapered double cantilever beam specimen, which is tested under out-of-plane normal load and measures the critical value of the mode I component of the strain energy release rate, G_{Ic}, to the "edge delamination specimen," a $[\pm 30/\pm 30/90/\overline{90}]_s$ specimen which is tested in a standard uniaxial manner and delaminates at the free edge. The conclusion is that either specimen could be used as a measure of the ability of a matrix to resist delamination, but that both G_c and G_{Ic} would be required to quantitatively characterize "toughness." In further work, O'Brien [27] proposed that G_I is the controlling parameter for delamination under static loading while the total G is the critical quantity for delamination onset under cyclic loading.

After further investigation, O'Brien et al. [28] determined that the value of G_c is a laminate parameter which is highly dependent on the percentage of the total G which is due to mode I. They varied the stacking sequence of a family of

laminates in order to compare laminates with similar total G values but greatly varied amounts of G_I. They found that brittle resins were affected only by the mode I component of G but that toughened resins could be characterized by critical values of total G where this G_c is highly dependent on the percentage of G that is mode I. This means that G_c is a strong function of laminate type for systems with toughened matrices.

Many researchers [24,25,29,30,31] have found transverse cracks in 90° plies before the onset of delamination. Wang and Crossman [23] dealt with the problem in terms of strain energy release rate. They computed the onset strains for delamination and transverse cracking for $[\pm 25/90_n]_s$ laminates. Although the transverse cracking onset strain was higher than the failure strain for $[90_n]$ specimens and approached it asymptotically for large values of n, they found good agreement between their predictions and the actual onset strains and damage types in the experimental portion of their work [24,31].

O'Brien [29] noted that "local delaminations" can form where the crack meets the neighboring ply. He proposed that these can grow unstably across the specimen and developed a simple formula for predicting onset of transverse cracking in terms of strain energy release rate. Using this equation and

the one proposed for predicting delamination [25], O'Brien was able to correlate onset strain and damage type of Crossman and Wang's data [31] and achieved good agreement.

2.4 Experimental Determination of Delamination Initiation

The investigation of delamination is strongly dependent on the ability to accurately determine the delamination initiation stress experimentally. Delamination criteria and their predictions can only be evaluated when supported by valid data. There are several methods described in the literature for the detection of delamination initiation. Kim and Soni [19] monitored the acoustic emission of their specimens during testing. They assumed that a rapid increase in the rate of emissions was indicative of delamination initiation.

Wang et al. [24] and O'Brien [25] used X-rays and a dye-penetrant to find the delaminated area of specimens which were loaded in small increments. Wang et al. plotted delaminated area as a function of stress and then extrapolated backwards to find the stress where the area was equal to zero. This was taken to be the estimated initiation stress. O'Brien determined the stress at which delamination initiates by assuming that the first stress at which a detectable delaminated area could be observed corresponded to the onset of nonlinear-

ity in the load-deflection curve. He achieved relatively good agreement with his X-ray data. It is important to note that these X-ray methods often detected transverse cracks across the width in the 90° plies of specimens before delamination detection. These transverse cracks probably have a significant effect on the interlaminar stress state and therefore the strain energy release rate components in these specimens before delamination.

Reifsneider et al. [32] continually monitored the attenuation of ultrasonic through the thickness of a specimen during testing by mounting an ultrasonic transducer on the front and back of the test section. The initiation stress was estimated as the point where the modulus appeared to change and a corresponding increase in ultrasonic attenuation occurred. It is not clear how difficult it was to judge exactly where the change in attenuation or modulus which respect to load occurred. An optical microscope was mounted on the testing machine to allow for observations and photographs of the specimen edge during testing. They always observed transverse cracks in the 90° plies of their quasi-isotropic specimens before delamination initiation. These cracks served as delamination initiation sites. An acoustic emission transducer was used on some specimens in a manner similar to that of Kim and Soni. For their $[0/90/\pm45]_s$ specimens, they found a change in

modulus without an observed delamination or increase in ultrasonic attenuation.

Klang and Hyer [33] investigated delamination initiation at circular boundaries. They loaded specimens to specific increments of load at which point the load was held and acetate film replications were made of the free surface. Six to twelve replications were made of each specimen before failure occurred. These replications were studied under a microscope for indications of delamination. The loading interval in which delamination occurred could be determined from these permanent records.

It is important to point out that in all the methods which involve changing the load in small increments, the initiation could conceivably have existed for some finite time before it is detected. The other methods described above do not give any quantitative criteria for determining how much of a change in a given parameter is indicative of delamination. In most of these cases, the change of the parameter is rather subtle, thus causing the precise initiation point to be obscured. It is important to any study of initiation that examination to determine if a delamination exists be made and as soon as possible after that delamination could have formed. For this, a method which can detect initiation almost instan-

taneously and with certainty is necessary so that the test can be stopped and the specimen examined.

Much work has been concentrated on explaining the transverse cracking phenomenon and its relationship to delamination. It is perhaps advisable, however, that when studying delamination, researchers restrict themselves to laminates which are not prone to massive transverse cracking. Generally, this would mean studying laminates which do not have 90° plies. This would allow for in-depth study of delamination isolated from transverse cracking. Once delamination by itself is fully understood, its interaction with transverse cracking could be explored in a more meaningful light.

CHAPTER 3

PROPOSED CRITERION

3.1 Selection of the Average Stress Approach

Of the methods for predicting delamination initiation which were reviewed in Chapter 2, the two which show the most promise in terms of simplicity and agreement with data seem to be the average stress and strain energy release rate approaches. Both methods have physical bases and attempt to account for the important contributors to delamination initiation.

The strain energy release rate seems to be the most popular method in the recent literature. It is a one parameter model. Once this parameter has been determined for a given laminate, the behavior of laminates with different ply thickness can be quickly estimated. Initiation stress is predicted to be proportional to the reciprocal of the square root of the ply thickness.

A strict strain energy release approach has two fundamental problems. First, the character of the decrease in initiation stress with ply thickness is restricted to an exponential decay. This is a vestige of the one parameter model. The model therefore predicts very low initiation

stresses for thick laminates despite the fact that the stresses at the free edge at these stress levels may be quite small. Second, the behavior of only a minority of laminates can be predicted using a single parameter determined for a material system. Due to the full three-dimensional state of stress at the free edge, there are generally both mode I and mode II contributions to the initiation process. Most laminates have brittle resins which seem to be primarily sensitive to the mode I component of the strain energy release rate. Determination of this component must presently be done using numerical methods such as finite elements. This complicates the procedure considerably. There is evidence to suggest that the critical value of the mode I component of strain energy release rate may be dependent on the fraction of total strain energy release rate which is due to mode I. These additional complications reduce the usefulness of this method in early design stages.

The average stress approach attempts to predict initiation using values of certain stress components averaged over a certain distance from the free edge and corresponding strength parameters. The average value of a stress component can easily be calculated for a given averaging dimension, x_{avg}:

$$\bar{\sigma}_{ij} = \frac{1}{x_{avg}} \int_{o}^{x_{avg}} \sigma_{ij}\, dx \qquad (3.1)$$

where x is the distance from the free edge. The strength parameters might be the interlaminar normal strength or interlaminar shear strength of the composite.

The average stress method has been difficult to apply because of the lack of simple analytical solutions for the interlaminar stress state at the free edge of the laminate. The stress state is generally determined for a specific mechanical and/or thermal loading. It has been necessary to numerically integrate stress components to determine average stresses. The advent of the Force Balance Method by Lagace and Kassapoglou [11,12] has removed this obstacle. The thermal and mechanical loading can be varied independently. The stress distribution funtions are sums of constant and exponential terms which can be easily integrated. This new ability to quickly calculate parameters which describe the average stress state under general loading make the average stress state much more attractive.

The average stress approach has the potential to describe all laminates of a given material system with one set of parameters. The criteria proposed by Kim and Soni [19,20] and the criterion proposed in this investigation depend on the determination of interlaminar strength parameters which would be

constant for all laminates made from a given material system. The other parameter of the average stress approach, the distance over which the stress components are averaged, is also believed to be a material system constant rather than a laminate constant, although continued experimentation will be needed to bear this out.

3.2 Quadratic Delamination Criterion

It has been shown in the literature that both the interlaminar normal stress (σ_{zz}) [2,15,16,19] and the interlaminar shear stress (σ_{1z}) [13,14,20] can be important in delamination initiation. Useful average stress criteria must include at least these stresses along with some measure of meaningful strength parameters. Kim and Soni [19,20] chose to deal only with the σ_{zz} or σ_{1z} component at one time. The opposite extreme would be to include all the components of stress, perhaps in the form of a Mises-Hencky equivalent stress:

$$\bar{\sigma}_{\varepsilon} = [\tfrac{1}{2}[(\bar{\sigma}_{11} - \bar{\sigma}_{22})^2 + (\bar{\sigma}_{22} - \bar{\sigma}_{zz})^2 + (\bar{\sigma}_{zz} - \bar{\sigma}_{11})^2] + 3[\bar{\sigma}_{12}^{\,2} + \bar{\sigma}_{2z}^{\,2} + \bar{\sigma}_{1z}^{\,2}]]^{1/2} \qquad (3.2)$$

This approach introduces the difficulty of determining an appropriate strength parameter. It has been suggested that the interlaminar normal strength can be approximated as the transverse strength of the composite and the interlaminar shear strength can be approximated as the shear strength of the composite. In the composite system used in this investigation, no one critical value of $\overline{\sigma}_E$ would give adequate agreement for both cases of delamination dominated by shear stresses and cases dominated by out-of-plane normal stresses.

The problem in developing a useful criterion is to determine which components of stress are most important in initiation. Delamination is essentially a failure of the interply matrix layer. Hashin [34] developed criteria for various damage modes of composite materials by comparing stress components to their related strength parameters. His criterion for tensile matrix damage contained both normal and shear stress terms. The criterion was formulated to be independent of the sign of shear stress. Thus, all shear stress terms were squared. The terms containing normal stresses were also of second order. When this criterion is applied to delamination using an average stress approach, it is evident that the contributions of in-plane stresses in the matrix layer are relatively small when compared to the contributions of the average out-of-plane interlaminar stress components. Hence, only

out-of-plane interlaminar shear and normal components need be considered in this approach.

It is obvious from the calculation of the interlaminar stress state that the square of the average value of the σ_{2z} component is overwhelmed by the square of the average value of the σ_{1z} component. This is due to the fact that the value of σ_{1z} is highest at the free edge whereas the boundary conditions require that σ_{2z} be zero at the free edge. Thus, the average value of σ_{1z} will always be considerably greater than the value of σ_{2z}. In the laminates studied in this investigation, the square of the average value of mechanical σ_{2z} never exceeds 0.7% of the square of the average value of mechanical σ_{1z}. If the shear strength of the composite is taken to be on the same order for the σ_{1z} and σ_{2z} stresses, then the $\overline{\sigma}_{2z}$ term will always be negligible when compared to the $\overline{\sigma}_{1z}$ term and can be ignored.

Tensile values of interlaminar normal stress are obviously important in initiating delamination. It is believed, however, that compressive values of interlaminar normal stress at the free edge do not affect initiation. Thus, compressive values of average interlaminar normal stress should be ignored. Laminates which have values of interlaminar normal stress which are identically zero or compressive at the free edge will never have tensile values of $\overline{\sigma}_{zz}$. Delamination in

these laminates is therefore controlled solely by the average value of σ_{1z}. Care should also be taken not to include the contributions of compressive values of σ_{zz} when calculating the average value of interlaminar normal stress for laminates which have tensile values at the free edge but have compressive values within the range of the averaging dimension.

It is therefore proposed that delamination will initiate when the following Quadratic Delamination Criterion is met at a ply interface:

$$\left(\frac{\bar{\sigma}_{1z}}{Z^s}\right)^2 + \left(\frac{[\bar{\sigma}_{zz}]}{Z^t}\right)^2 = 1 \qquad (3.3)$$

where $[\overline{\sigma}_{zz}] = 0$ if $\overline{\sigma}_{zz}$ is compressive

$\overline{\sigma}_{zz}$ if $\overline{\sigma}_{zz}$ is tensile

Z^t = interlaminar tensile normal strength

Z^s = interlaminar shear strength.

This Quadratic Delamination Criterion accounts for the contributions of the two stress components that are believed to be primarily responsible for delamination initiation. The criterion compares the average stress components with their related strength parameters. This single criterion can there-

fore describe delamination initiations which are dominated by significant values of interlaminar shear, tensile interlaminar normal stress, or any combination thereof.

3.3 Implementation of Quadratic Delamination Criterion Using the Force Balance Method

3.3.1 General Application

The Force Balance Method is very well suited for use with the Quadratic Delamination Criterion. The general forms of the σ_{zz} and σ_{1z} stresses are:

$$\sigma_{zz} = f_m(\lambda_m e^{-\lambda_m \phi_m X} - e^{-\phi_m X})\sigma_{ff} + f_t(\lambda_t e^{-\lambda_t \phi_t X} - e^{-\phi_t X})\Delta T \tag{3.4a}$$

$$\sigma_{1z} = h_m e^{-\phi_m X} \sigma_{ff} + h_t e^{-\phi_t X} \Delta T \tag{3.4b}$$

where: f,h = interlaminar stress constants determined for a specific interface via the Force Balance Method

ϕ, λ = interlaminar stress constants determined for the laminate via the Force Balance Method

x = distance from the free edge

σ_{ff} = far field mechanical stress

ΔT = laminate temperature minus curing temperature

m,t = subscripts denoting mechanical or thermal contributions.

The interlaminar stress distributions of σ_{zz} and σ_{1z} due to thermal loading and unit mechanical loading are depicted for the +15°/-15° interfaces of the three types of laminates used in this investigation in Appendix A. The +15°/-15° interface has been determined to be the critical interface for each of these laminates. Upon choosing a value for x_{avg}, the averaged stress components become:

$$\bar{\sigma}_{zz} = \frac{f_m}{\phi_m x_{avg}} \left[e^{-\phi_m x_{avg}} - e^{-\lambda_m \phi_m x_{avg}} \right] \sigma_{tt} + \frac{f_t}{\phi_t x_{avg}} \left[e^{-\phi_t x_{avg}} - e^{-\lambda_t \phi_t x_{avg}} \right] \Delta T \qquad (3.5a)$$

$$\bar{\sigma}_{1z} = \frac{h_m}{\phi_m x_{avg}} \left[1 - e^{-\phi_m x_{avg}} \right] \sigma_{ff} + \frac{h_t}{\phi_t x_{avg}} \left[1 - e^{-\phi_t x_{avg}} \right] \Delta T \qquad (3.5b)$$

Once the interlaminar stress parameters have been determined, the application of the Quadratic Delamination Criterion becomes quite simple.

3.3.2 Effect of Ply Thickness

It has been shown through the reasoning of dimensional analysis [35] that ϕ is the only interlaminar stress parameter that varies as the ply thickness of the laminate changes. The results of the Force Balance Method show that ϕ is inversely proportional to ply thickness. The result of this is that the distributions of the various components "spread out" with respect to distance from the free edge as ply thickness increases. This is shown for the σ_{zz} distribution of a $[\pm 15_n/0_n]_s$ laminate in Figure 3.1. It is important to note that the shape of the stress distribution remains the same and the value of stress at the free edge is constant for a given thermal and/or mechanical load. This behavior is the same for all components of stress.

This has specific implications in the average stress method. As ply thickness increases, the region of high stress near the free edge widens. Since the averaging dimension remains constant, the average σ_{zz} and σ_{1z} stress components increase for a given far field stress. This implies that initiation will occur at lower far field stresses for laminates with larger ply thicknesses as observed experimentally. The limit of this effect occurs when the ply thickness becomes large with respect to the averaging dimension. When this hap-

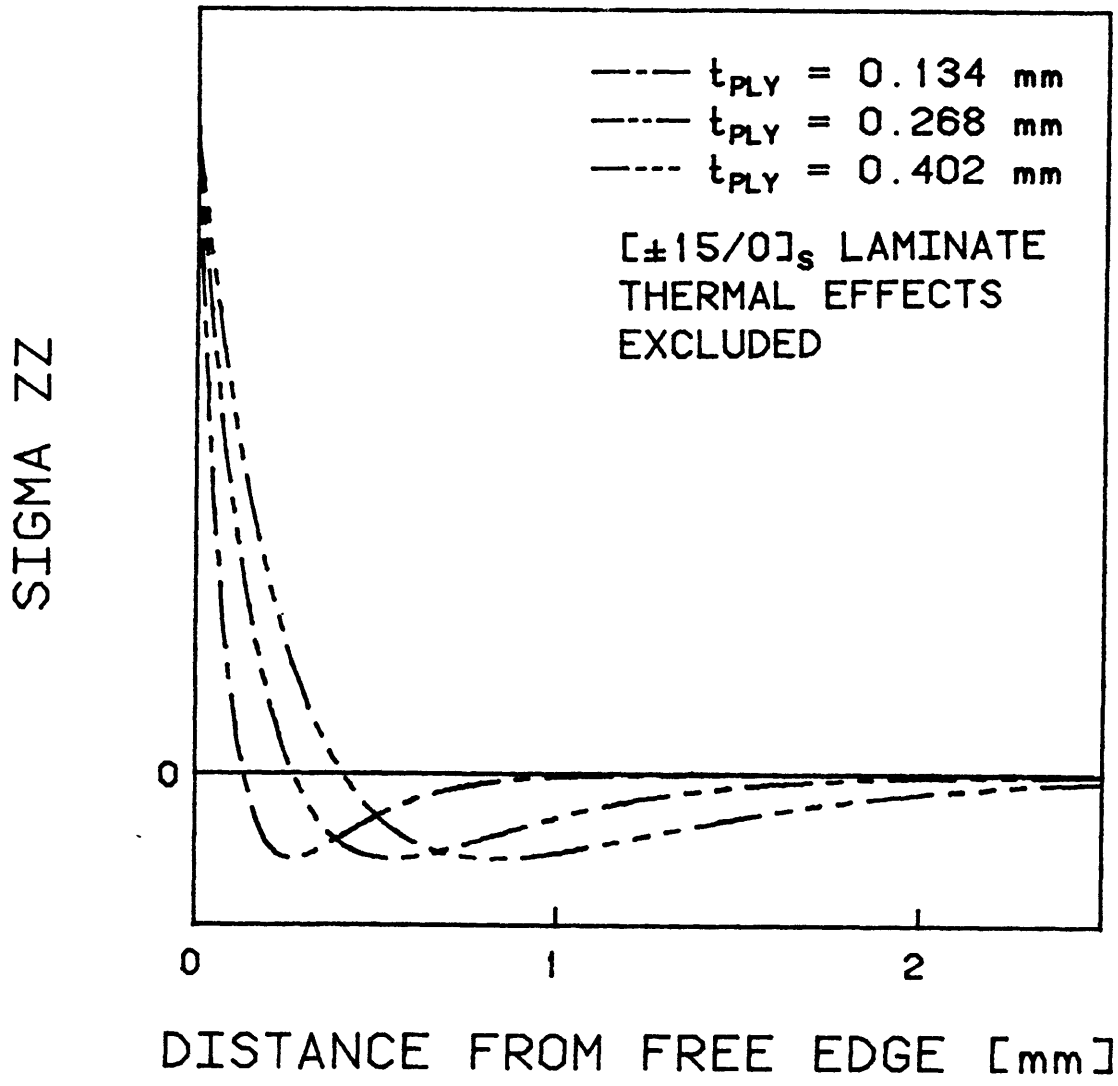

FIGURE 3.1 EFFECT OF PLY THICKNESS ON THE INTERLAMINAR STRESS STATE

pens, the average stress components asymptotically approach the values at the free edge. Thus, the predicted initiation stress asymptotically approaches a lower bound as ply thickness increases.

3.3.3 Effect of Averaging Dimension

Changing the chosen averaging dimension has an effect which is similar to that of changing the ply thickness. As the averaging dimension is increased, the region of the stress distribution over which the stress components are averaged is increased. This is relatively the same effect as that of decreasing the ply thickness. These two effects are illustrated in Figure 3.2 for $\overline{\sigma}_{1z}$. All other stress components exhibit the same sensitivity relative to changes in the averaging dimension. Thus, average stress components and, more importantly, predicted initiation stresses can be expressed in terms of ply thickness normalized by averaging dimension as illustrated in Figure 3.3. Thus, calculations may be made using a convenient averaging dimension. The curve that corresponds to a different averaging dimension can be found easily by scaling the effective ply thickness axis by a factor equal to the reciprocal of the change in the averaging dimension. The curve does not change its shape; it merely shifts horizon-

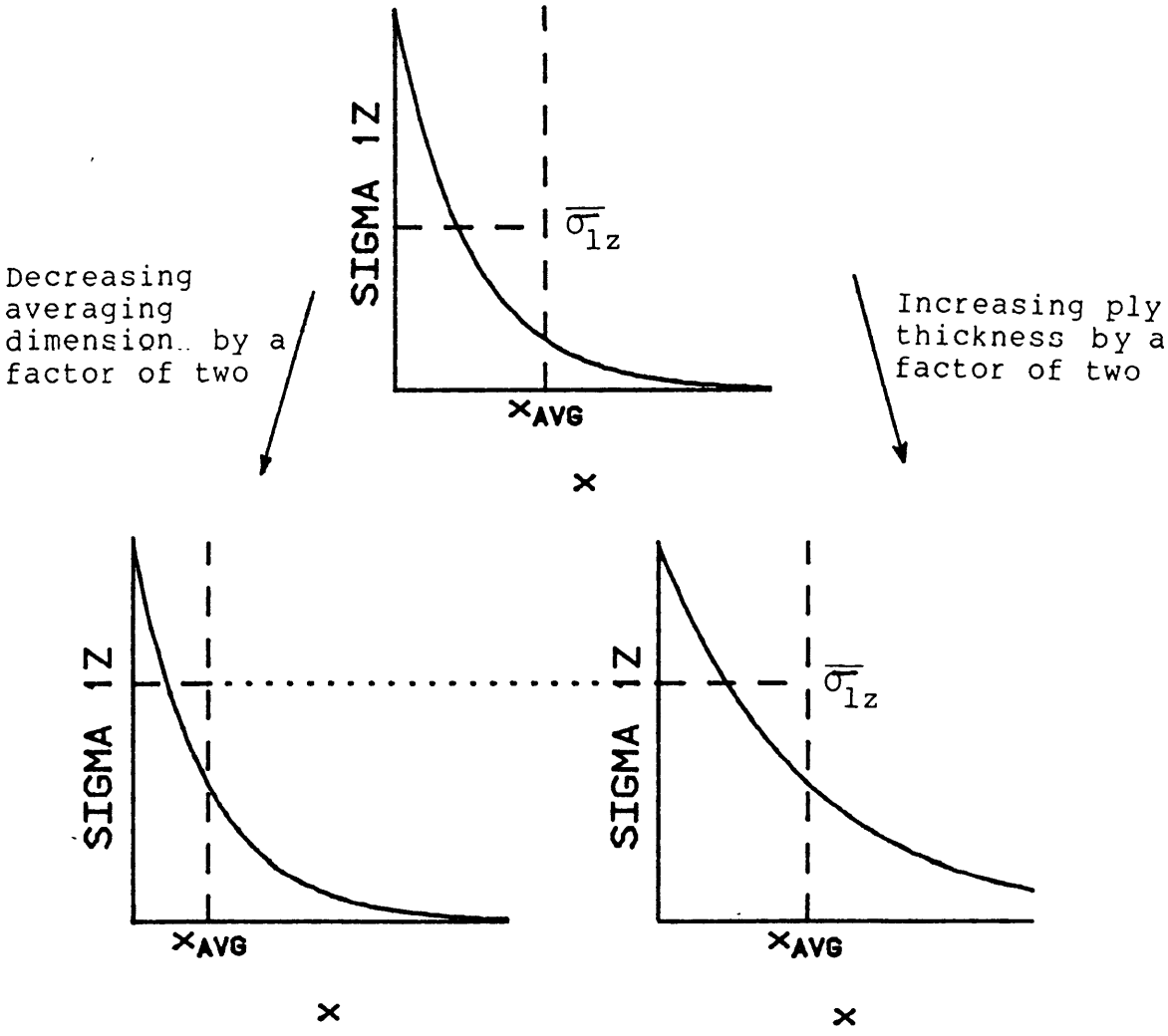

FIGURE 3.2 EFFECTS OF PLY THICKNESS AND AVERAGING DIMENSION ON THE AVERAGE STRESS

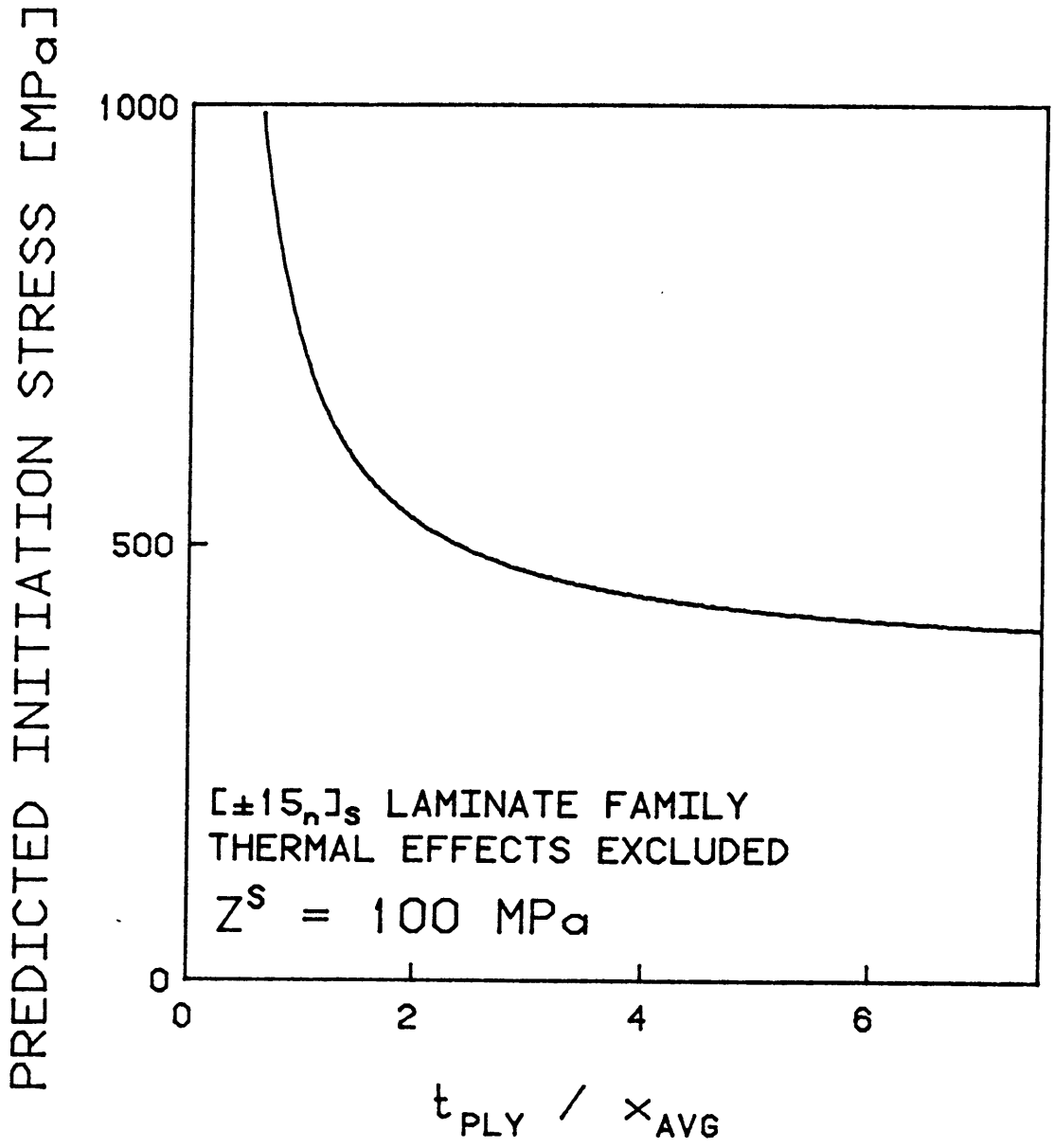

FIGURE 3.3 EFFECT OF NORMALIZED PLY THICKNESS ON PREDICTED DELAMINATION INITIATION STRESS

tally as illustrated in Figure 3.4. This allows for the easy exploration of several averaging dimensions in the search for a best fit value.

As noted in Section 3.2, care must be taken when the averaging dimension is greater than the distance from the free edge to the point where σ_{zz} changes sign. It is not believed that the compressive stress affects delamination initiation. Therefore, compressive values should not be included in the calculation of average stress components. This is not to say, however, that laminates with compressive values of σ_{zz} at the free edge should ever be considered to have an average value of σ_{zz} which is tensile.

3.3.4 Effect of Interlaminar Strength Parameters

It is obvious that a change in the interlaminar strength parameters will have an important effect on the predicted delamination initiation stress, regardless of the averaging dimension. To illustrate this sensitivity, consider the cases where $[\overline{\sigma}_{zz}]$ is taken to be zero (i.e. when σ_{zz} is identically zero or compressive at the free edge). The Quadratic Delamination Criterion reduces to the simple shear criterion used by Kim and Soni [20]:

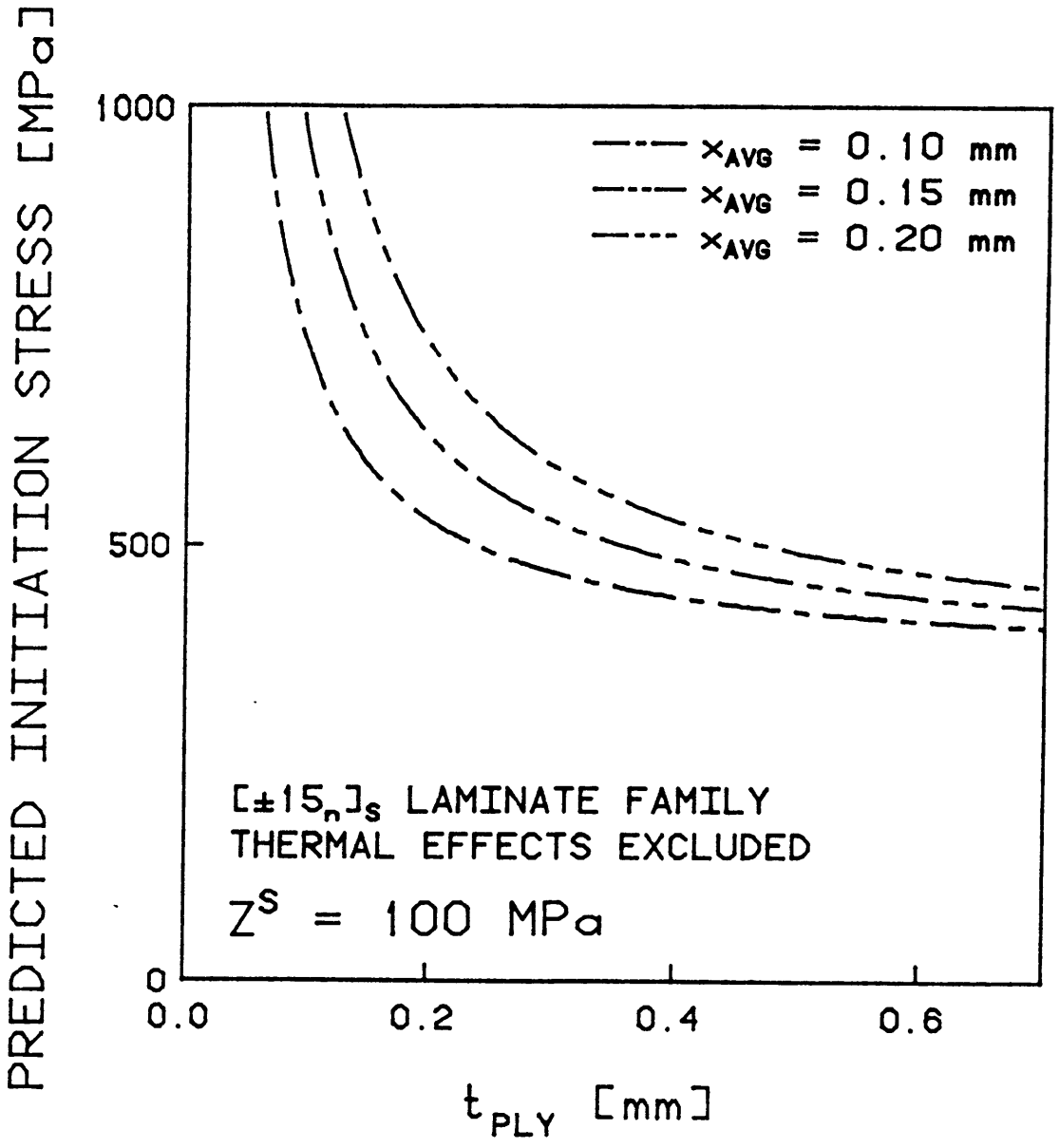

FIGURE 3.4 EFFECT OF AVERAGING DIMENSION ON PREDICTED DELAMINATION INITIATION STRESS

$$\bar{\sigma}_{1z} = Z^S \tag{3.6}$$

If the contributions of thermal stresses are ignored, it is evident that the shape of the predicted initiation stress versus ply thickness curve will remain the same, but will shift upward by a factor equal to the proportional change of interlaminar shear strength. This effect is depicted in Figure 3.5.

When specimens are dominated by mechanical shear stress but have both σ_{zz} and thermal stress contributions, a change in the interlaminar shear strength will still have the same general effect but the increase in predicted strength will not be perfectly linear. There will be some shape change of the predicted initiation stress curve as the thermal and normal stress components become more important in the Quadratic Delamination Criterion. For example, Figure 3.6 illustrates the effect of changing the assumed value of the interlaminar shear strength on the predicted curve for $[\pm 15_n/0_n]_s$ specimens. It can be seen that increasing the interlaminar shear strength causes the predicted strength to increase for all ply thicknesses. The percentage change in predicted strength varies, however, as the contributions of the thermal and normal stresses change.

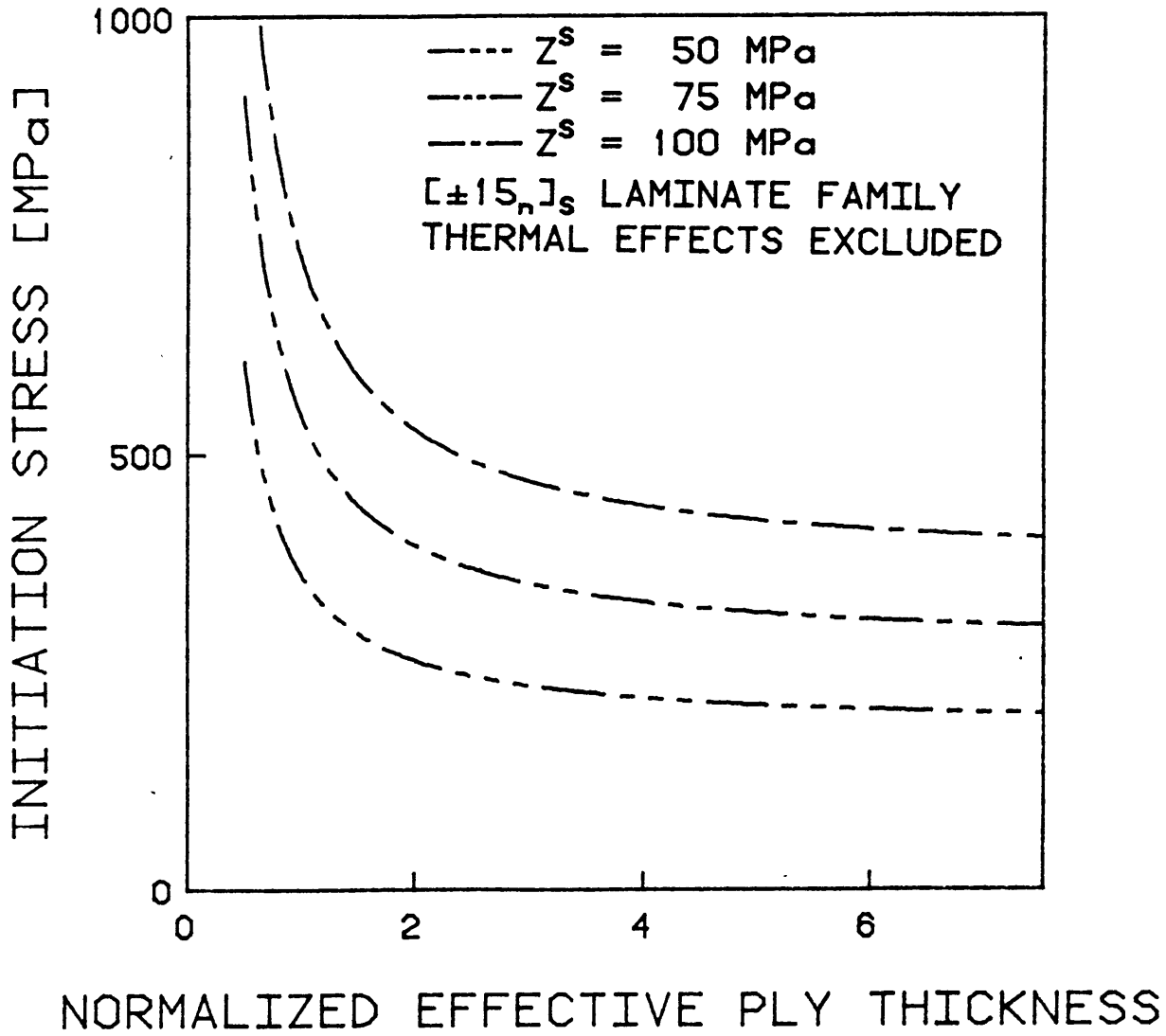

FIGURE 3.5 EFFECT OF INTERLAMINAR SHEAR STRENGTH ON PREDICTED DELAMINATION INITIATION STRESS OF SPECIMENS DOMINATED SOLELY BY MECHANICAL INTERLAMINAR SHEAR STRESS

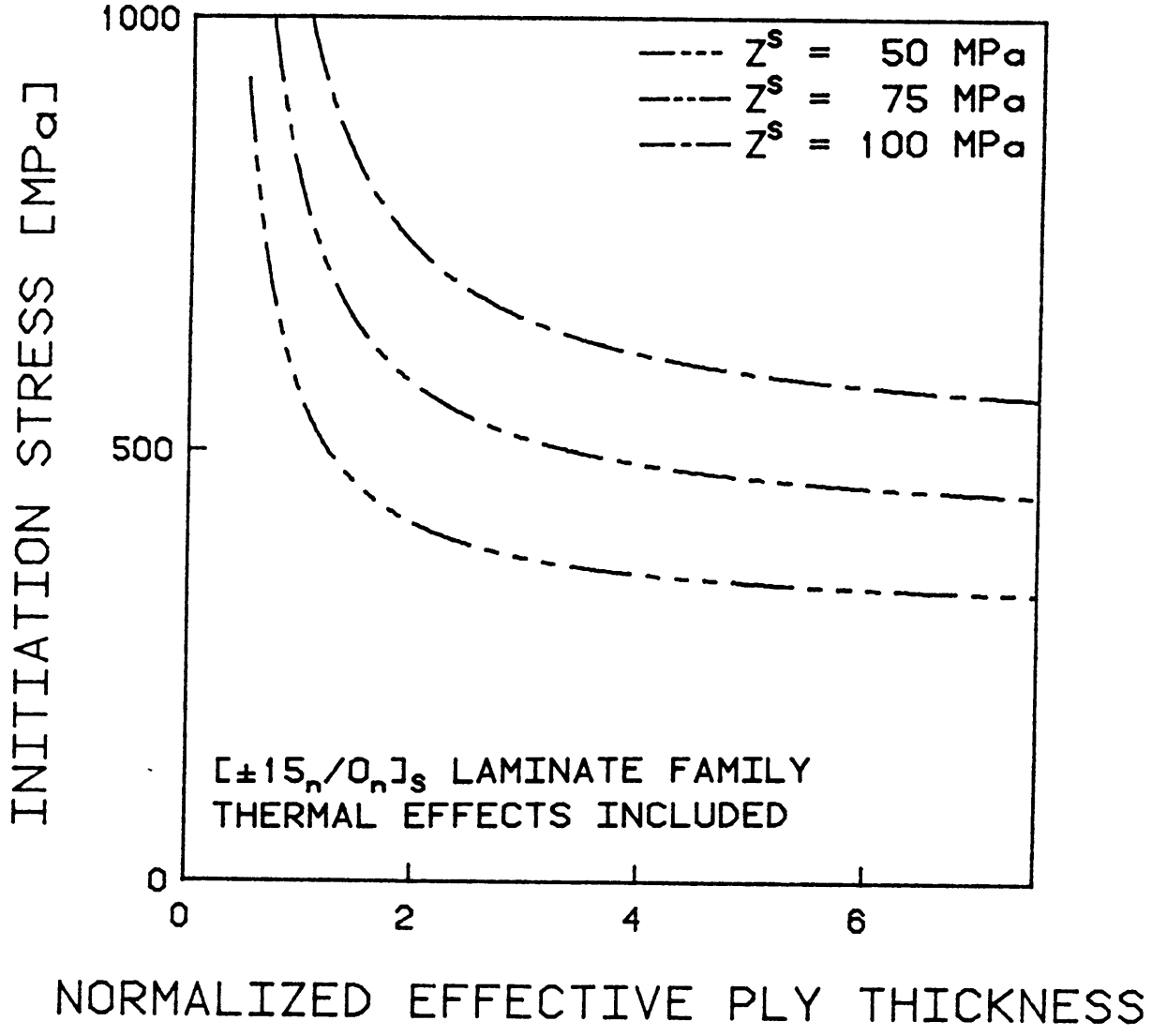

FIGURE 3.6 EFFECT OF INTERLAMINAR SHEAR STRENGTH ON PREDICTED DELAMINATION INITIATION STRESS OF SPECIMENS WITH THERMAL AND INTERLAMINAR NORMAL STRESS CONTRIBUTIONS

CHAPTER 4

THE EXPERIMENT

4.1 Specimen, Material, and Laminate Choice

The specimen used in this investigation is the standard TELAC specimen. This specimen is a straight-edged coupon which is 350 mm long and 50 mm wide. Glass/epoxy loading tabs 75 mm long and 50 mm wide are bonded onto the ends of the specimen using American Cyanamid FM-123 film adhesive. The layup of the loading tabs is $[0/90]_{ns}$ where n is sufficient for the loading tab to be 1.5 to 4 times as thick as the laminate as is suggested by the American Society for Testing and Materials [36]. Table 4.1 contains a summary of loading tab thicknesses used for the various laminate thicknesses in this experiment. The test section of this coupon is thus 200 mm by 50 mm. The specimen is illustrated in Figure 4.1.

All specimens were made from Hercules AS1/3501-6 graphite/epoxy. This material contains unidirectional AS1 graphite fibers in a 3501-6 thermosetting epoxy matrix. This composite is supplied as a preimpregnated tape nominally 305 mm in width with the epoxy in a semicured state. The "prepreg" must therefore be stored at -18°C or below until

TABLE 4.1

NOMINAL LAMINATE AND TAB THICKNESSES

LAMINATE	NOMINAL LAMINATE THICKNESS [mm]	NOMINAL TAB THICKNESS [mm]	NOMINAL TAB TO LAMINATE THICKNESS RATIO
$[\pm 15]_s$	0.536	2.03	3.79
$[\pm 15_*]_s$	0.678	2.03	2.99
$[\pm 15_2]_s$	1.07	3.05	2.85
$[\pm 15_3]_s$	1.61	4.06	2.52
$[\pm 15_4]_s$	2.14	6.10	2.85
$[\pm 15_5]_s$	2.68	6.10	2.28
$[\pm 15/0]_s$, $[0/\pm 15]_s$	0.804	2.03	2.52
$[\pm 15_*/0_*]_s$	1.02	3.05	2.99
$[\pm 15_2/0_2]_s$, $[0_2/\pm 15_2]_s$	1.61	4.06	2.52
$[\pm 15_3/0_3]_s$, $[0_3/\pm 15_3]_s$	2.41	6.10	2.52
$[\pm 15_4/0_4]_s$, $[0_4/\pm 15_4]_s$	3.22	6.10	1.89
$[\pm 15_5/0_5]_s$, $[0_5/\pm 15_5]_s$	4.02	8.13	2.02

Note: Subscript "*" indicates laminates made from 190g/m^2 prepreg

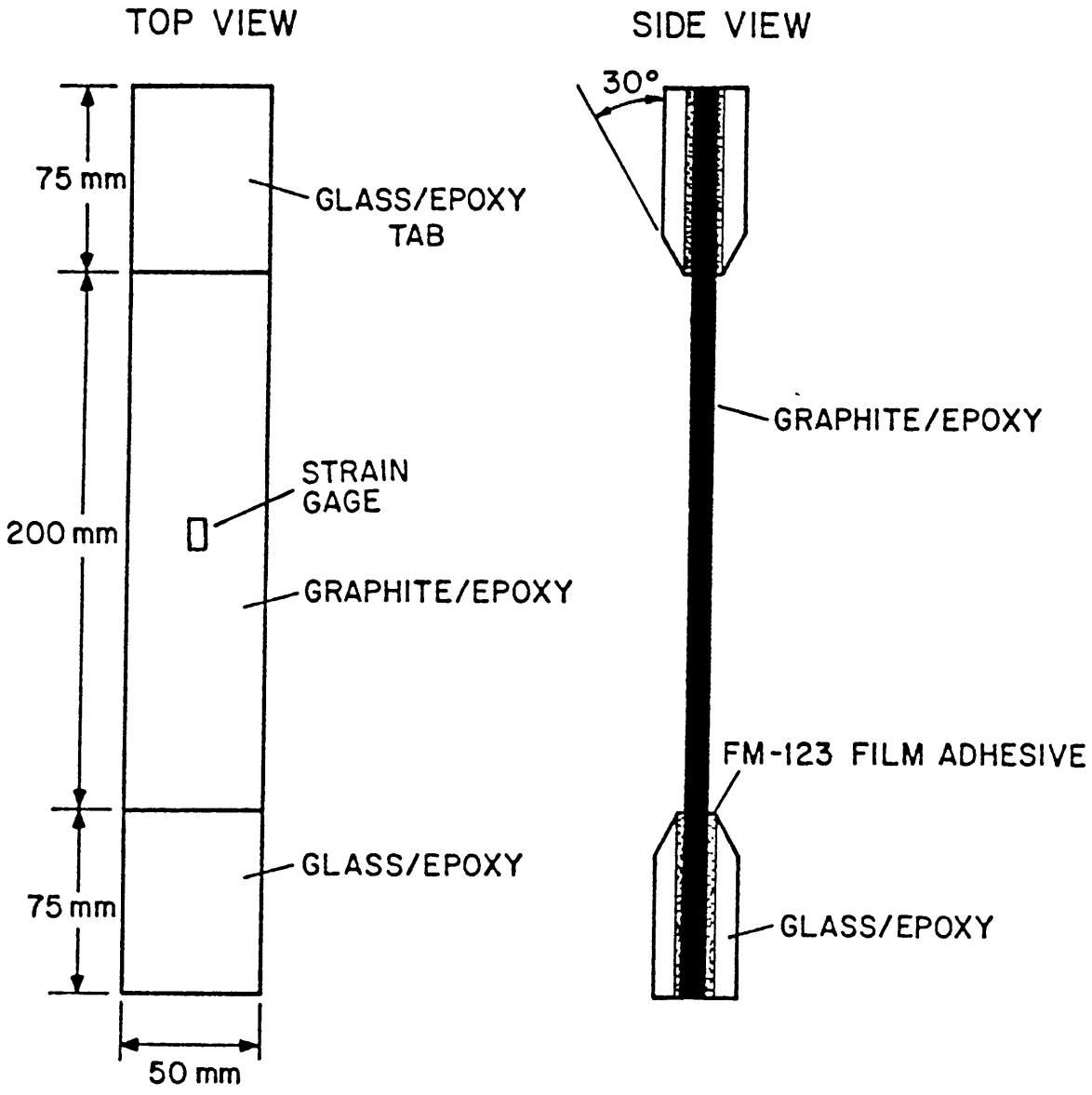

FIGURE 4.1 STANDARD TELAC TEST SPECIMEN

laminate manufacture. The basic elastic properties of the unidirectional ply of this material are reported in Table 4.2.

Three different laminate "types" were chosen for this investigation: $[\pm 15_n]_s$, $[\pm 15_n/0_n]_s$, and $[0_n/\pm 15_n]_s$. These laminates were chosen for their relative propensity to delaminate as observed in previous experiments at TELAC [2,21] and for their respective interlaminar stress states. The $[\pm 15_n]_s$ laminates delaminate although their calculated interlaminar normal stress, σ_{zz}, is identically zero. The $[\pm 15_n/0_n]_s$ laminates were chosen because both interlaminar shear stress, σ_{1z}, and tensile σ_{zz} exist in significant magnitudes at the free edge. The $[0_n/\pm 15_n]_s$ laminates exhibit delamination despite compressive values of σ_{zz} at the free edge. The interlaminar σ_{1z} distribution is similar at the +15°/-15° interfaces in the last two laminates. The calculations of interlaminar stresses were performed using the Force Balance Method of Lagace and Kassapoglou [11,12].

In order to examine the effect of ply thickness on the initiation of delamination, the ply thickness of these laminates was varied in two ways. In most cases, standard Hercules AS1/3501-6 graphite/epoxy with a nominal areal weight of 150 g/m² and cured per ply thickness of 0.134 mm was used. To vary the "effective ply thickness", a number of plies of the same orientation were stacked on top of one another as il-

TABLE 4.2

ELASTIC PROPERTIES OF AS1/3501-6 GRAPHITE/EPOXY

E_L	130 GPa
E_T	10.5 GPa
E_Z	10.5 GPa
G_{LT}	6 GPa
G_{LZ}	6 GPa
G_{TZ}	4.8 GPa
ν_{LT}	0.28
ν_{LZ}	0.28
ν_{TZ}	0.54

lustrated in Figure 4.2. For example, the effective ply thickness of a $[\pm 15]_s$ laminate is taken to be 0.134 mm. The effective ply thickness of a $[\pm 15_5]_s$ laminate is taken to be five times that value, or 0.670 mm. For each of the three laminate types mentioned above, specimens were constructed with values of normalized effective ply thickness (effective ply thickness divided by 0.134 mm), n, equal to 1, 2, 3, 4, and 5. It is important to note the fact that in previous experiments [21] these "multiple-thick" plies always behaved as a unit (i.e. there was never any delamination within a group of plies with the same angular orientation). Thus, they can be analyzed as single plies of a different ply thickness.

The second method for varying effective ply thickness was to use a special AS1/3501-6 prepreg with a nominal areal weight of 190 g/m² originally prepared by Hercules for Boeing Aircraft Co. This material has a nominal ply thickness of 0.169 mm and therefore a value of normalized effective ply thickness of 1.27. Specimens of $[\pm 15]_s$ and $[\pm 15/0]_s$ laminate types were made from this material. A laminate of the third type, $[0_n/\pm 15_n]_s$, was found to be improperly constructed and did not yield relevant data.

There were therefore five or six normalized effective ply thicknesses for each laminate type (n = 1, 2, 3, 4, 5, and 1.27 for the $[\pm 15]_s$ and $[\pm 15/0]_s$ laminate types). The five

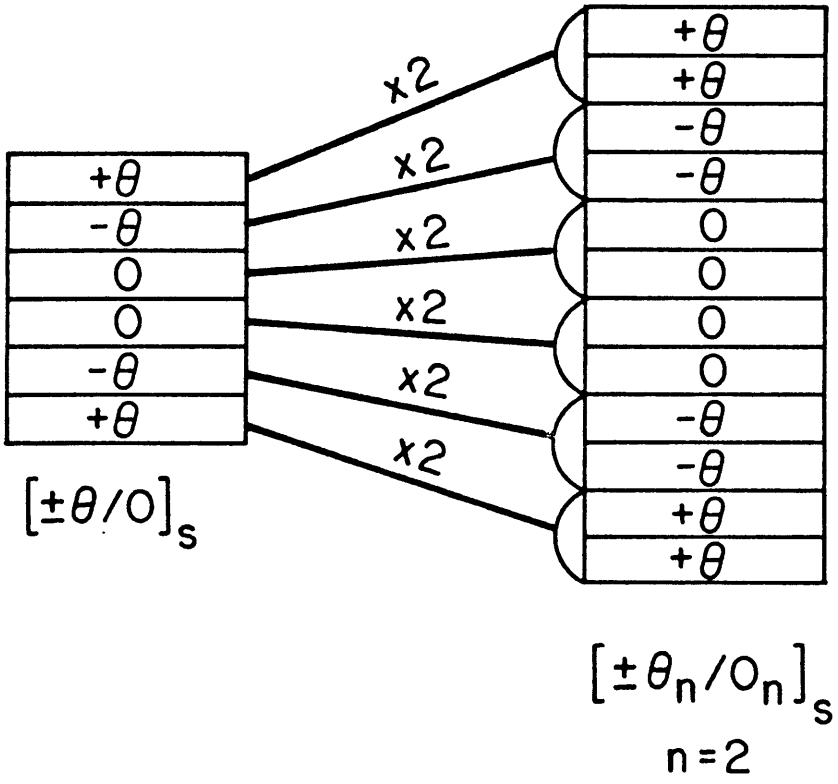

FIGURE 4.2 EFFECTIVE PLY THICKNESS CONCEPT

or six resulting laminates of the same basic orientation, albeit different effective ply thicknesses, constitute a "laminate family." These values of n were chosen because they gave a wide region over which to study the effects of ply thickness. The value of 1.27 was chosen specifically to "fill in the gap" between n equal to 1 and 2. This is important when one considers that the value of normalized ply thickness is doubling in this important region of the initiation stress versus ply thickness curve. Five specimens of each laminate type and ply thickness were manufactured. The total testing program is denoted in Table 4.3.

4.2 Nomenclature

The method for identifying specimens is an adaptation of the standard three bit TELAC code. The first bit contains a shorthand laminate notation of the form $n\theta Qm$. The θ represents the angular orientation of the angled plies in degrees. The Q represents a letter which denotes the location of any 0° plies. An "A" denotes that the 0° plies are located at the midplane while a "B" denotes that they are on the outside of the laminate. The m denotes the number of 0° ply groups in each half of the symmetric laminate. Hence, 15A0 represents a

TABLE 4.3

TESTING PROGRAM

n	$[\pm 15_n]_s$	$[\pm 15_n/0_n]_s$	$[0_n/\pm 15_n]_s$
1	5[a]	5	5
1.27	5	5	b
2	5	5	5
3	5	5	5
4	5	5	5
5	5	5	5

[a]Numbers indicate the number of specimens of each type

[b]Laminate was layed up incorrectly

$[\pm 15]_s$ laminate, 15A1 represents a $[\pm 15/0]_s$ laminate, and 15B1 represents a $[0/\pm 15]_s$ laminate.

For this experiment, the prefix n is added to this designation when the normalized effective ply thickness is different from one. Since the angular orientation in degrees of any unidirectional ply can be represented by a single number between -90 and +90, the addition of a preceding integer greater than one would lead to no ambiguity. This normalized effective ply thickness is used for this prefix. The only exception is that an asterisk is used for the laminates constructed of the 190 g/m² composite. Hence, 315A1 denotes a $[+15_3/-15_3/0_3]_s$ laminate.

The second bit in the three bit code is reserved for the nominal size of the manufactured notch normalized by 1.59 mm (1/16 inch). Since all of the specimens in this experiment were unnotched, the second bit of the code is zero for all specimens.

The third bit is an individual specimen number. To avoid confusion between the specimens manufactured for different projects, TELAC has adopted a practice of sequentially numbering all specimens of a given laminate type and notch size. This means that the first specimen of a given laminate type in a given investigation might not be specimen number one. This is the case for most of the specimens in this experiment as

these laminate types have been used in several previous investigations. The exceptions are the specimens manufactured from the 190 g/m² composite as these are the first specimens in TELAC constructed of this material.

4.3 Manufacture of Specimens

The eighty-five specimens manufactured for this investigation were constructed using the procedures developed at TELAC [37]. A review of these procedures is given.

The graphite/epoxy comes in rolls of semicured unidirectional preimpregnated tape or "prepreg". The nominal width of the 150 g/m² composite is 305 mm while the nominal width of the 190 g/m² composite is 75 mm. To prevent curing of the matrix before the laminates were manufactured, the composites were stored in freezers at or below -18°C. When manufacturing was to begin, the composite was left at room temperature in a sealed bag for at least 30 minutes. This prevents condensation from forming on the composite.

The prepreg was layered into uncured laminates in a "clean room" which is air-conditioned to keep room temperature below 25°C and the relative humidity low. Surgical gloves were used whenever handling uncured composite to avoid contamination from skin oil. The composite was cut into trapezoidal

shapes which could be placed together to make 305 mm by 350 mm plies with specific fiber orientations. These shapes were designed such that there were no fiber breaks in any ply, that is, the edges of the shapes which butted up were parallel to the fiber direction. Thus, the only joints were "matrix joints" which became indistinguishable during curing. The plies were cut from the prepreg using teflon-covered aluminum templates, which were machined to tolerances of one millimeter, and razor blades.

Several "curing materials" were used to insure proper curing of the composite. The surface of the composite layup was protected throughout the curing process by a peel-ply. This is a nylon-like fabric which is porous to the epoxy. The uncured laminate encased in peel-ply was placed onto an aluminum caul plate which was protected by a nonporous teflon-coated glass fabric (TCGF). A layer of porous TCGF was placed on top of the laminate. Several layers of a paper bleeder material were placed on top of the porous TCGF in order to absorb excess epoxy resin which flows out of the laminate during the bleed stage of the cure. For laminates of the standard 150 g/m^2 prepreg, the number of layers of paper bleeder was one half the number of plies in the laminate. Three and four plies of paper bleeder were used for the four-ply and six-ply laminates of the 190 g/m^2 material, re-

spectively. Aluminum top plates wrapped in nonporous TCGF were placed on top of the paper bleeder. Each laminate was bordered on two sides by aluminum dams and on two sides by dams of a corprene rubber material (cork). The dams prevented shifting of the composites during curing. The corner of the aluminum dams provided a sharp "good corner" which could be used for reference of the fiber orientations.

The curing plate was large enough to handle all six laminates of a laminate family in a single cure. The six laminates and their top plates were covered by a sheet of porous TCGF and a heavy fiberglass fabric air breather which provided a path for air and other gases to escape into the vacuum system. The entire assembly was vacuum bagged with a high-temperature nylon bagging material and Schnee-Morehead vacuum tape. Figure 4.3 is a schematic representation of the cure set up for a laminate.

The curing of the composite is a two-stage process which takes place in an autoclave at 0.59 MPa (85 psig) pressure and an applied vacuum of at least 740 mm Hg (29 inches Hg). The first stage is a one hour "flow stage" at 117°C in which the epoxy is at its minimum viscosity. This allows for "bleeding" off of excess epoxy resin, proper bonding of the plies, and the removal of possible voids by the vacuum and pressure. The second stage of the cure is a two hour "set stage" at 177°C.

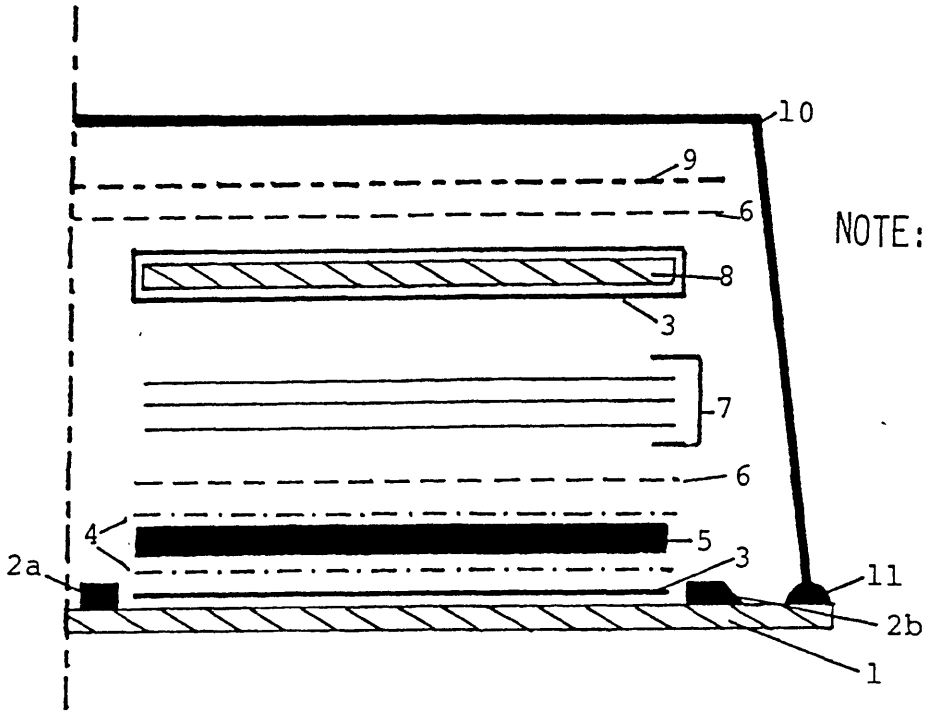

1. Aluminum Caul Plate, 3/8" thick MIC 6 aluminum with thin uniform coat of mold release 225 baked on
2a. Cork dam (Corprene), 1/8" x 1" with adhesive backing
b. Aluminum dam, 1/4" x 1", screwed down
3. Guaranteed non-porous teflon, TCGF-EHV .003, premium
4. Peel-ply #3921
5. Prepreg layup (laminate)
6. Porous teflon, TCGF .001-P porous
7. Paper bleeder (1 bleeder/2 plies of prepreg)
8. Aluminum Caul Plate, 1/4" thick MIC 6 aluminum with thin uniform coat of mold release 225 baked on
9. Air breather, #7781 fiberglass with volan finish
10. HS-6262 nylon vacuum bagging, 2 mils thick
11. Vacuum tape

FIGURE 4.3 STANDARD TELAC CURE ASSEMBLY

This is where most of the chemical crosslinking of the polymer chains in the epoxy takes place. All heat-up and cool-down rates were in the range of 1 to 3°C/min to avoid thermally shocking the composite. A postcure of eight hours at 177°C in an unpressurized oven was used. The entire cure cycle is illustrated in Figure 4.4.

Each cured laminate was machined into five 50 mm by 350 mm specimens using a water-cooled diamond grit cutting wheel. Approximately 25 mm was cut from the reference edge of the laminate and discarded before the specimens were cut. The cutting wheel was attached to a specially outfitted milling machine to avoid any tapering of the specimens.

The specimens were measured for width at three points using a caliper and for thickness in nine places using a micrometer. The exact location of the measurement points is shown in Figure 4.5. The average values for width and thickness for each specimen are reported in the data tables. It should be noted that thickness measurements are used simply as a quality control check. It can be readily seen under a microscope that "dimpling" of a surface layer of epoxy due to the presence of the peel-ply during curing can distort thickness measurements. This apparent extra thickness is most evident for thinner laminates. Thus, nominal thicknesses were used in all stress calculations. The thicker laminates showed some decrease in

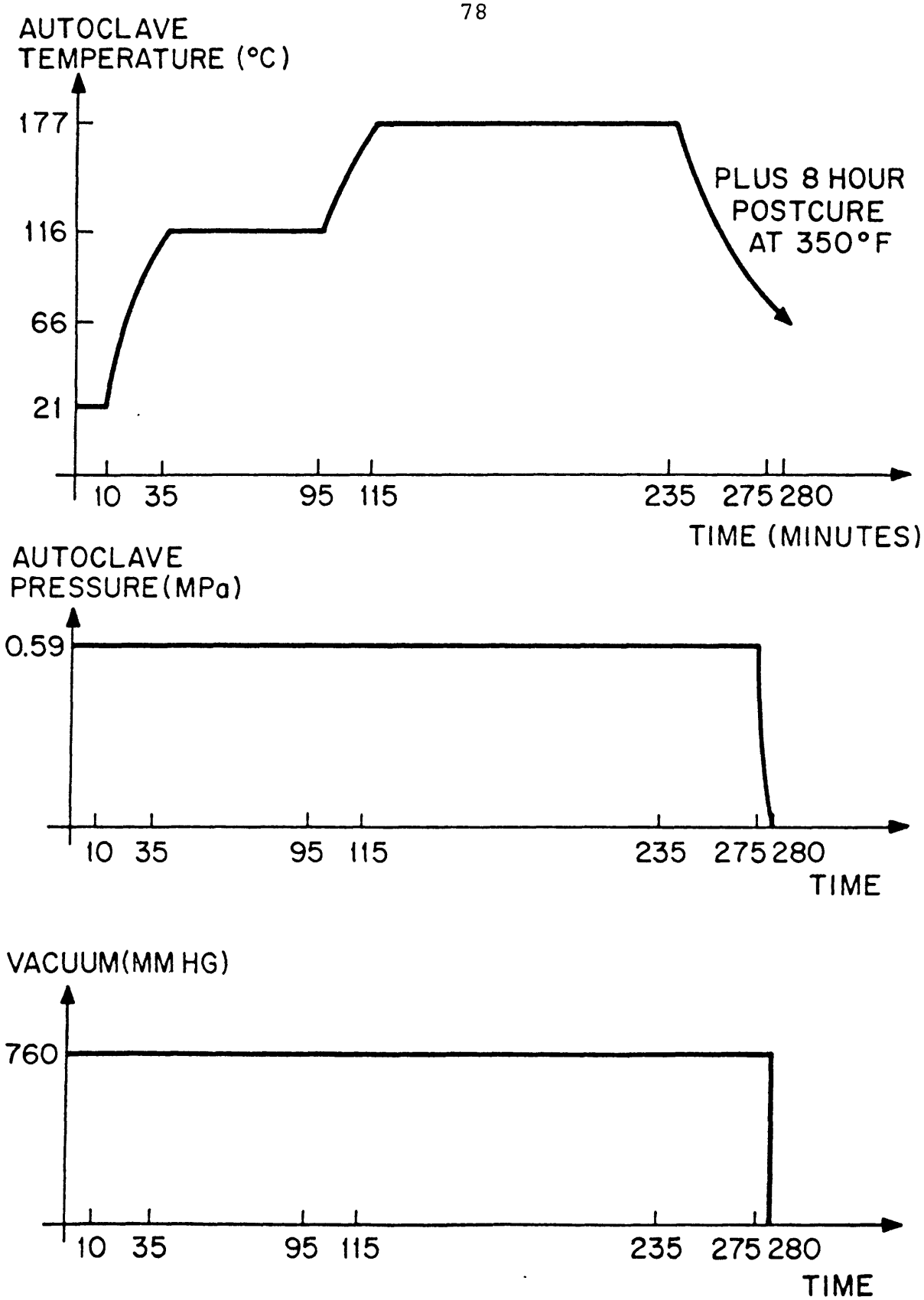

FIGURE 4.4 STANDARD TELAC CURE CYCLE FOR AS1/3501-6 GRAPHITE/EPOXY

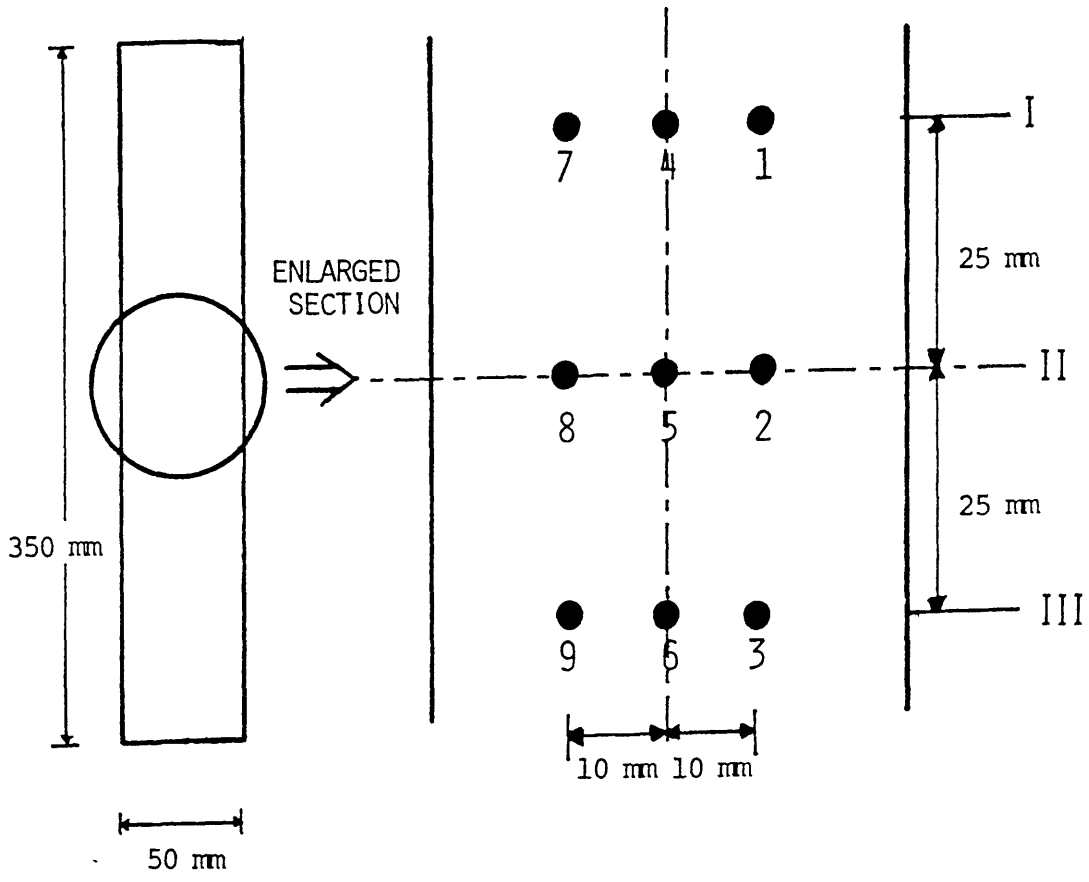

FIGURE 4.5 LOCATIONS ON THE SPECIMEN WHERE THICKNESS AND WIDTH MEASUREMENTS WERE MADE

thickness toward the laminate edge. This increased the coefficient of variation of thicknesses of the specimens of a given laminate as well as decreasing the average ply thickness slightly below the asymptotic level of the nominal value. Actual laminate and average ply thicknesses are reported in Table 4.4. The average value of ply thickness for the laminates constructed of the 150 g/m² prepreg is 0.132 mm with a coefficient of variation of 5.5%. The average value of ply thickness for the laminates constructed of the 190 g/m² prepreg is 0.168 mm with a coefficient of variation of 3.9%. These average values of ply thickness are within 2% of the nominal values of 0.134 mm and 0.169 mm, respectively.

Glass/epoxy loading tabs, as described in Section 4.1, were manufactured from 3M SP-1003 unidirectional preimpregnated glass/epoxy. These laminates were cured according to procedures outlined in Reference 37. The cure cycle consisted of a single stage cure of two hours at 166°C under vacuum and an applied pressure of 0.34 MPa (50 psig). Manufactured laminates were 305 mm by 710 mm and were cut into individual tabs measuring 50 mm by 75 mm. One of the 50 mm edges of each tab was bevelled to a 30° angle to the plane of the tab using a belt sander.

Tabs were bonded onto the specimen with American Cyanamid FM-123-2 film adhesive. The adhesive was applied directly to

TABLE 4.4

AVERAGE LAMINATE AND PLY THICKNESSES FOR EACH LAMINATE

Laminate	Average Laminate Thickness [mm]	Average Ply Thickness [mm]	Coefficient of Variation
$[\pm 15]_s$	0.59	0.148	1.4%
$[\pm 15_*]_s$	0.70	0.174	3.3%
$[\pm 15_2]_s$	1.06	0.132	3.3%
$[\pm 15_3]_s$	1.56	0.130	3.1%
$[\pm 15_4]_s$	2.08	0.130	3.5%
$[\pm 15_5]_s$	2.60	0.130	3.6%
$[\pm 15/0]_s$	0.83	0.138	1.7%
$[\pm 15_*/0_*]_s$	0.99	0.166	2.4%
$[\pm 15_2/0_2]_s$	1.55	0.129	3.0%
$[\pm 15_3/0_3]_s$	2.25	0.125	3.7%
$[\pm 15_4/0_4]_s$	3.06	0.127	3.2%
$[\pm 15_5/0_5]_s$	3.73	0.124	3.0%
$[0/\pm 15]_s$	0.84	0.141	2.7%
$[0_2/\pm 15_2]_s$	1.56	0.130	4.9%
$[0_3/\pm 15_3]_s$	2.30	0.128	3.9%
$[0_4/\pm 15_4]_s$	3.17	0.132	3.0%
$[0_5/\pm 15_5]_s$	3.93	0.131	4.1%

Note: Subscript "*" indicates laminates made from 190g/m^2 prepreg

the tab. The film, which is stored at -18°C, becomes tacky enough at room temperature to hold the tab in place on the specimen while preparing the bonding cure. The specimens were placed on an aluminum plate covered with nonporous TCGF. The specimens were covered with another layer of TCGF and a steel top plate placed on top of each specimen. Air breather was placed over the top plates and the entire assembly vacuum bagged. The film adhesive was cured for two hours at 114°C. An applied vacuum and an autoclave pressure of 0.068 MPa (10 psig) on the top plates yielded an absolute pressure of approximately 0.34 MPa (50 psia) on the bonding surface.

4.4 Instrumentation of Specimens

A strain gage was attached to each specimen to monitor longitudinal strain during testing. The gage was mounted in the center of the test section as shown in Figure 4.1. All gages are Micro Measurements EA-06-031DE-120 strain gages with a 3.175 mm square constantan wire element on a 0.025 mm thick polyimide backing. The gages were aligned with the longitudinal axis of the coupon specimen using lines that were lightly scribed on the thin epoxy layer of the laminate surface. The gages were bonded onto the specimen with M-Bond 200 adhesive.

The resistance of the gages is 120 ohms ± 0.15% and the gage factor is 2.04 ± 0.5%.

4.5 Edge Replication Procedures

The edge replication technique was used to monitor and inspect the specimen edges for delamination. An edge replication involves the use of a strip of acetate film to make an impression of an edge of a specimen. The specimen edges had to be carefully polished before testing. The polishing was done with 25 mm diameter felt bobs mounted in a drill press. The felt bobs were continually dipped in a colloidal solution of a fine abrasive, Kaopolite-SF, with an average particle size of 0.7 microns. The solution was hand-mixed and contained approximately two parts tap water for each part of abrasive. A smooth back and forth motion of the specimen edge against the felt bob was used for polishing. After polishing, the edges were quickly rinsed to prevent the solution from solidifying on the edge. This gave the specimen edge a glossy finish.

In this investigation, edge replications were made of both edges of each specimen before testing and after each test. Replications were therefore made while the specimen was both outside the testing machine and inside the testing ma-

chine while under load. To make a replication, a strip of replicating tape 25 mm in width is cut to the correct length to replicate the portion of the free edge which is not inaccessible, i. e., not within the grips of the testing machine. The edge is wiped with cheesecloth soaked in acetone. The acetone is allowed to evaporate and the replicating tape placed up against the corner of the edge as depicted in Figure 4.6. A squirt bottle containing acetone is held up to the tape and used to squirt acetone over the surface of the tape which is facing the edge of the specimen. This softens the tape for replication. The tape is then smoothed against the edge with a finger or other smooth object and allowed to dry for approximately one minute. During this time, a mark is placed on the tape using a magic marker. This corresponds to a similar mark which had been made on the specimen about 30 to 40 mm from the tab. These marks are used for reference of distance along the free edge. This is necessary as the tabs are not exposed enough when the specimen is in the testing machine to allow the end of the tab to be a longitudinal reference point.

Once the replications dry, they are removed. Replications are carefully examined to see if sufficient pressure was applied to the entire surface. If insufficient pressure were applied, smudges can be seen with the naked eye. If areas are

FIGURE 4.6 POSITION OF REPLICATING TAPE DURING APPLICATION OF ACETONE

seen to be improperly replicated, the replication is discarded and the specimen is rereplicated. If the replications are acceptable, they are labelled with a piece of masking tape and placed between two clean flat surfaces to finish drying. This prevents curling of the replications. The replication techniques used in this investigation were refined during preliminary investigative work.

When properly done, replications may show features as small as individual fibers. Differences in plies, interlaminar resin layers, and an occasional microvoid can easily be seen. Softened acetate can seep into tight transverse cracks and delaminations, especially when they are susceptible to being "opened" when under load. The difference in surface texture of the replications of these features gives replications the unique ability to highlight these difficult-to-detect features when viewed under a microscope. This detection is nearly impossible to do when viewing the actual specimen under an optical microscope as these features appear as dark lines against a dark background. The replications were illuminated from behind while being viewed under the microscope. This enhanced the different surface texture and made initiation detection more reliable.

4.6 Load Drop Phenomenon

An important extension of the load-displacement curve approach of O'Brien [25] was made in this work in an effort to detect delamination initiation directly. When delamination initiates, strain continuity is no longer applicable in the delaminated region since the delaminated sublaminates are no longer rigidly bonded. O'Brien suggested that the modulus of this region is the average modulus of the remaining sublaminates weighted by the thickness of the sublaminates. Energy considerations suggest that this modulus will always be less than the original modulus. When this decrease in modulus is a result of an instantaneous delamination in a laminate which is being statically loaded under displacement (stroke) control, the result is an instantaneous drop in load. Hence, it is believed that a drop in load in a quasistatically loaded specimen may be indicative of delamination initiation. For the small amount of delaminated area expected to occur at initiation, the change in effective modulus of the test section is small. The point of change of modulus would be difficult to detect using stress-strain data. In contrast, a drop in load can be pinpointed as long as data are taken with enough frequency that the load drop is not obscured by the increase in load due to normal loading of the specimen.

A computer program was therefore written for the testing of specimens which allowed the automatic termination of a test when a drop in load was detected. The ability of the computer to detect a drop in load was dependent on several factors. First, the size of the load drop is a function of the size of the delaminated area. O'Brien [25] showed:

$$\frac{A_{del}}{A_{tot}} = \frac{E_{eff} - E_{lam}}{E_{avg} - E_{lam}} \qquad (4.1)$$

where: A_{del} = delaminated area

A_{tot} = total test section area

E_{eff} = longitudinal modulus of partially delaminated specimen

E_{avg} = weighted average modulus of the sublaminates

E_{lam} = longitudinal modulus of undelaminated laminate.

If linear stress-strain behavior is assumed under stroke control, a decrease in load proportional to the decrease in modulus is expected. That is, since the stroke is assumed constant at any given point, the load divided by the specimen stiffness must remain constant. Since the total area remains unchanged this yields:

$$\frac{P_{del}}{P_{und}} = \frac{E_{eff}}{E_{lam}} \tag{4.2}$$

where: P_{del} = load applied to partially delaminated specimen

P_{und} = load applied to undelaminated specimen.

Solving for E_{eff}, and substituting this result into Equation 4.1 yields, upon simplification:

$$\frac{A_{del}}{A_{tot}} = \frac{\left(\frac{P_{del} - P_{und}}{P_{und}}\right) E_{lam}}{E_{avg} - E_{lam}} \tag{4.3}$$

If the fractional load drop is defined as:

$$\Delta P_{fr} = \frac{P_{del} - P_{und}}{P_{und}} \tag{4.4}$$

Equation 4.3 can be manipulated to obtain:

$$\Delta P_{fr} = \left(\frac{E_{avg} - E_{lam}}{E_{lam}}\right) \frac{A_{del}}{A_{tot}} \tag{4.5}$$

Assuming that the interface which is most likely to delaminate can be predicted, the percentage drop in load can be directly related to the area of delamination. Thus the load drop is given by:

$$\Delta P = \Delta P_{fr} \cdot P_{und} = \left(\frac{E_{avg}}{E_{lam}} - 1 \right) \frac{A_{del}}{A_{tot}} P_{und} \qquad (4.6)$$

The ability to detect the load drop is a function of the parameters of the data acquisition system and the strain rate at which the test is conducted. Load data from the testing machine is available to the computer data acquisition software through analog-to-digital conditioners. These conditioners digitize the analog voltage data representing the applied load by discrete "computer units". The value of a computer unit of load is dependent on the load range setting of the testing machine. The ranges used in this investigation were 44.5 kilonewtons (10,000 pounds), 89.0 kilonewtons (20,000 pounds), and 222.4 kilonewtons (50,000 pounds). The full range was divided into 2048 computer units. Thus, a computer unit was equivalent to 21.7 N with the machine in the 44.5 kN range, 43.4 N in the 89.0 kN range, and 108.6 N in the 222.4 kN range.

The data was sampled automatically at discrete time intervals. The stress rate is a function of the modulus and the strain rate:

$$\dot{\sigma} = E \dot{\varepsilon} \tag{4.7}$$

The loading rate is given by the stress rate times the cross-sectional area of the test section:

$$\dot{P} = \dot{\sigma} A_{cs} = EA_{cs} \dot{\varepsilon} \tag{4.8}$$

where A_{cs} is the cross-sectional area of the test section. Assuming linear stress-strain behavior, the increase of load per time interval is simply the loading rate times the time increment between data acquisition:

$$\Delta P = \dot{P} \Delta t = EA_{cs} \dot{\varepsilon} \Delta t \tag{4.9}$$

It is imperative that this increase in load be less than the expected drop in load due to delamination described by Equation 4.6. Otherwise, the load increase would obscure the load drop as illustrated in Figure 4.7. To be detectable by the computer program, the load drop must be at least one computer unit greater than the load increase. If P_{cu} is defined

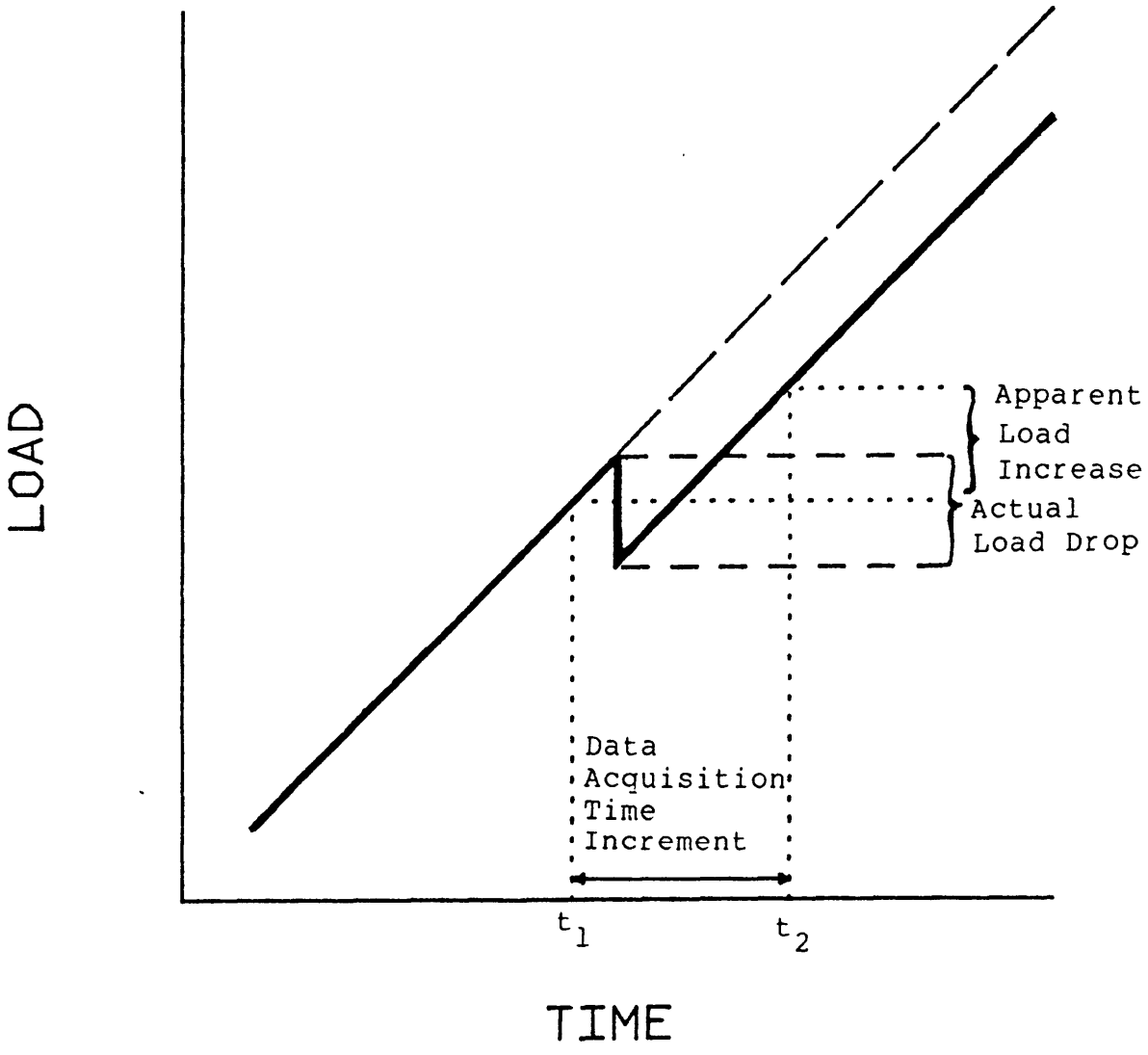

FIGURE 4.7 LOAD INCREASE OBSCURING A LOAD DROP

as the load equivalent to one computer unit, the following inequality must be satisfied:

$$\left|\left(\frac{E_{avg}}{E_{lam}} - 1\right)\frac{A_{del}}{A_{tot}} P_{und}\right| \geq EA_{cs}\dot{\epsilon}\Delta t + P_{cu} \qquad (4.10)$$

It is assumed that it is known which interface will delaminate so that various terms in Equation 4.10 can be determined. In addition, the load range for a specific laminate is chosen based on maximum loads as previously observed for these laminates in tests to failure. The load at which delamination takes place, P_{und}, is linked to the minimum delamination area which can be detected, A_{del}. Thus, the sensitivity of this technique is defined by the resulting A_{del} in that the delamination of such an area will induce a detectable load drop.

To be conservative, P_{und} was taken to be one half of the ultimate tensile stress. Thus, the minimum detectable A_{del} can be directly related to the actual strain rate and thus the chosen time increment. There is a limit as to how short the data acquistion time increment can be. It must not be so short that the computer data file (which is limited in size to 1314 data points) is filled before the specimen can reach expected delamination load plus a margin of safety. Also, the

noise of the system must be taken into account. The variation of load measurement can vary by as much as plus or minus 1 or 2 computer units. If the time increment is too short, this noise can be larger than the expected rise in load per time increment. When this occurs, the test can be stopped erroneously. Trial and error were used to determine time increments which were short enough to provide adequate sensitivity but long enough to avoid problems with noise. In all cases, it was decided to err slightly on the side of choosing a time increment which is too short. This was decided because it was reasoned that it was better not to miss a real initiation and chance having to retest the specimen than to have an initiation missed and the specimen go on to final failure without having given any information about initiation. The time increments chosen for each specimen type are tabulated in Table 4.5. The actual strain rate and A_{del} that can be detected, as determined from Equation 4.10, are also listed.

4.7 Testing Procedures

All specimens were tested in an MTS 810 Material Test System equipped with hydraulic grips. Tests were conducted under quasistatic monotonic tensile loading. The machine was always run under stroke control with a constant stroke rate of

TABLE 4.5

LOAD DROP TESTING PARAMETERS FOR EACH LAMINATE

Laminate	Data Aquisition Time Increment [Sec]	Average Actual Strain Rate [Microstrain/ Sec]	Minimum Detectable Delamination Area [mm^2]
$[\pm 15]_s$	0.30	71.2 (2.6%)[a]	220
$[\pm 15_*]_s$	0.30	71.9 (3.7%)	231
$[\pm 15_2]_s$	0.20	70.2 (2.9%)	188
$[\pm 15_3]_s$	0.15	67.9 (2.2%)	189
$[\pm 15_4]_s$	0.11	65.1 (4.8%)	152
$[\pm 15_5]_s$	0.11	61.8 (2.6%)	145
$[\pm 15/0]_s$	0.18	70.3 (3.1%)	161
$[\pm 15_*/0_*]_s$	0.16	69.9 (1.8%)	187
$[\pm 15_2/0_2]_s$	0.16	65.5 (1.5%)	188
$[\pm 15_3/0_3]_s$	0.12	60.3 (3.4%)	151
$[\pm 15_4/0_4]_s$	0.12	55.2 (2.8%)	196
$[\pm 15_5/0_5]_s$	0.12	53.0 (3.3%)	168
$[0/\pm 15]_s$	0.18	71.0 (3.1%)	138
$[0_2/\pm 15_2]_s$	0.16	65.0 (0.9%)	166
$[0_3/\pm 15_3]_s$	0.12	60.5 (1.9%)	121
$[0_4/\pm 15_4]_s$	0.12	57.4 (3.7%)	168
$[0_5/\pm 15_5]_s$	0.12	54.1 (2.7%)	150

[a]Numbers inparentheses are coefficients of variation

Note: Subscript "*" indicates a laminate made from $190 g/m^2$ prepreg

1.07 mm/min. This translates to a nominal strain rate of approximately 90 microstrain/sec over the 200 mm test section.

Specimens were aligned in the grips using a machinist's square. The upper grip was closed and the lower grip positioned around the lower tab. This was considered the "zero load" position at which strain gage calibration was done. The strain gages were monitored by computer using Vishay strain gage conditioners. The computer stored data which was retrieved from the strain gage conditioners or testing machine through analog-to-digital devices which divided the full range of the channel into ±2048 digital units as described in Section 4.6. In this investigation, the stroke range is 12.7 mm. Thus a computer unit of stroke is equivalent to 0.0062 mm. It should be noted that stroke could not be used as an accurate measure of the stretching of the test section due to the significant shearing of plies of the loading tabs relative to each other. This effect is more pronounced in the thicker specimens since they have thicker tabs.

The value of a computer unit of strain could be adjusted using the gain control on the strain gage conditioner. In this investigation, the conditioner was calibrated before each test so that each computer unit represented six microstrain. The gage was first "balanced" so that zero strain registered in the zero load position. A calibration resistance was con-

nected in parallel with the strain gage in order to calibrate the system.

The testing machine was run under computer control such that data aquisition and load application would start simultaneously. The test can be stopped in three ways. One, a test can be stopped by intentionally interrupting the test. Two, a test can be stopped automatically when the data file collecting load, stroke, and strain data is filled. The third possibility, which was the normal procedure, is that a test is stopped when the detected load at one data point is lower than the value at the previous point. This apparent load drop is taken as an indication of possible delamination initiation.

Once the test had been stopped, maximum load and stroke values from the testing machine were recorded in the laboratory notebook. It is desirable that edge replications be made while the specimen is under load. As the machine had a tendency to gradually increase load while being held at a given point, the computer was used to decrease the stroke (and thus the load) by a factor of approximately two. Two edge replications were taken of both edges of the specimen while it was loaded at this lower level. The specimen was then completely unloaded and removed from the testing machine.

The replications were carefully examined under a microscope at magnifications ranging from 14X to approximately 50X.

When a replication showed a delamination that was not in a previous replication (replications were taken of the specimens before testing to serve as initial comparisons), the test was considered to have detected an initiation point. If no such feature was discovered, the specimen was retested. When a specimen was retested, the computer program ignored any perceived load drop which occurred before the specimen reached its previous maximum load since these load drops were artifacts of the procedure and not indicative of delamination initiation.

One specimen of each laminate family with a normalized effective ply thickness of one (specimens 15A0-0-9, 15A1-0-21, and 15B1-0-18) was tested in a slightly different manner. The testing set up was identical, but instead of stopping the test at a drop in load, the specimen was incrementally loaded to specific loads needed to achieve stresses in increments of 50 MPa. After each stress level was achieved, the load was reduced by a factor of approximately two and two replications were made of each side. The specimen was unloaded but not removed from the testing machine between tests. These tests were repeated until final failure occurred. This allowed for an initial indication of the growth of delamination after initiation. More importantly, these tests serve as a check that delamination does not initiate prior to the stress levels de-

tected by the load drop technique. This is assured by these tests when the specimens are inspected at regular intervals and do not show any signs of delamination initiation on the replications taken at stresses lower than the delamination initiation stress determined from other specimens.

CHAPTER 5

RESULTS

5.1 Stress-Strain Behavior

The stress-strain behavior of all specimens in this investigation was linear until delamination initiation, at which point the test was terminated. The stress calculations were made using load data from the testing machine, measured width, and nominal thickness. The longitudinal moduli of individual specimens are listed in the data tables. A summary of the average longitudinal moduli for the various laminates is reported in Table 5.1. In all cases, the reported modulus is for the final test of a given specimen, that is for loading from no load to the load at which delamination initiates. The values for most laminates were within experimental scatter of the values predicted by Classical Laminated Plate Theory which are 107 GPa for the $[\pm 15_n]_s$ laminates and 116 GPa for the $[\pm 15_n/0_n]_s$ and $[0_n/\pm 15_n]_s$ laminates.

For the vast majority of specimens, the modulus did not vary by more than 5% from this final value from test to test. This is within the expected range of experimental scatter. Typical stress-strain plots for specimens of each family are depicted in Figures 5.1 through 5.3.

TABLE 5.1

AVERAGE LONGITUDINAL MODULUS OF EACH LAMINATE

Laminate	Average Longitudinal Modulus [GPa]
$[\pm 15]_s$	110 (2.3%)[a]
$[\pm 15_*]_s$	104 (2.8%)
$[\pm 15_2]_s$	102 (7.6%)
$[\pm 15_3]_s$	103 (6.4%)
$[\pm 15_4]_s$	105 (6.4%)
$[\pm 15_5]_s$	103 (7.1%)
$[\pm 15/0]_s$	117 (1.3%)
$[\pm 15_* 0_*]_s$	114 (4.3%)
$[\pm 15_2/0_2]_s$	112 (5.7%)
$[\pm 15_3/0_3]_s$	113 (8.0%)
$[\pm 15_4/0_4]_s$	108 (4.4%)
$[\pm 15_5/0_5]_s$	109 (5.8%)
$[0/\pm 15]_s$	115 (2.8%)
$[0_2/\pm 15_2]_s$	112 (6.5%)
$[0_3/\pm 15_3]_s$	112 (6.3%)
$[0_4/\pm 15_4]_s$	107 (8.7%)
$[0_5/\pm 15_5]_s$	104 (5.3%)

Note: Subscript "*" indicates a laminate made from 190g/m^2 prepreg

[a]Numbers in parentheses are coefficients of variation

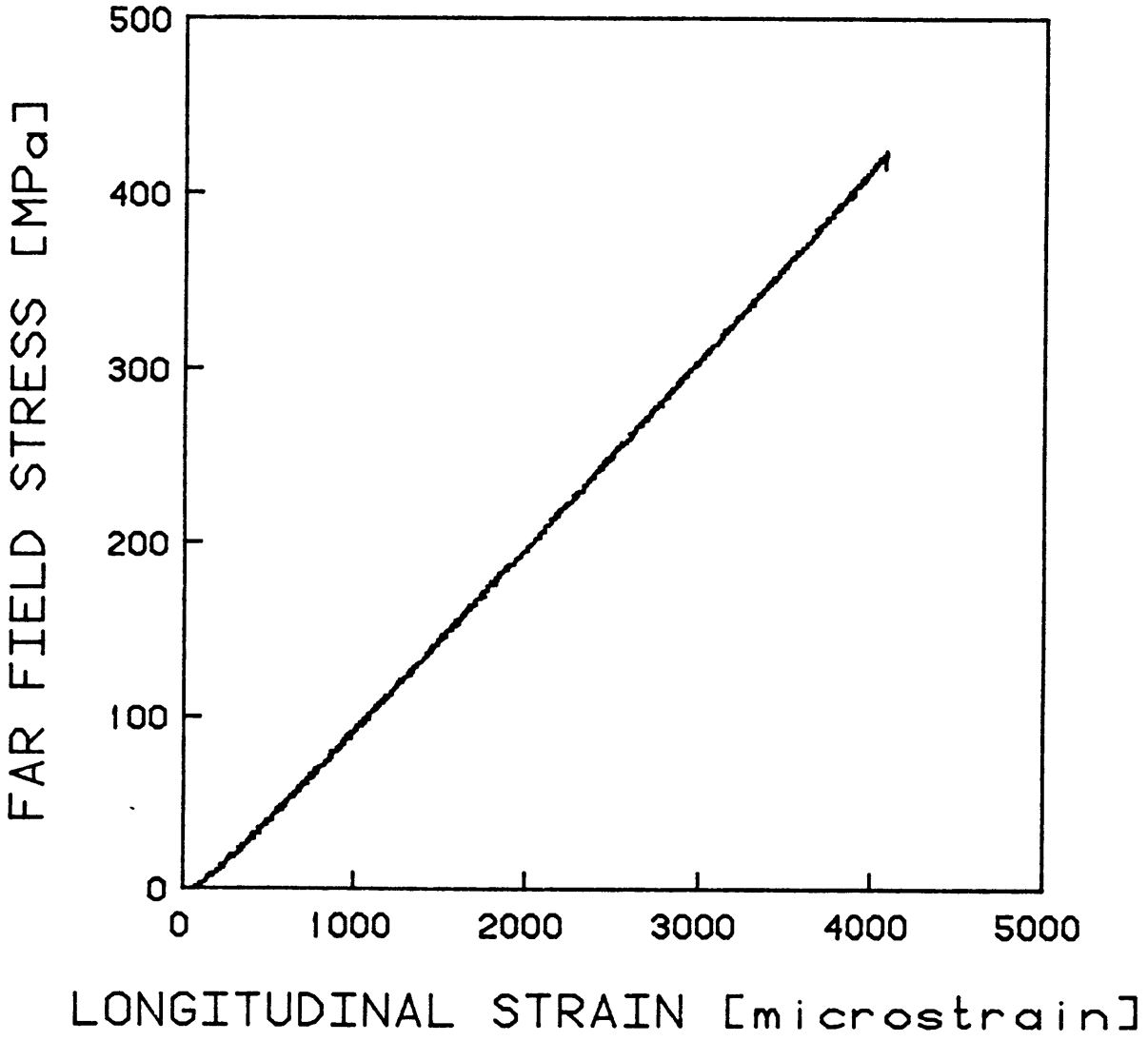

FIGURE 5.1 TYPICAL STRESS-STRAIN CURVE OF A $[\pm 15_n]_s$ SPECIMEN

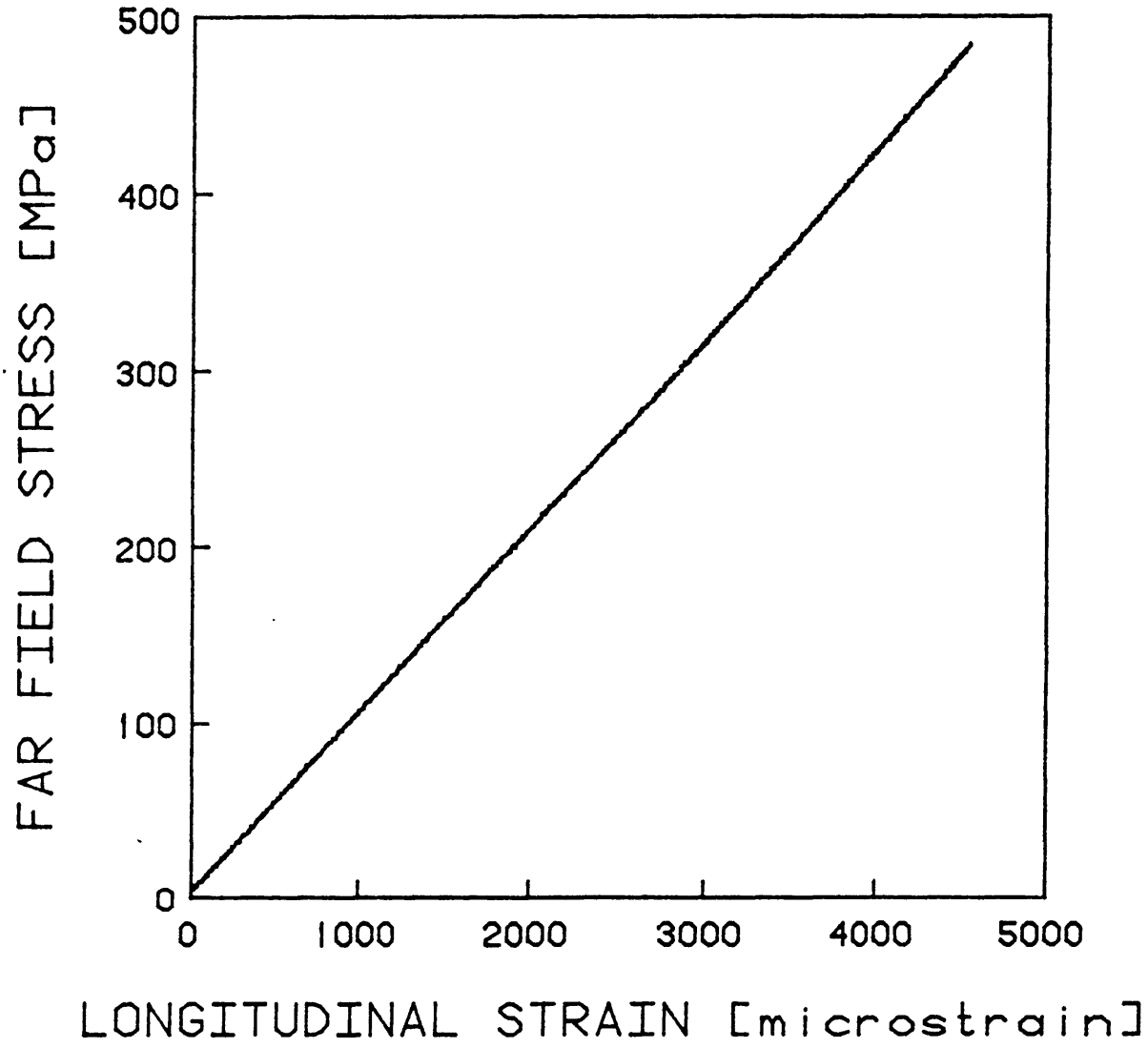

FIGURE 5.2 TYPICAL STRESS-STRAIN CURVE OF A $[\pm 15_n/0_n]_s$ SPECIMEN

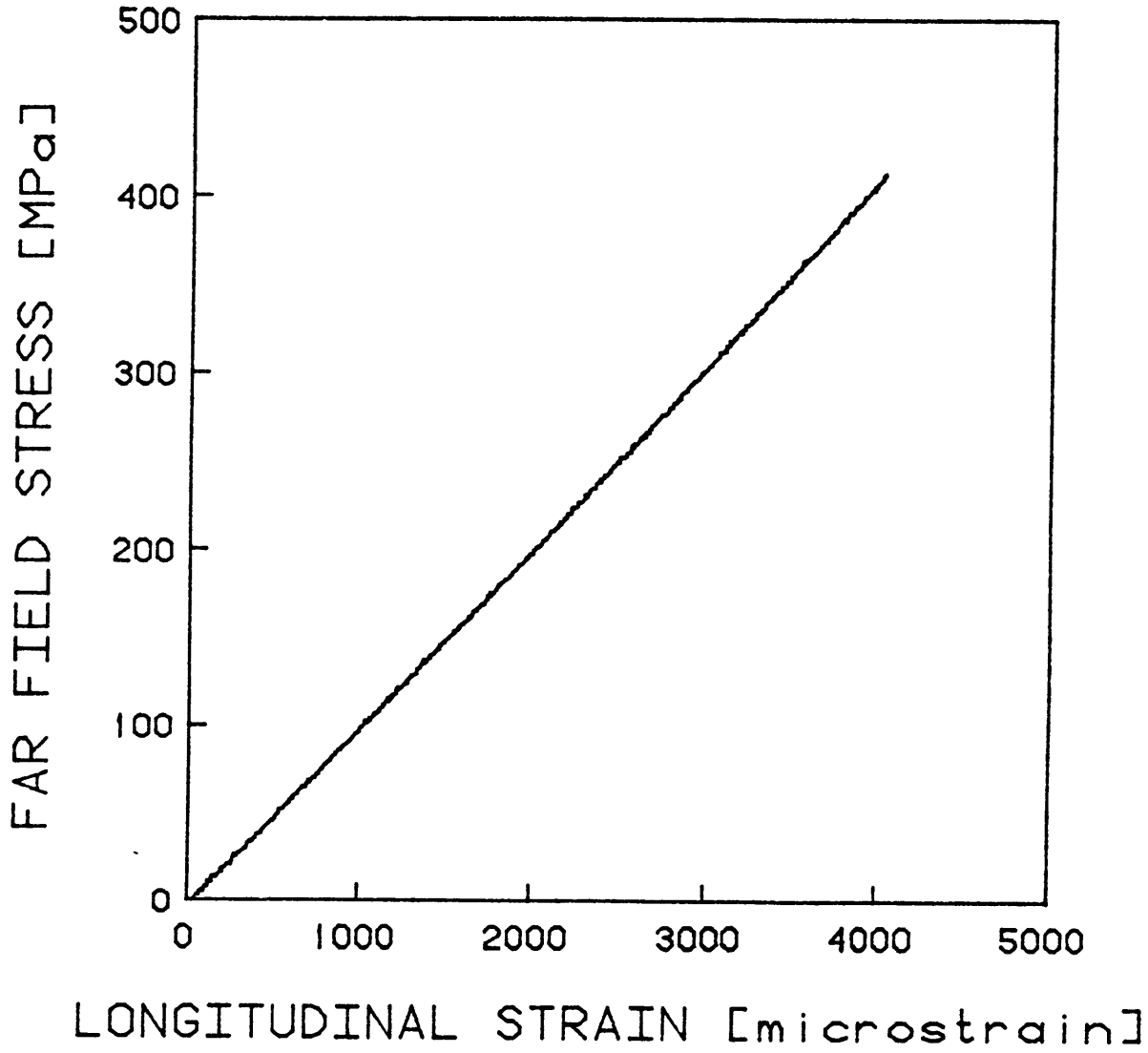

FIGURE 5.3 TYPICAL STRESS-STRAIN CURVE OF A $[0_n/\pm 15_n]_s$ SPECIMEN

5.2 Detection of Delamination Initiation

Delamination detection is a two step procedure as described in Chapter 4. Tests were stopped at load drops which could have been caused by initiation. Initiation was verified by comparing replications taken after the test (while the specimen was still partially loaded) with replications taken before any testing occurred.

It took some experience to determine exactly what a delamination looked like on a replication. The dark regions between plies were originally thought to indicate delamination. Upon examination of the replication taken before testing, however, it was evident that these were merely interlaminar resin layers. Small flaws could be seen on some of the original replications. These ranged from small interlaminar voids to transverse cracks which could have been introduced during specimen handling. Figure 5.4 contains photographs of some of these inherent features. In general, however, the polished free edge was clean, smooth, and free of flaws as depicted in Figure 5.5.

Delamination initiation appeared in several ways. In most cases, initiations were detected on edge replications as light white lines which followed the ply interfaces. This "hairline" initiation was the type of initiation that was expected. The

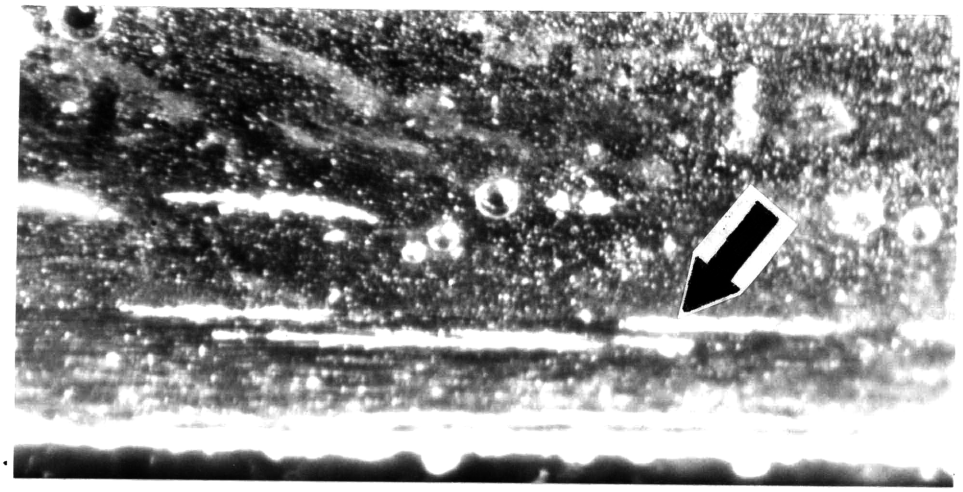

Inherent Microvoid

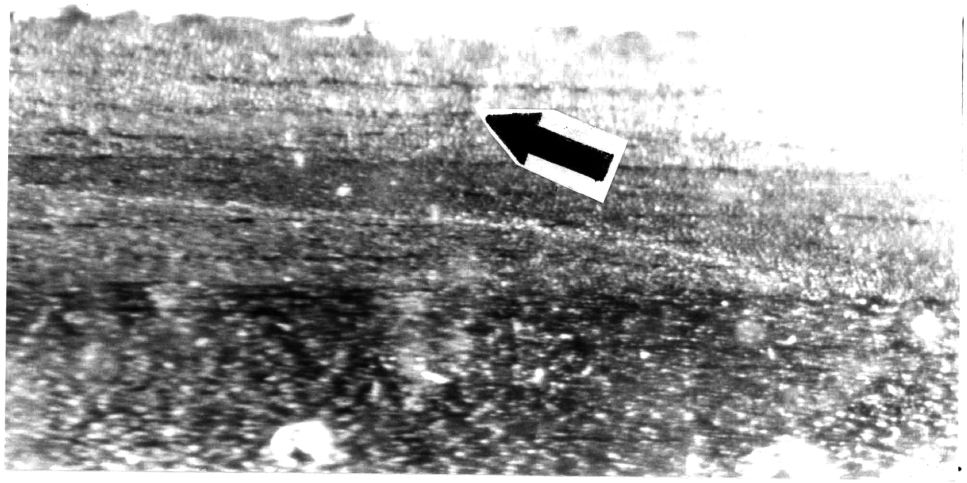

Inherent Transverse Crack (Top Center)

FIGURE 5.4 PHOTOGRAPHS OF REPLICATIONS SHOWING INHERENT DEFECTS ON THE FREE EDGE (14X)

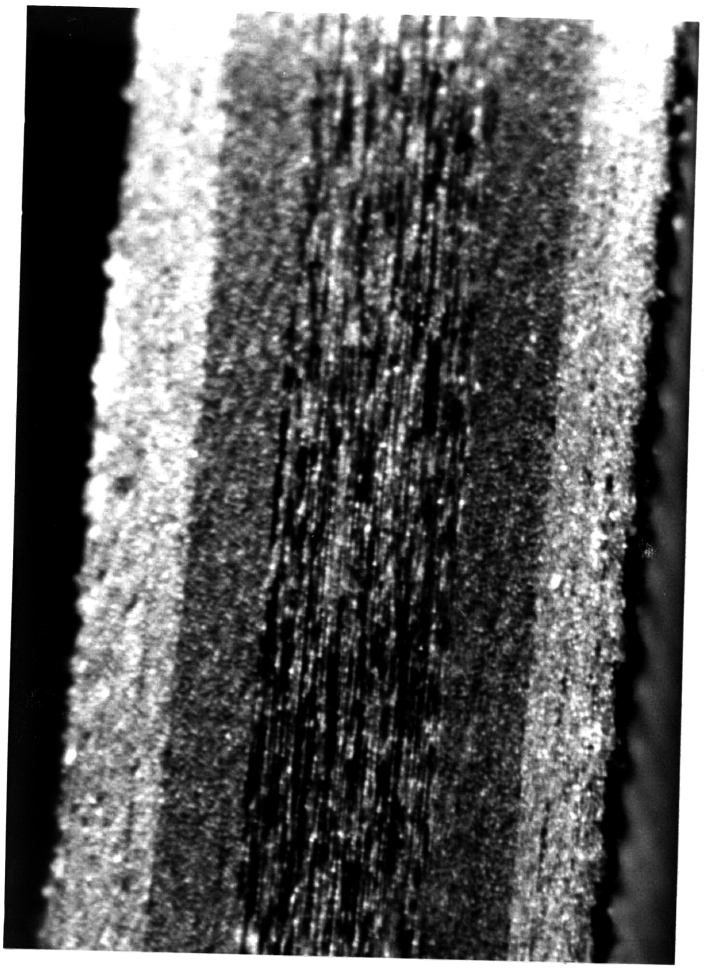

FIGURE 5.5 PHOTOGRAPH SHOWING A TYPICAL CLEAN SURFACE OF A FREE EDGE (40X)

white line on the replication was probably caused by the difference in surface texture between the initation and the surrounding material. A typical initiation can be seen in the photograph in Figure 5.6. Detection tended to be easier on replications with more contrast. The degree of contrast may be a function of the amount of polishing of the specimen edge. It is important to point out that in a majority of specimens, no transverse cracking was detected. In no case was a transverse crack detected in a region where no transverse crack had previously existed unless it was associated with a small delamination separation. The newly formed transverse cracks were only seen on the branch of the initiation in the immediate vicinity of the delamination separation and occurred at the termination of these initiation branches as can be seen in Figure 5.7.

Some specimens exhibited delamination initiations which appeared to initiate at previously existing flaws such as interlaminar microvoids or transverse cracks and microvoids. Examples of these initiations are visible in the photographs in Figure 5.8. The initiation stresses for such specimens is occasionally lower than that of similar specimens which were free of preexisting flaws.

In some cases, there was visible out-of-plane separation. This ranged from small edge delaminations measuring up to

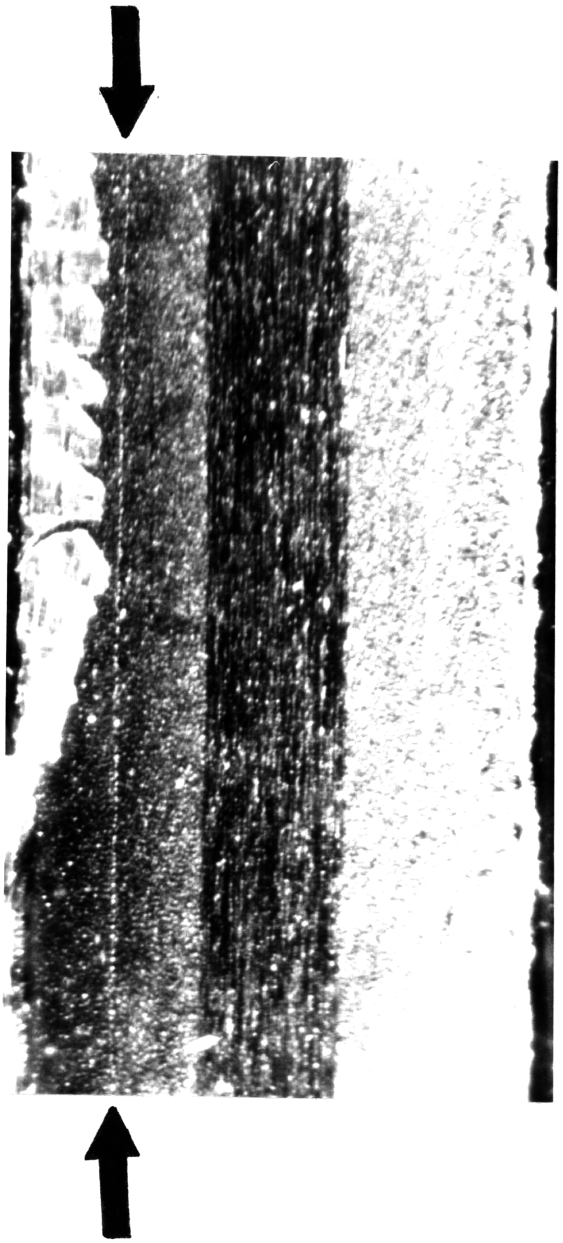

FIGURE 5.6 PHOTOGRAPH OF REPLICATION SHOWING A TYPICAL DELAMINATION INITIATION (40X)

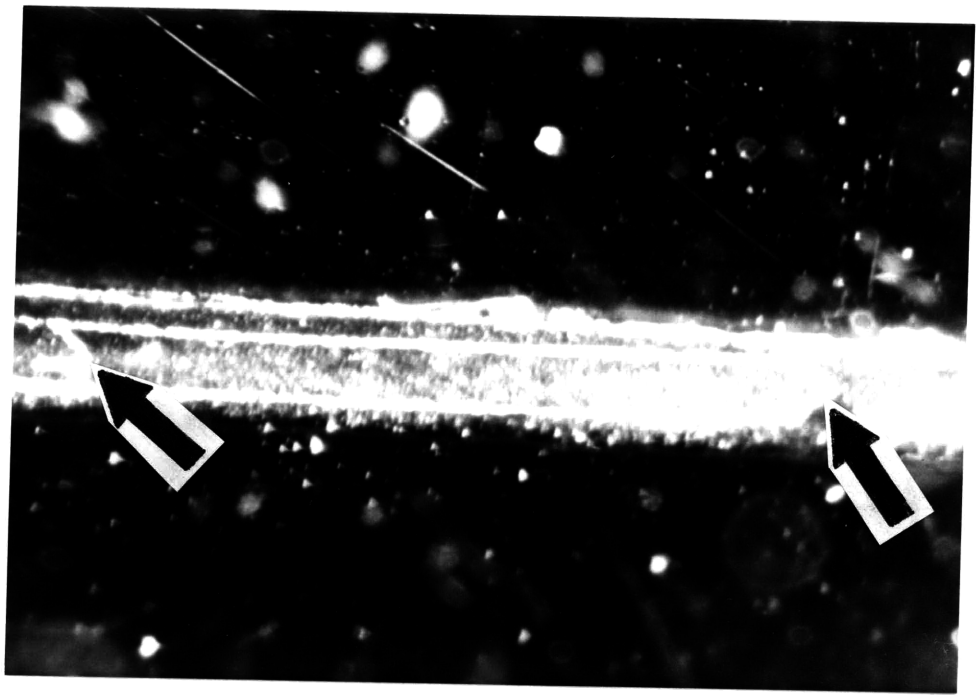

FIGURE 5.7 PHOTOGRAPH OF REPLICATION SHOWING TRANSVERSE CRACK DAMAGE NEAR A SMALL DELAMINATION (14X)

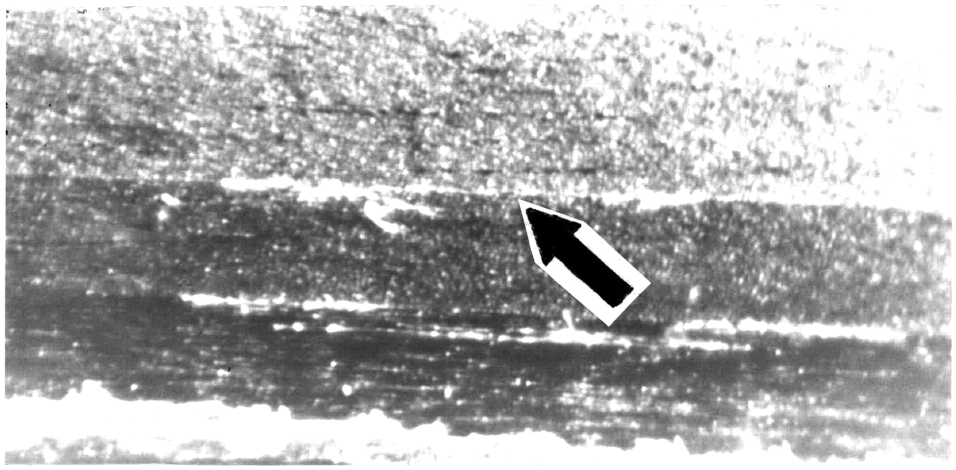

Delamination Initiation at a Microvoid

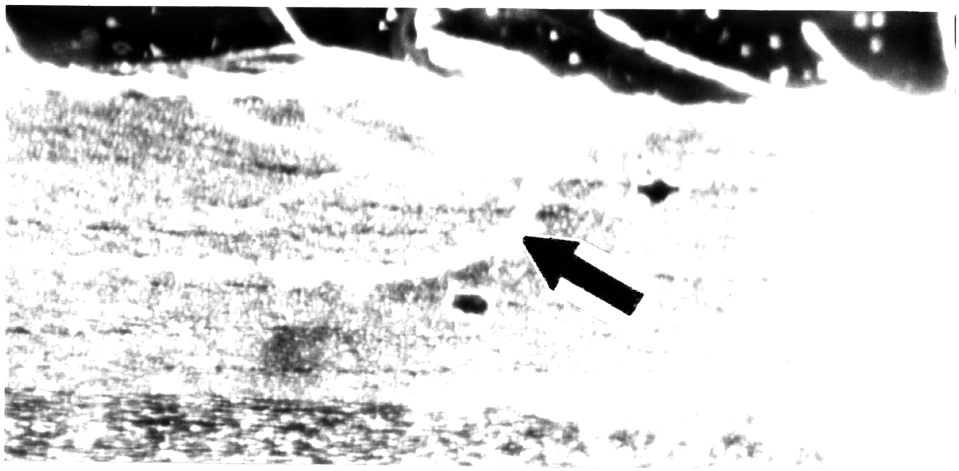

Delamination Initiation at an Inherent Transverse Crack

FIGURE 5.8 PHOTOGRAPHS OF REPLICATIONS SHOWING DELAMINATION INITIATIONS AT DEFECTS (14X)

20 mm in length to massive delamination failure. Figure 5.9 contains photographs of these types of delaminations. The small delaminations were usually symmetric with respect to the midplane. That is, if part of the front surface ply delaminated, a similar delamination was found on the corresponding part of the back surface.

It is difficult to determine the validity of the data generated by the specimens exhibiting large delaminations. Their delamination stresses tended to be greater than the initiation stresses of similar specimens. It is possible that the load drop due to initiation came at a load slightly less than the maximum load in the previous test. This could be due to experimental scatter. The testing program would ignore this load drop and loading could continue until final delamination failure could occur.

The four types of delamination initiations were classified as follows: Type A initiations were hairline initiations. Type B initiations were hairline initiations from a defect. Type C initiations were small delamination separations. Type D initiations were massive delamination failures. The type of initiation exhibited by each specimen is indicated in the data tables. Table 5.2 shows the number of each specimen type that exhibited each type of initiation. The

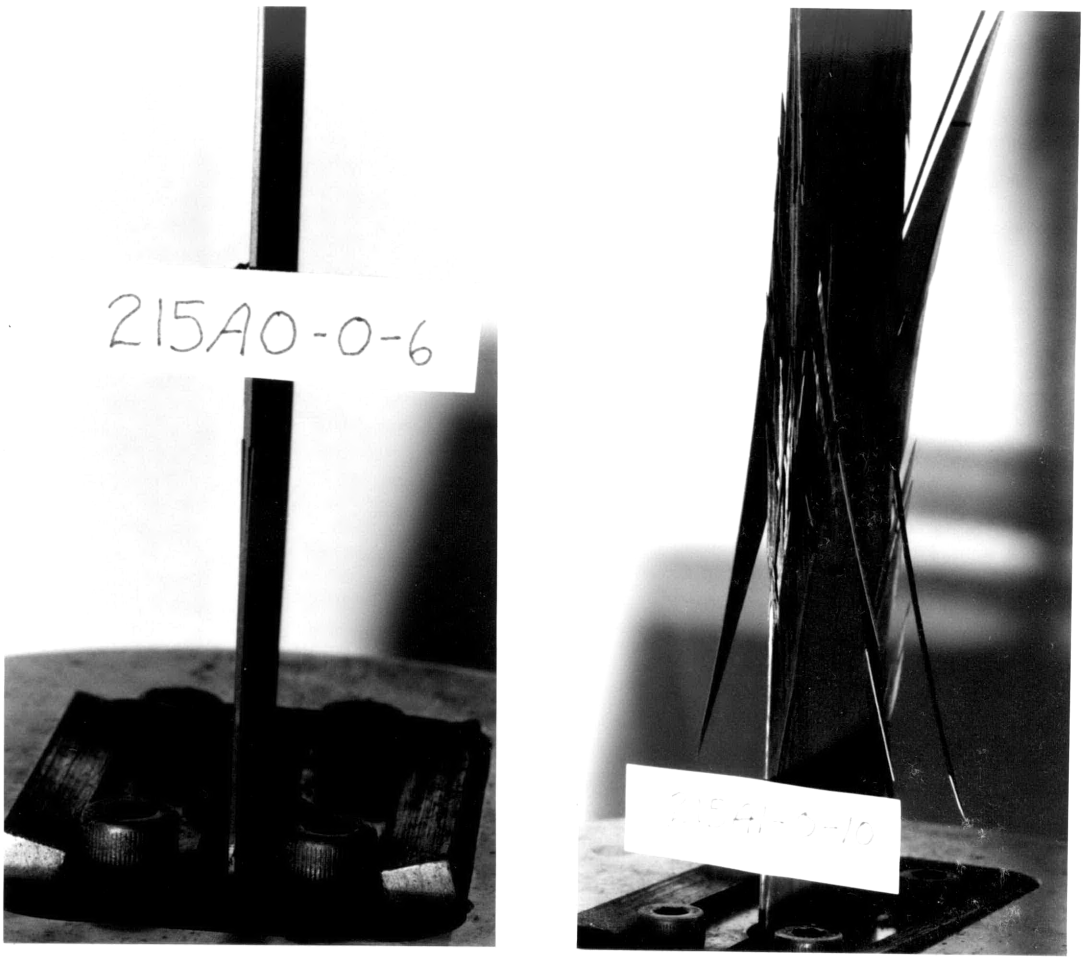

FIGURE 5.9 PHOTOGRAPHS OF SMALL AND LARGE DELAMINATIONS

TABLE 5.2

DISTRIBUTION OF DELAMINATION TYPES FOR EACH LAMINATE

Laminate	Delamination Type Detected[a]			
	A	B	C	D
$[\pm 15]_s$	1[b]	0	2	1
$[\pm 15_*]_s$	1	1	0	2
$[\pm 15_2]_s$	0	1	4	0
$[\pm 15_3]_s$	2	1	0	2
$[\pm 15_4]_s$	3	2	0	0
$[\pm 15_5]_s$	2	1	0	2
$[\pm 15/0]_s$	4	0	0	0
$[\pm 15_*/0_*]_s$	5	0	0	0
$[\pm 15_2/0_2]_s$	4	1	0	0
$[\pm 15_3/0_3]_s$	2	2	0	1
$[\pm 15_4/0_4]_s$	4	1	0	0
$[\pm 15_5/0_5]_s$	3	1	0	1
$[0/\pm 15]_s$	4	0	0	0
$[0_2/\pm 15_2]_s$	3	1	0	1
$[0_3/\pm 15_3]_s$	4	1	0	0
$[0_4/\pm 15_4]_s$	3	2	0	0
$[0_5/\pm 15_5]_s$	5	0	0	0

Note: Subscript "*" indicates a laminate made from 190g/m^2 prepreg

[a]Key: Type A - Hairline initiation
Type B - Hairline initiation from a defect
Type C - Small delamination
Type D - Massive delamination

[b]Values indicate the number of specimens exhibiting each delamination type

numbers include the incrementally loaded specimens which all exhibited hairline (Type A) initiation.

The specific character of the Type A and Type B hairline initiations was quite variable. They always occurred at +15°/-15° interfaces. In a majority cases, the damage was restricted to one free edge of the specimen. The Type B initiations were generally single initiations only a few millimeters long and were usually restricted to one +15°/-15° interface. Type A initiations ranged in size from sporadic initiations several millimeters long scattered along the free edge to initiations which ran along the entire length of the free edge. There did not seem to be any distinct trend as to whether the initiations were symmetric with respect to the midplane (i.e. whether they occurred at both +15°/-15° interfaces in a laminate or at just one). The number of occurrences of each type was approximately equal.

Two specimens, *15A0-0-5 and *15B1-0-1, were not included in the data. Due to unexpected features of the testing machine while in computer control, they were inadvertently destroyed before they yielded initiation data.

5.3 Initiation Stresses and Strains

The initiation stresses were taken to be the computed stress at the point where the final load drop occurred in the test of a specimen which showed delamination initiation in its replication. The initiation strains were taken to be the strain in the computer data file which corresponded to the initiation stress. These stresses and strains are listed for each specimen in the data tables.

It can be noted that the specimens which exhibited initiations from initial defects often had initiation stresses which were lower than those of similar specimens and specimens which exhibited massive delamination failure often exhibited "initiation stresses" which were considerably higher than those of similar specimens. It is difficult to say which of these specimens yielded valid data. For example, initiation at a defect may have occurred only instantaneously before initiation would have occurred normally or it may be the result of a stress concentration near the defect which caused it to be considerably premature. Massive delamination may be the result of substantial growth due to having missed the real initiation point or merely a result of a large "pop-in" delamination area. Due to these ambiguities, it was decided to omit from the calculated averages the initiation stresses and

strains obtained from specimens which exhibited initiation at a defect and had an initiation stress lower than any other valid data of similar specimens and specimens which exhibited massive delamination and had "initiation stresses" greater than any similar specimen. Table 5.3 lists all specimens which were omitted. Table 5.4 shows the effect on the average initiation stress and coefficient of variation for the laminates which were affected. Table 5.5 shows average valid initiation stress and strain for all laminates.

5.4 Delamination Area

The delaminated area for each specimen which exhibited a Type A or a valid Type B initiation was computed from the measured loading rate (per time increment) and measured fractional load drop using Equation 4.3. The computed area for each specimen, as well as the magnitude that would be introduced by conditioner noise equivalent to one computer unit, is included in Appendix B. The values for detected delamination area ranged from just under 50 mm^2 to nearly 600 mm^2. The average detected area was 150 mm^2. For virtually all specimens, the delaminated area was more than two to three times the area that would be caused by system noise of one computer unit.

TABLE 5.3

SPECIMENS OMITTED FROM THE DATA BASE

*15A0-0-2
*15A0-0-3
215A0-0-10
315A0-0-8
515A0-0-6
515A0-0-7
515A0-0-9
215A1-0-9
315A1-0-7
315A1-0-10
515A1-0-8
515A1-0-10
215B1-0-7
215B1-0-8
415B1-0-6
415B1-0-19

TABLE 5.4

AVERAGE DELAMINATION INITIATION STRESSES OF LAMINATES WITH AND WITHOUT OMITTED DATA

Laminate	Average Delamination Initiation Stress With Omitted Data [MPa]		Average Delamination Initiation Stress With Omitted Data [MPa]	
$[\pm 15_*]_s$	691	(11.6%)[a]	696	(0.5%)
$[\pm 15_2]_s$	571	(19.2%)	618	(5.4%)
$[\pm 15_3]_s$	541	(19.1%)	508	(16.4%)
$[\pm 15_5]_s$	358	(54.4%)	402	(19.2%)
$[\pm 15_2/0_2]_s$	527	(41.6%)	625	(5.0%)
$[\pm 15_3/0_3]_s$	553	(19.8%)	539	(5.2%)
$[\pm 15_5/0_5]_s$	473	(12.7%)	452	(1.1%)
$[0_2/\pm 15_2]_s$	669	(21.5%)	645	(8.4%)
$[0_4/\pm 15_4]_s$	511	(18.6%)	566	(9.8%)

Note: Subscript "*" indicates a laminate made from 190g/m^2 prepreg

[a]Numbers in parentheses are coefficients of variation

TABLE 5.5

AVERAGE DELAMINATION INITIATION STRESS AND STRAIN FOR EACH LAMINATE

Laminate	Average Delamination Initiation Stress [MPa]	Average Delamination Initation Stress [MPa]
$[\pm 15]_s$	859 (8.7%)[a]	7517 (7.9%)
$[\pm 15_*]_s$	696 (0.5%)	6327 (0.1%)
$[\pm 15_2]_s$	618 (5.4%)	5802 (4.7%)
$[\pm 15_3]_s$	508 (16.4%)	4991 (14.5%)
$[\pm 15_4]_s$	383 (27.1%)	3618 (19.6%)
$[\pm 15_5]_s$	402 (19.2%)	3903 (5.8%)
$[\pm 15/0]_s$	734 (12.3%)	6089 (13.3%)
$[\pm 15_*/0_*]_s$	641 (14.2%)	5395 (9.5%)
$[\pm 15_2/0_2]_s$	624 (5.0%)	5334 (6.7%)
$[\pm 15_3/0_3]_s$	539 (5.2%)	4542 (11.5%)
$[\pm 15_4/0_4]_s$	481 (2.7%)	4240 (5.0%)
$[\pm 15_5/0_5]_s$	452 (1.1%)	4070 (2.3%)
$[0/\pm 15]_s$	757 (2.6%)	6246 (5.6%)
$[0_2/\pm 15_2]_s$	645 (8.4%)	5690 (7.9%)
$[0_3/\pm 15_3]_s$	484 (12.0%)	4271 (10.8%)
$[0_4/\pm 15_4]_s$	566 (9.8%)	4898 (8.3%)
$[0_5/\pm 15_5]_s$	539 (13.7%)	4909 (9.1%)

Note: Subscript "*" indicates a laminate made from 190g/m^2 prepreg

[a]Numbers in parentheses indicate coefficient of variation

This indicates that the load drops were most likely those that are associated with initiation.

The fact that it was possible to detect delaminated areas smaller than the minimum detectable area as reported in Table 4.5 is a result of the fact that the delamination initiation load was much higher than the conservative estimate of one half of the previously determined failure load. As a given delamination area causes a given fractional load drop, the minimum detectable area is inversely proportional to the delamination initiation load.

The delaminations which occurred were usually confined to one free edge of the specimen. The delamination initiation occasionally ran along the entire free edge but often there were one or more small delaminations. The total delamination length was usually 50 mm or more. The average computed delamination area was 150 mm^2. This implies that the initiations penetrated on the order of one to three millimeters toward the center of the test section.

5.5 Incrementally Loaded Specimens

The results of the incremental loading tests were consistent with the results of the other tests. All incrementally loaded specimens exhibited Type A hairline initiations. Ta-

ble 5.6 compares the initiation stress range of the incremental specimens with the average initiation stress and range of the specimens tested in a normal manner. It is important to remember that for the specimens which were incrementally loaded, the stress at which delamination initiates can only be narrowed to a 50 MPa range since the specimens were replicated at 50 MPa intervals. The initiation stress ranges found for these specimens were comparable to the initiation stress values found using using the load drop method. Figures 5.10 through 5.12 show the progression of damage for each specimen from before initiation to the replication taken just prior to final failure for the region where delamination initiation first occurred.

5.6 Calculation of Theoretical Parameters

5.6.1 Quadratic Delamination Criterion

The Quadratic Delamination Criterion contains three important parameters: the averaging dimension x_{avg}, the interlaminar shear strength Z^s, and the interlaminar normal strength Z^t. The interlaminar strengths are values for a material which in principle can be determined directly from tests. In practice, however, it is difficult to apply pure

TABLE 5.6

DELAMINATION INITIATION STRESS RANGE
OF INCREMENTALLY LOADED SPECIMENS
VERSUS AVERAGE DELAMINATION INITIATION STRESS

Laminate	Delamination Initiation Stress Range Of Incrementally Loaded Specimen [MPa]	Average Delamination Initiation Stress Of Remaining Four Specimens [MPa]
$[\pm 15]_s$	701 - 754	859 (8.7%)[a]
$[\pm 15/0]_s$	700 - 752	734 (12.3%)
$[0/\pm 15]_s$	801 - 852	757 (2.6%)

[a]Numbers in parentheses are coefficients of variation

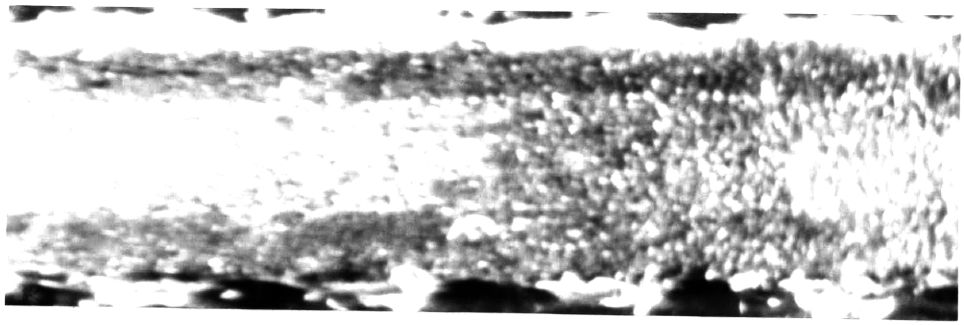

701 MPa

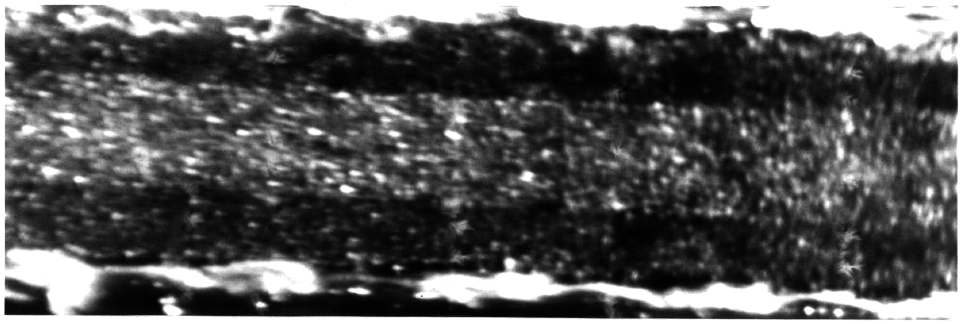

754 MPa

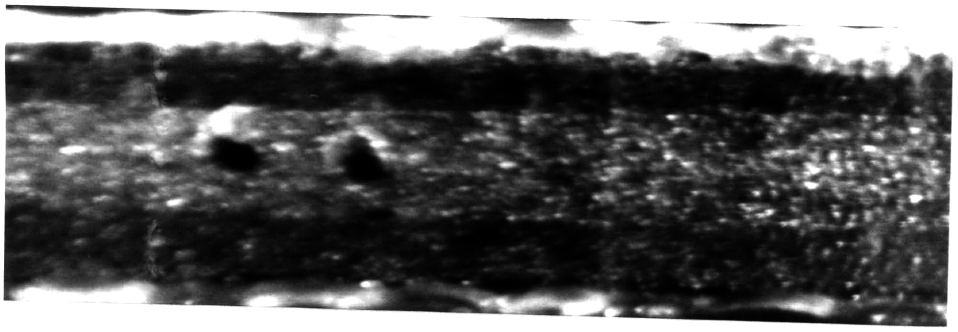

802 MPa

FIGURE 5.10 PHOTOGRAPHS OF REPLICATIONS SHOWING DAMAGE PROGRESSION OF THE INCREMENTALLY LOADED $[\pm 15]_s$ SPECIMEN (30X)

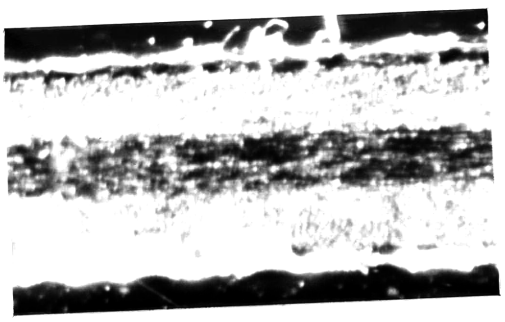

700 MPa

752 MPa

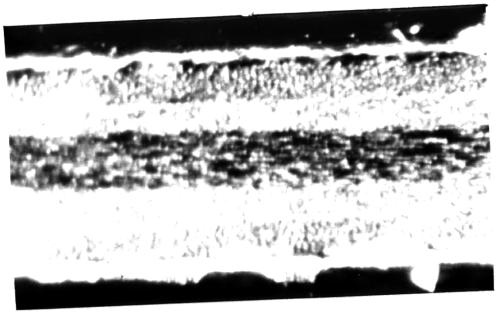

801 MPa

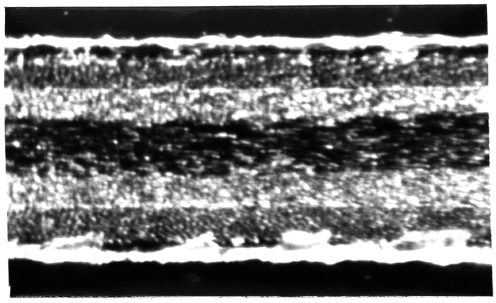

901 MPa

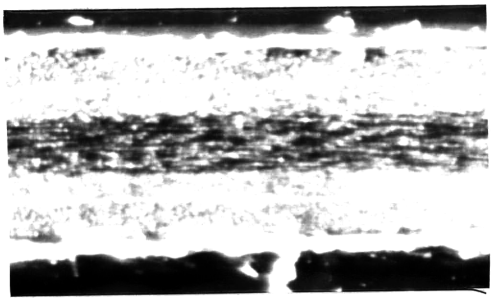

952 MPa

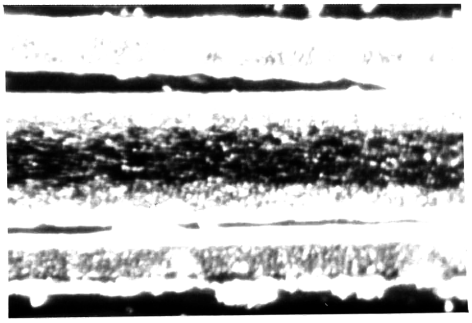

1002 MPa

FIGURE 5.11 PHOTOGRAPHS OF REPLICATIONS SHOWING DAMAGE PROGRESSION OF THE INCREMENTALLY LOADED $[\pm 15/0]_S$ SPECIMEN (14X)

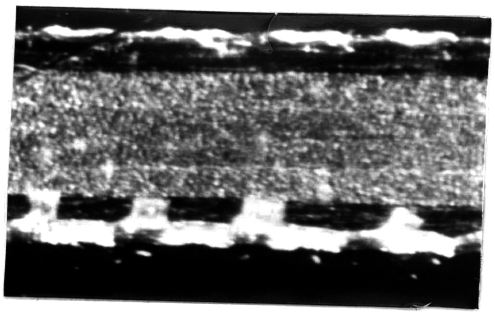

801 MPa

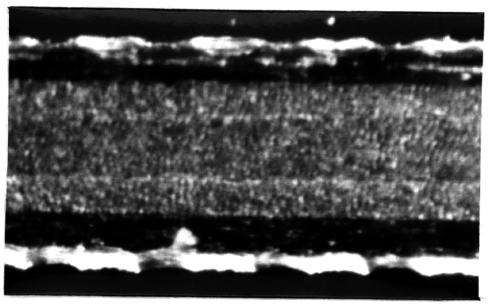

852 MPa

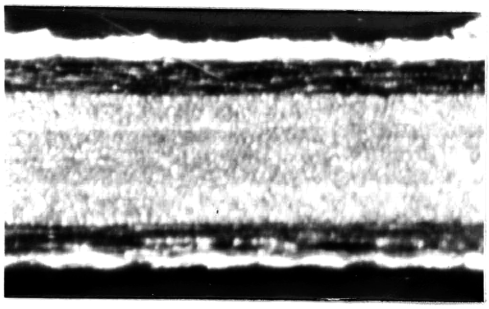

901 MPa

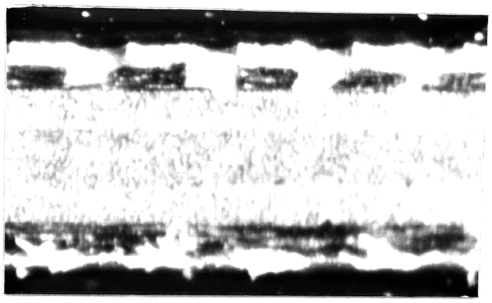

1001 MPa

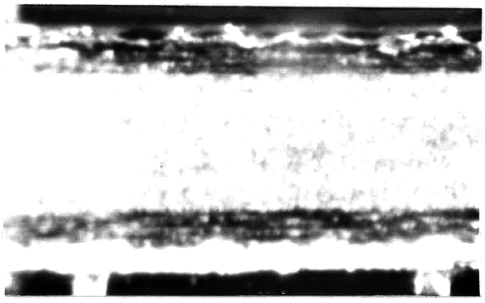

1103 MPa

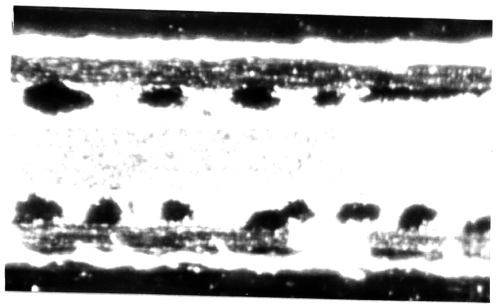

1201 MPa

FIGURE 5.12 PHOTOGRAPHS OF REPLICATIONS SHOWING DAMAGE PROGRESSION OF THE INCREMENTALLY LOADED $[0/\pm15]_s$ SPECIMEN (14X)

σ_{1z} or σ_{zz} to a laminate and no measured values for these parameters have been reported. However, approximations have been made for these parameters. Kim and Soni [19,20] suggested Z^s could be approximated by the in-plane shear strength of the composite and Z^t could be approximated by the transverse tensile strength of the composite. The accuracy of these approximations is difficult to ascertain, however. Thus, until Z^s and Z^t can be conclusively determined, they can be treated as variables in the analysis.

If values of the interlaminar strengths are known or assumed, values of the averaging dimension can be determined numerically from the initiation stress data and the Quadratic Delamination Criterion. These values, however, can be misleading due to the asymptotic nature of the criterion. At low values of effective ply thickness, the predicted values of initiation stress are quite sensitive to the averaging dimension. Thus, "backfiguring" an averaging dimension (i.e. numerically determining what averaging dimension will yield a predicted initiation stress which equals the actual initiation stress) can be relatively accurate for data collected at these low values of effective ply thickness.

In contrast, the predicted initiation stress is rather insensitive to averaging dimension when the effective ply thickness is relatively large. Thus, there can be a signif-

icant change in the backfigured averaging dimension when normal experimental scatter occurs. Figure 5.13 illustrates this problem: if the average value for initiation stress falls slightly above the asymptote, the backfigured value of effective ply thickness divided by the averaging dimension can be very much lower than its realistic value (thereby yielding a value of x_{avg} which is too high). Similarly, if the initiation stress falls slightly below the asymptote, the Quadratic Delamination Criterion can not predict initiation no matter what value of averaging dimension is used and no real value of x_{avg} can be obtained.

It is therefore necessary to use another method for determining the best fit values of the Quadratic Delamination Criterion parameters. It was decided to compare various sets of assumed values of the parameters on the basis of the actual initiation stresses normalized by the predicted initiation stresses. A set of parameters (that is the averaging dimension and interlaminar strength parameters) is deemed acceptable if the average normalized initiation stress for the data being considered is equal to one. A set of parameters is deemed the best fit if its values of normalized initiation stress have the lowest coefficient of variation.

Calculations were made both with and without the effects of thermal stresses included. This was done to ascertain the

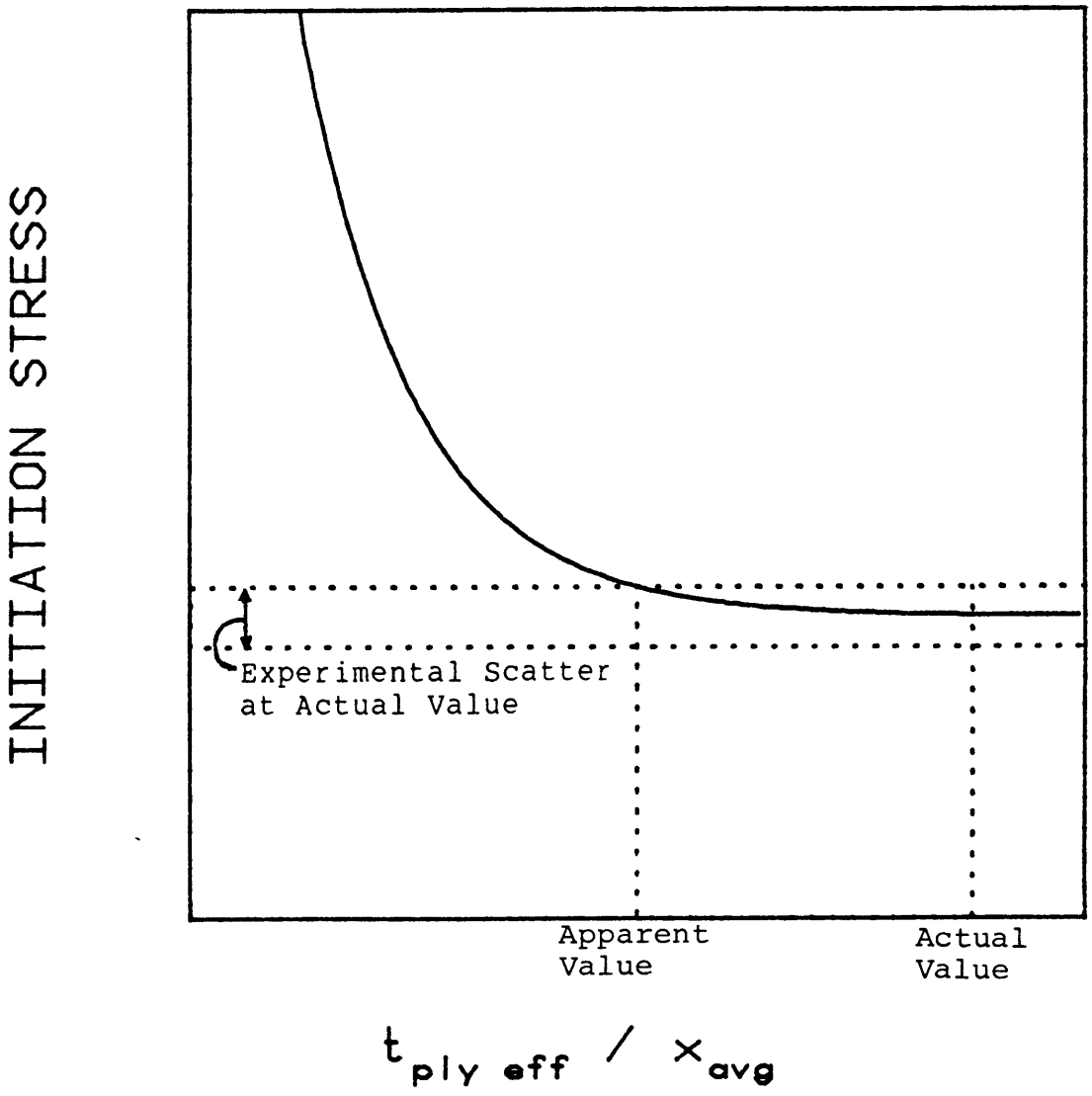

FIGURE 5.13 PROBLEMS ASSOCIATED WITH "BACKFIGURING" AN AVERAGING DIMENSION

significance of thermal stresses on the computed parameters. The thermal difference used in this calculation is the difference between the set temperature of the epoxy, 177°C, and room temperature (20°C). If it is assumed that these fabrication stresses provide a limiting value for the thermal interlaminar stress state, then the two cases analyzed act as reasonable bounds to the actual problem.

Since only two coordinates of data were available (ply thickness and initiation stress), it was only possible to determine two parameters from one set of data. This was adequate for data from the $[\pm 15_n]_s$ and $[0_n/\pm 15_n]_s$ laminate families as the value of $[\overline{\sigma}_{zz}]$ was zero. These cases thus reduced to the simple shear criterion which required only the determination of the averaging dimension and the interlaminar shear strength.

For the data from the $[\pm 15_n/0_n]_s$ laminate family, it was impossible to determine all three parameters from the available data. It was necessary to assume one of the parameters to evaluate assumed values of the other two. One solution would be to assume a value of interlaminar shear strength or averaging dimension such as the value suggested by Kim and Soni [20]. A best fit value of the interlaminar normal strength could then be estimated and used in the calculation

of the best fit values for interlaminar shear strength and averaging dimension.

There is a problem with this approach for the laminate families selected. The average value of σ_{zz} and thus the square of the quantity $\overline{\sigma}_{zz}$ divided by interlaminar normal strength is quite small for the $[\pm 15_n/0_n]_s$ laminate family. As the interlaminar shear stress state is very similar for the $[\pm 15_n/0_n]_s$ and $[0_n/\pm 15_n]s$ laminate families, the difference between the experimental values must be attributed wholely to the normal stress contribution. Since the average value of σ_{zz} is small, the value of interlaminar normal strength must be small in order to make the square of the quantity $\overline{\sigma}_{zz}$ divided by interlaminar normal strength significant. The value of interlaminar normal strength is therefore unreasonably sensitive to experimental scatter and assumed values of averaging dimension and interlaminar shear strength.

Values of interlaminar normal strength were computed for an assumed value of interlaminar shear strength equal to 105 MPa (the shear strength of the composite, as suggested by Kim and Soni [20]). For the case in which thermal stresses are included, the value of interlaminar normal strength is 3.9 MPa. This value is so small that the Quadratic Delamination Criterion predicts initiation at the midplane of the $[\pm 15_n/0_n]_s$ laminates before the +15°/-15° interface. It also

predicts initiation at stress levels much lower than are actually seen. All $[\pm 15_n/0_n]_s$ specimens exhibited initiation at the +15°/-15° interface. When thermal stresses were not included, no value of interlaminar normal strength could be determined. In this case, the coefficient of variation approached an asymptote as interlaminar normal strength increased, implying that the best fit occurs when the interlaminar normal strength is infinite.

It is clear that assuming a value of interlaminar shear strength would not give acceptable results for the $[\pm 15_n/0_n]_s$ laminate family. Thus, it was decided to instead assume that the value of interlaminar normal strength be equal to the transverse strength of the composite (53.9 MPa), as suggested by Kim and Soni [19]. The parameters which best fit the data were then determined.

Best fit values of interlaminar shear strength and averaging dimension were determined for each individual laminate family as well as for the entire data base. All these calculations were made both including and excluding the thermal effects on the interlaminar stress state. These determined values, as well as the coefficients of variation of the normalized initiation stresses, are reported for each case in Table 5.7 and the results plotted in Figures 5.14 through 5.19. In Figures 5.14 through 5.16, the theoretical curves of delam-

TABLE 5.7

BEST FIT PARAMETERS FOR THE QUADRATIC DELAMINATION CRITERION

Laminate Family	Thermal Effects Included			Thermal Effects Excluded		
	Averaging Dimension X_{avg} [mm]	Inter-laminar Shear Strength Z^S [MPa]	Coefficient Of Variation Of Normalized Delamination Initiation Stresses	Averaging Dimension X_{avg} [mm]	Inter-laminar Shear Strength Z^S [MPa]	Coefficient Of Variation Of Normalized Delamination Initiation Stresses
$[\pm 15_n]_s$	0.374	64	8.36%	0.279	88	7.92%
$[\pm 15_n/0_n]_s$	0.192	81	5.91%	0.144	108	5.64%
$[0_n/\pm 15_n]_s$	0.155	93	8.05%	0.116	121	8.05%
All Specimens	0.242	78	9.90%	0.178	105	9.70%

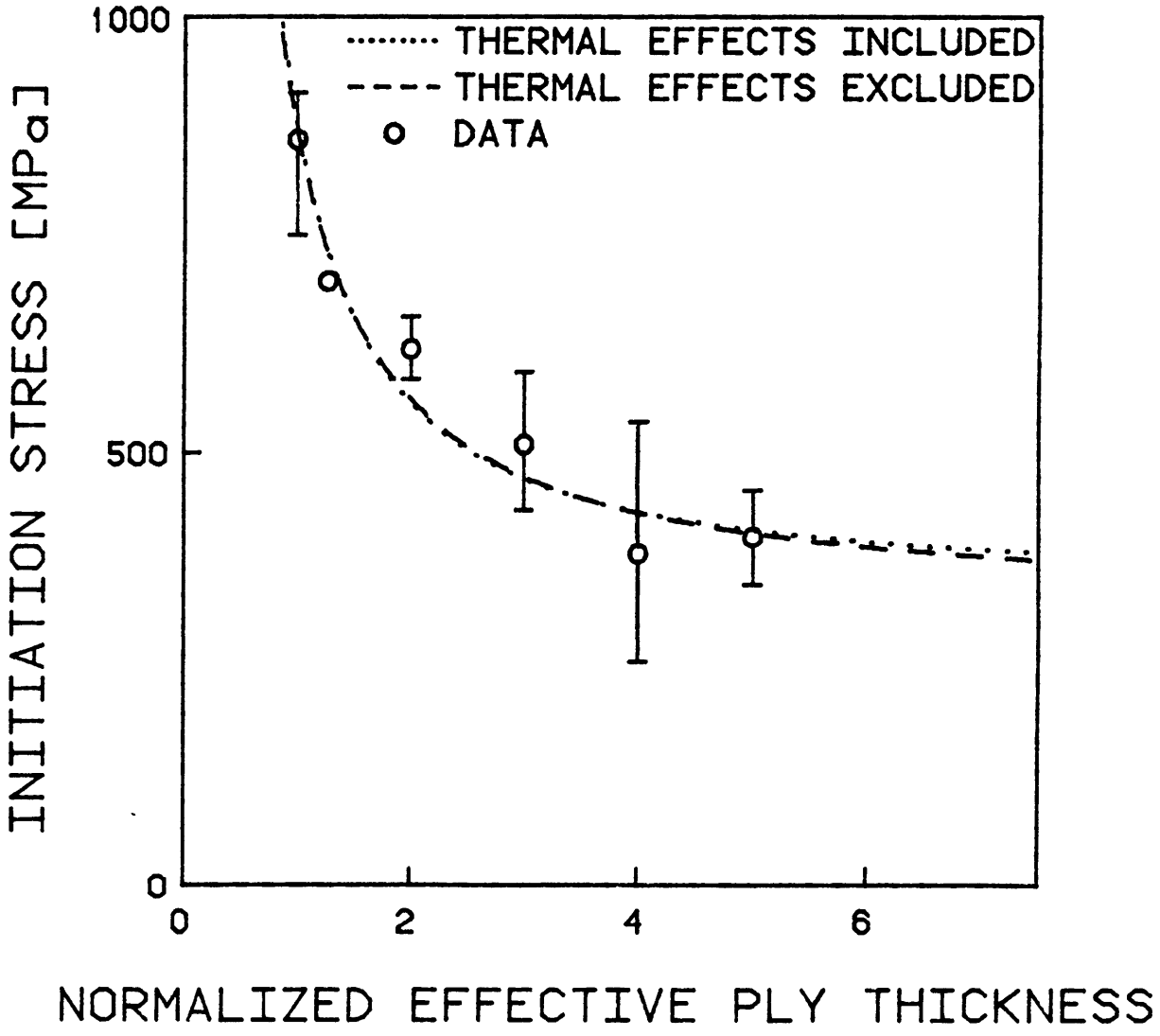

FIGURE 5.14 PREDICTED DELAMINATION INITIATION STRESS USING THE QUADRATIC DELAMINATION CRITERION (PARAMETERS DETERMINED USING DATA FROM THIS LAMINATE FAMILY) VERSUS DATA FOR THE $[\pm 15_n]_s$ SPECIMENS

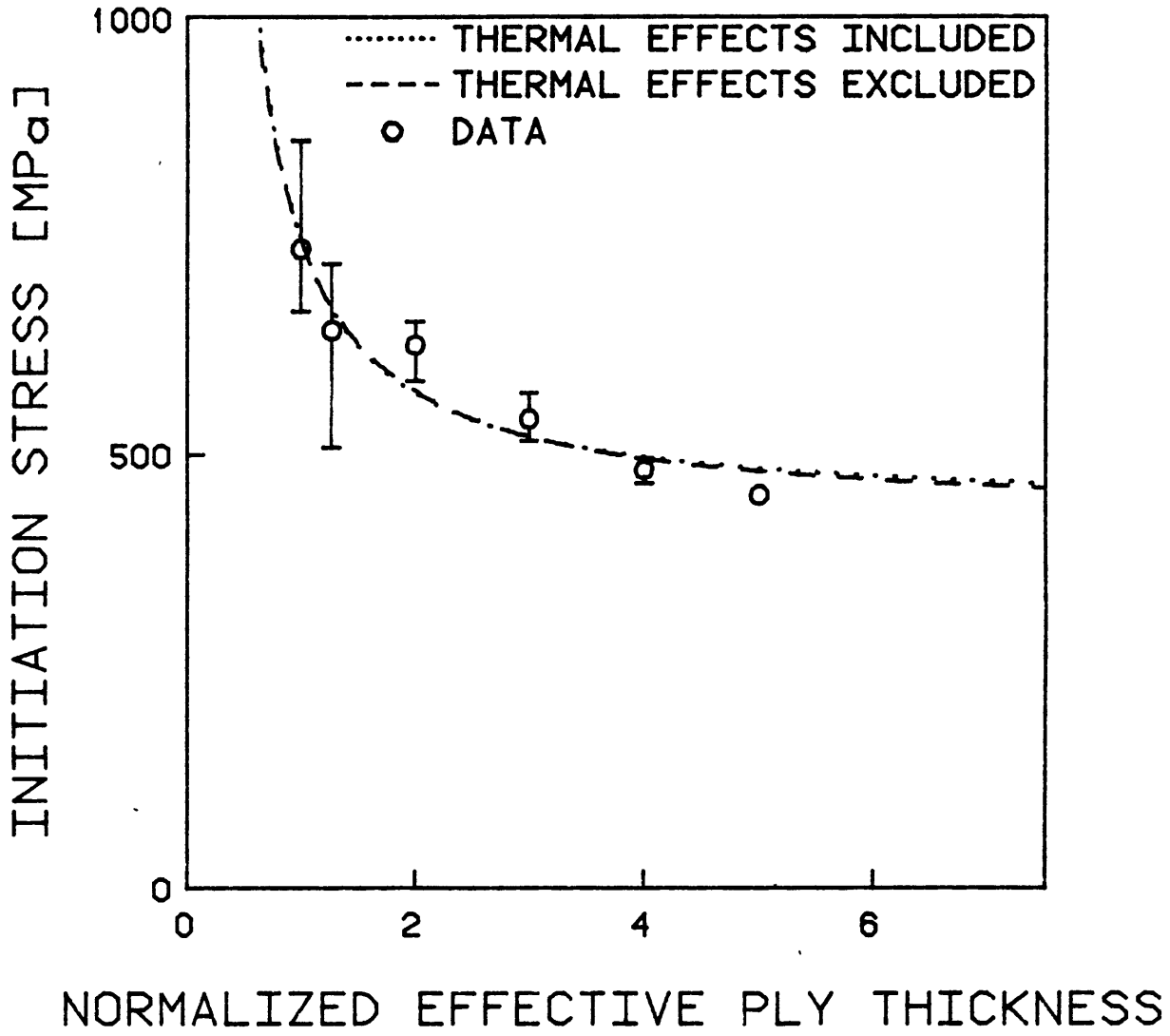

FIGURE 5.15 PREDICTED DELAMINATION INITIATION STRESS USING THE QUADRATIC DELAMINATION CRITERION (PARAMETERS DETERMINED USING DATA FROM THIS LAMINATE FAMILY) VERSUS DATA FOR THE $[\pm 15_n/0_n]_s$ SPECIMENS

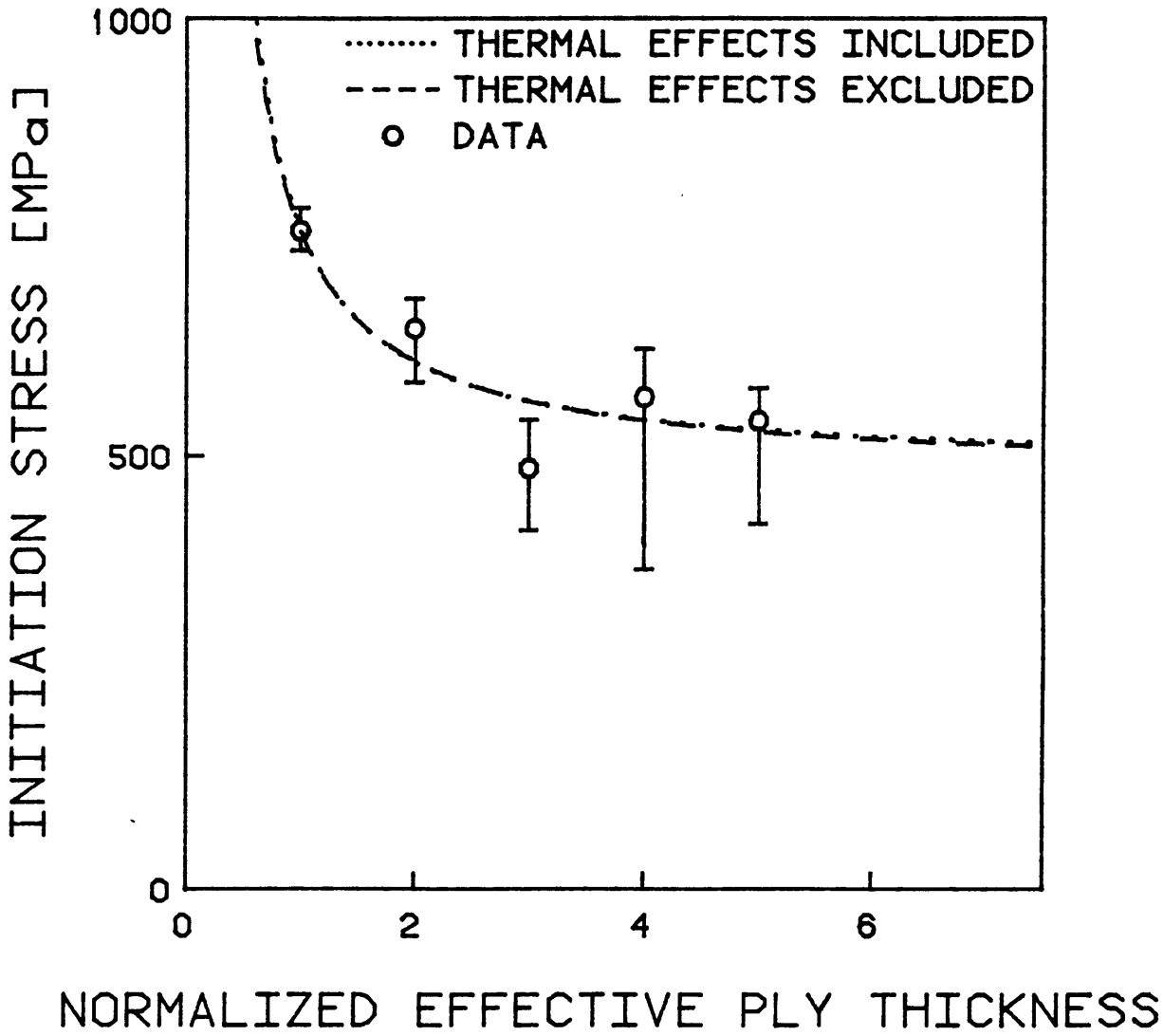

FIGURE 5.16 PREDICTED DELAMINATION INITIATION STRESS USING THE QUADRATIC DELAMINATION CRITERION (PARAMETERS DETERMINED USING DATA FROM THIS LAMINATE FAMILY) VERSUS DATA FOR THE $[0_n/\pm 15_n]_s$ SPECIMENS

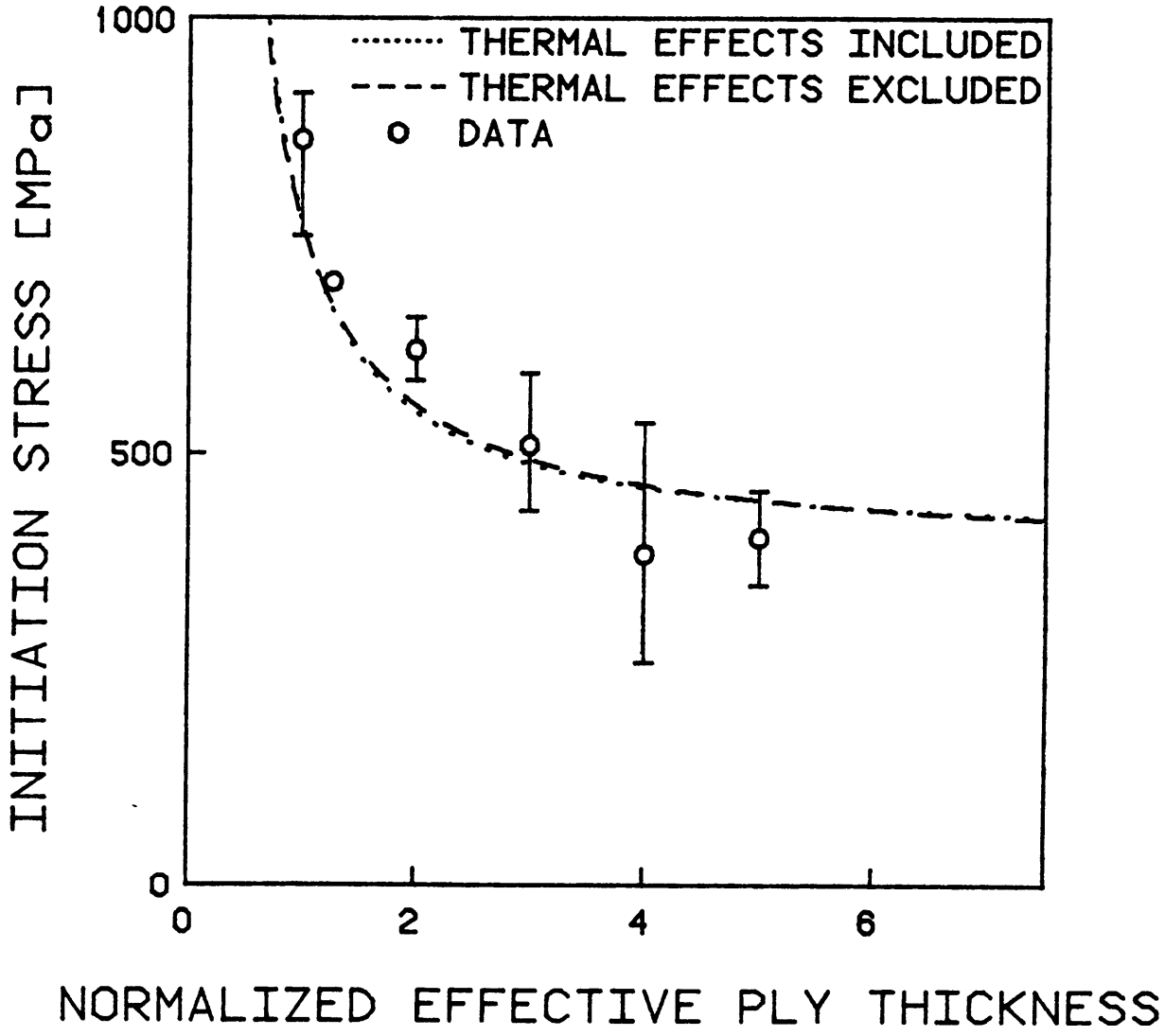

FIGURE 5.17 PREDICTED DELAMINATION INITIATION STRESS USING THE QUADRATIC DELAMINATION CRITERION (PARAMETERS DETERMINED USING ALL DATA) VERSUS DATA FOR THE $[\pm 15_n]_s$ SPECIMENS

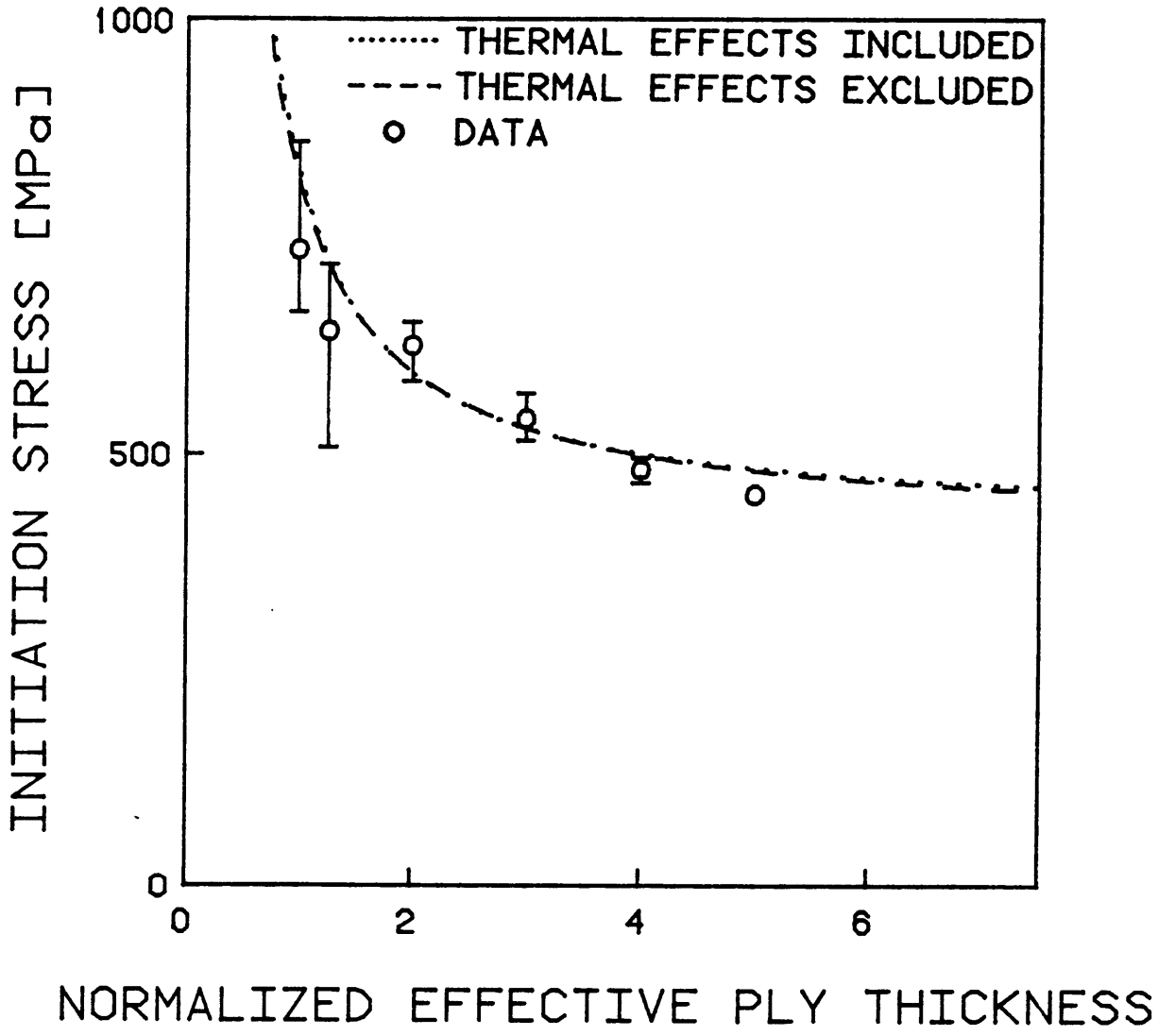

FIGURE 5.18 PREDICTED DELAMINATION INITIATION STRESS USING THE QUADRATIC DELAMINATION CRITERION (PARAMETERS DETERMINED USING ALL DATA) VERSUS DATA FOR THE $[\pm 15_n/0_n]_s$ SPECIMENS

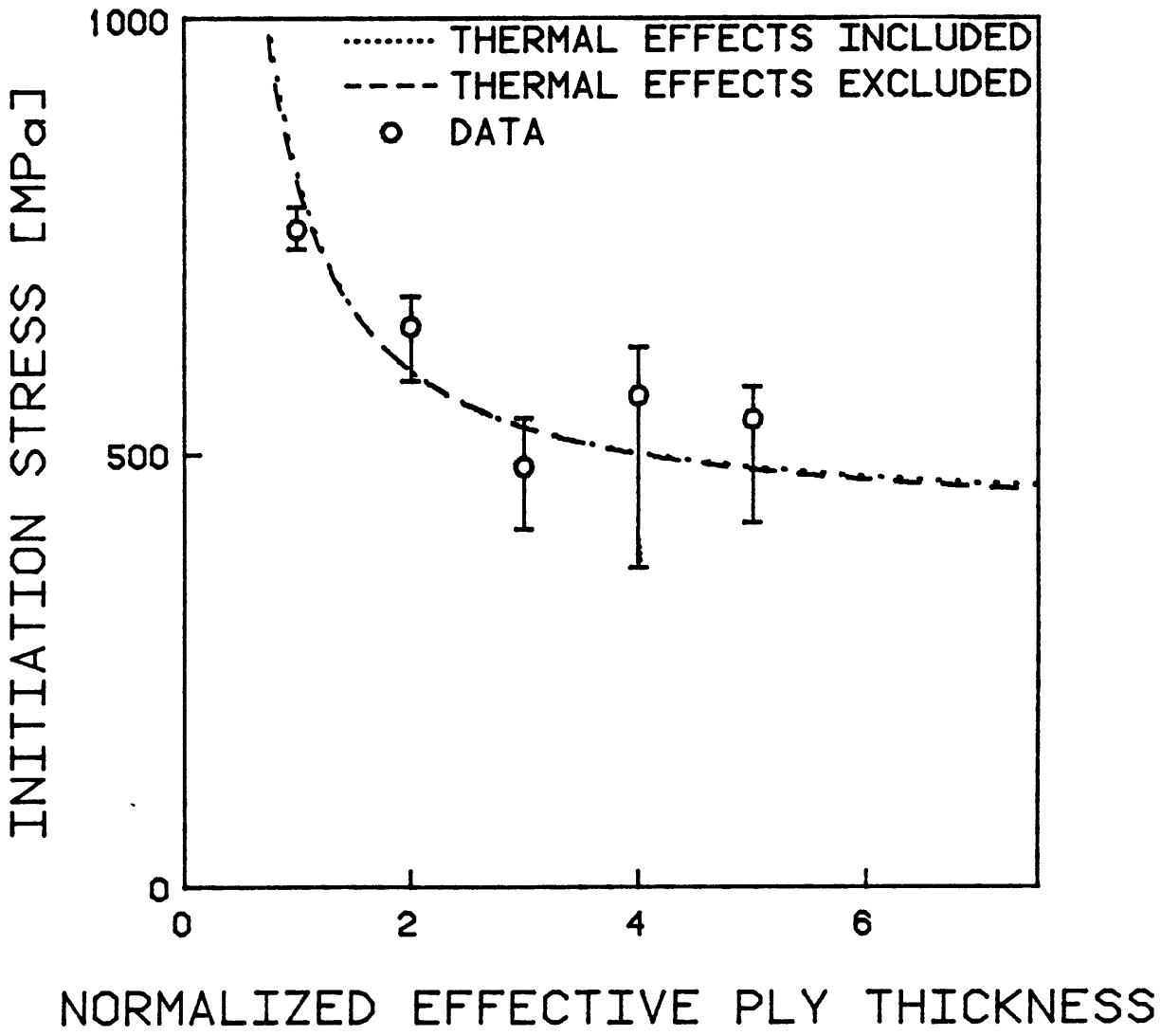

FIGURE 5.19 PREDICTED DELAMINATION INITIATION STRESS USING THE QUADRATIC DELAMINATION CRITERION (PARAMETERS DETERMINED USING ALL DATA) VERSUS DATA FOR THE $[0_n/\pm 15_n]_s$ SPECIMENS

ination initiation stress versus ply thickness are shown using the best fit parameters for the individual laminate families. The actual initiation stress data is plotted on these graphs. The "error bars" indicate the range of the valid data. The theoretical curves obtained when the best fit parameters are determined from the entire data base are shown for each laminate family in Figures 5.17 through 5.19. These figures also include actual delamination initiation stress data.

5.6.2 Strain Energy Release Rate Approach

The critical value of strain energy release rate was determined for each value of effective ply thickness of each laminate family using Equation 2.1. Average valid delamination initiation strains and theoretical moduli were used in these calculations. Table 5.8 summarizes the critical values of the total strain energy release rate calculated for each laminate along with the average value and coefficient of variation for these values for each laminate family. It appears that G_c increases significantly with effective ply thickness for the $[\pm 15_n/0_n]_s$ and $[0_n/\pm 15_n]_s$ laminate families. The value of G_c is expected to differ from laminate family to laminate family due to the different fraction of total strain energy release rate due to mode I for each laminate family. Fig-

TABLE 5.8

COMPUTED CRITICAL STRAIN ENERGY RELEASE RATES

Laminate	Computed Critical Strain Energy Release Rate [Joules/m^2]
$[\pm 15]_s$	750
$[\pm 15_*]_s$	673
$[\pm 15_2]_s$	893
$[\pm 15_3]_s$	991
$[\pm 15_4]_s$	695
$[\pm 15_5]_s$	1010
	835 (17.9%)[a]
$[\pm 15/0]_s$	421
$[\pm 15_*/0_*]_s$	419
$[\pm 15_2/0_2]_s$	646
$[\pm 15_3/0_3]_s$	703
$[\pm 15_4/0_4]_s$	816
$[\pm 15_5/0_5]_s$	940
	658 (31.9%)
$[0/\pm 15]_s$	443
$[0_2/\pm 15_2]_s$	735
$[0_3/\pm 15_3]_s$	621
$[0_4/\pm 15_4]_s$	1089
$[0_5/\pm 15_5]_s$	1367
	851 (43.8%)

Note: Subscript "*" indicates a laminate made from 190g/m^2 prepreg

[a]Numbers in parentheses are coefficients of variation

ures 5.20 through 5.22 show the theoretical curves for each laminate family. The average value of G_c for each particular laminate family was used in determining these theoretical curves.

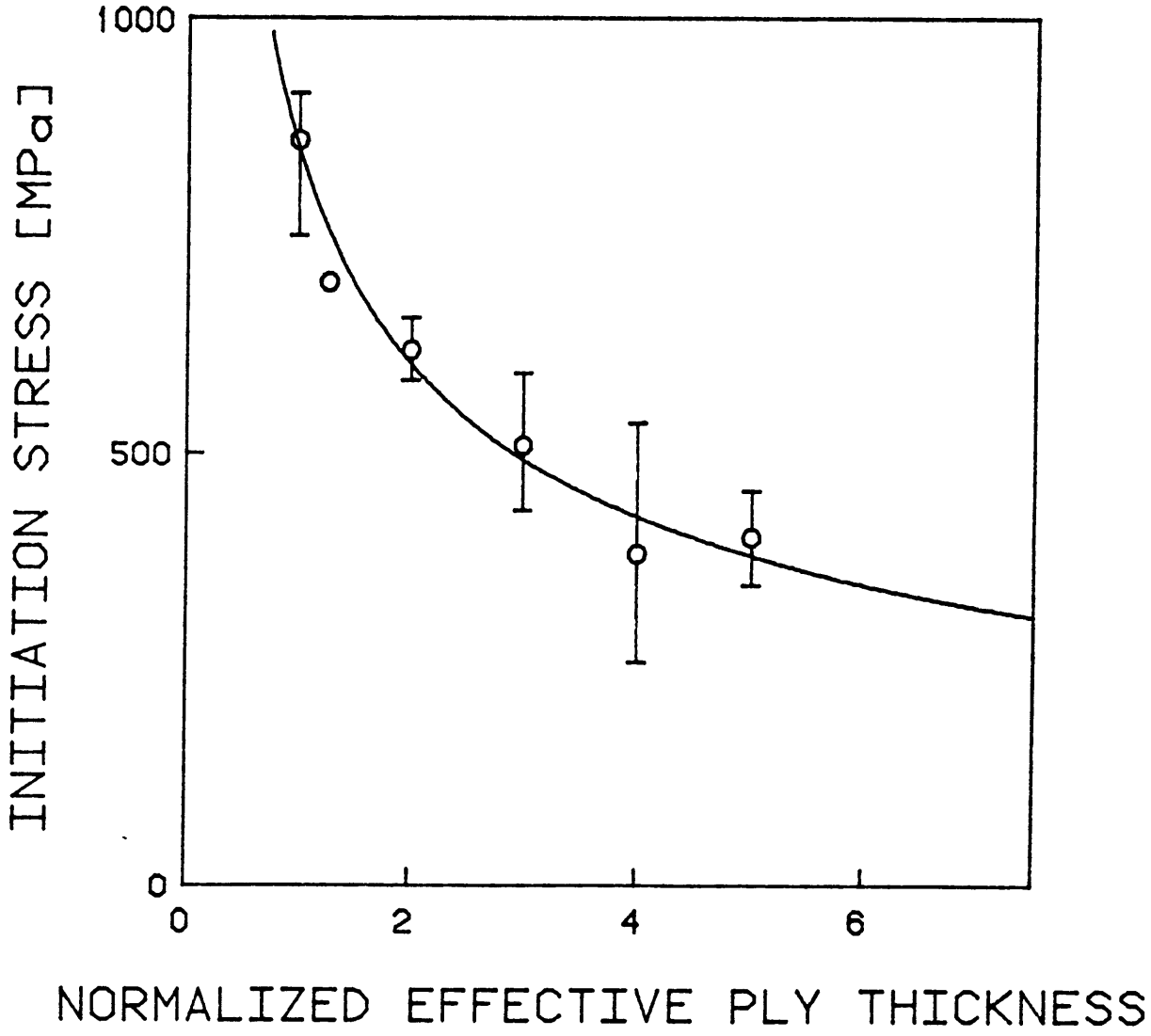

FIGURE 5.20 PREDICTED DELAMINATION INITIATION STRESS USING THE STRAIN ENERGY RELEASE RATE APPROACH VERSUS DATA FOR THE $[\pm 15_n]_s$ SPECIMENS

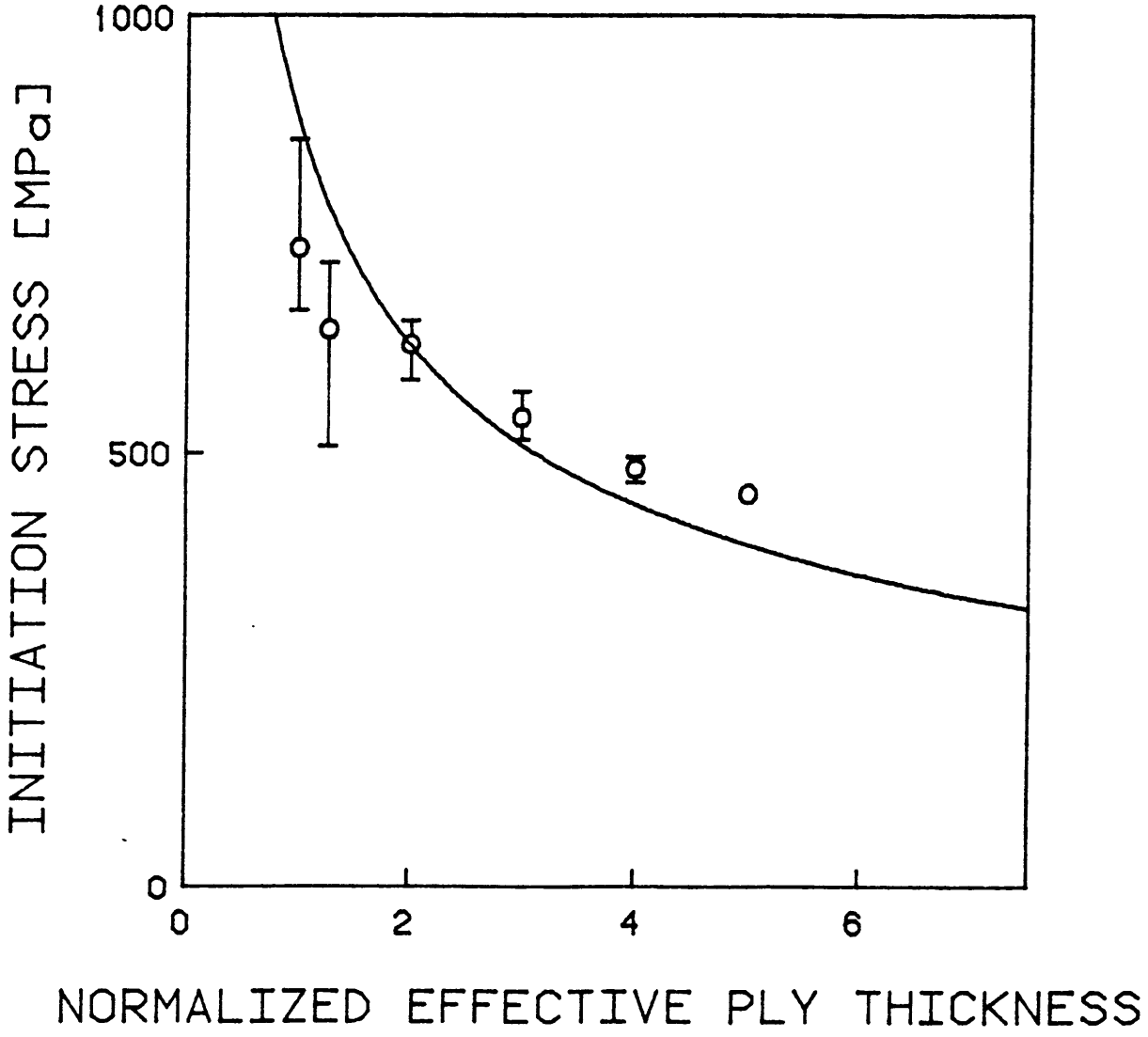

FIGURE 5.21 PREDICTED DELAMINATION INITIATION STRESS USING THE STRAIN ENERGY RELEASE RATE APPROACH VERSUS DATA FOR THE $[\pm 15_n/0_n]_s$ SPECIMENS

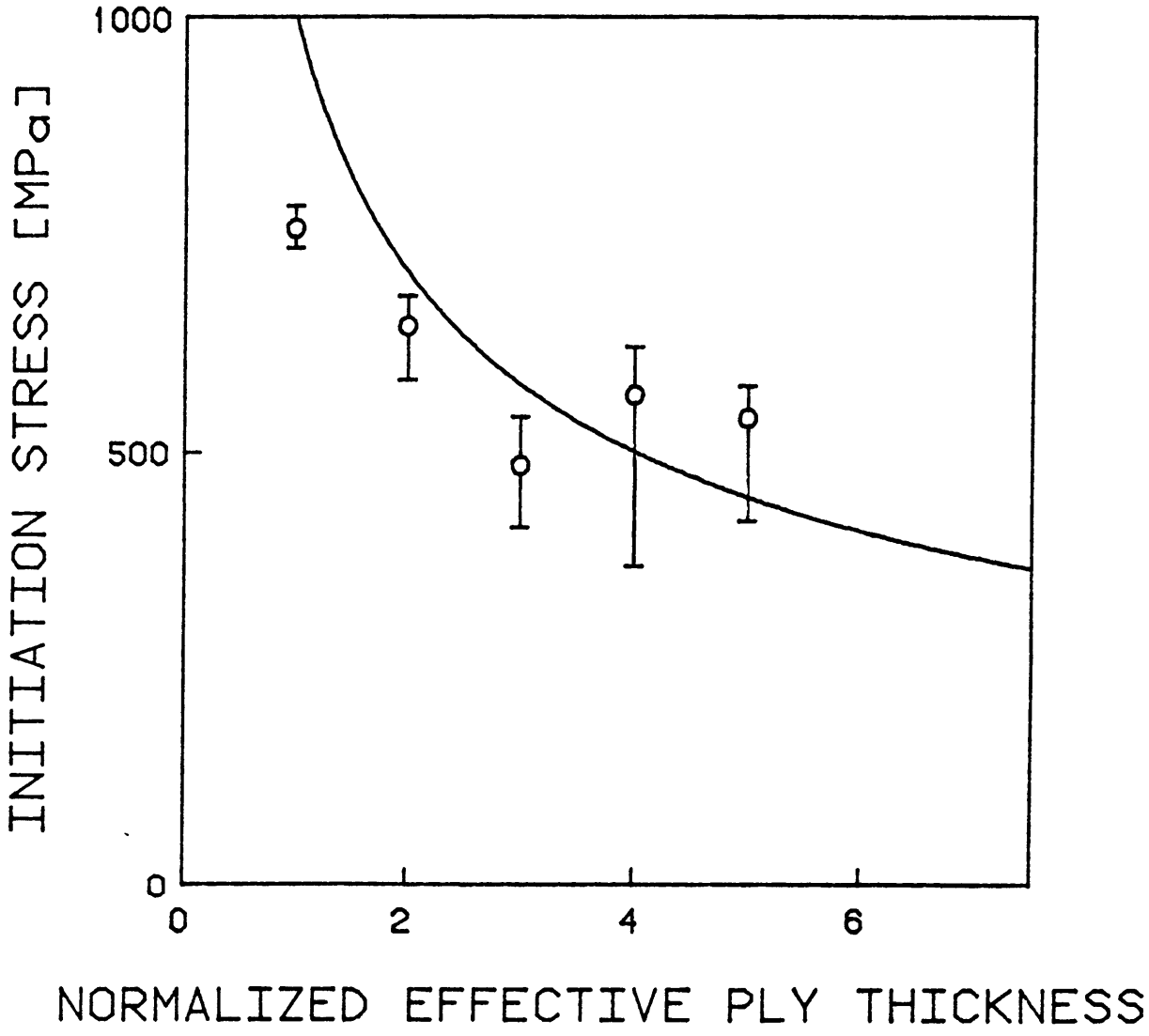

FIGURE 5.22 PREDICTED DELAMINATION INITIATION STRESS USING THE STRAIN ENERGY RELEASE RATE APPRAOCH VERSUS DATA FOR THE $[0_n/\pm 15_n]_s$ SPECIMENS

CHAPTER 6

DISCUSSION

6.1 Evaluation of the Testing Procedure

There is a need for a method which can detect delamination instantaneously during a test so that accurate values of delamination initiation stress and strain can be confidently obtained. This will also allow for the examination of such delamination initiation before any substantial additional growth occurs. The load drop method described herein combined with a nondestructive evaluation (such as the edge replications used in this investigation) seems to be an excellent way to achieve this goal.

Another possible nondestructive testing method is X-rays combined with a dye penetrant that is opaque to X-rays. This is a more expensive procedure than edge replication, but X-rays do have the advantage of being able to determine the delaminated area directly. This area can then be compared to the computed value of delaminated area. The X-rays, however, may not be able to detect initiation at defects as easily as replication techniques.

The testing method used in this investigation appears to have worked quite well. The delaminations seen were usually

of the hairline type, as would be expected. The fact that there were variations in the length and symmetry (with respect to the midplane) of the delaminations has important implications. Initiation is thought to be a "pop-in" phenomenon in which rapid but limited growth occurs. It would be expected that it would take little additional load for a delamination initiation to cause symmetric damage which runs along much of the length of the free edge. The presence of many cases of unsymmetric and small uncoalesced initiations implies that tests were stopped soon after the initial pop-in commenced.

The delaminated area calculated for the valid hairline initiations were generally the result of a total load drop of three or more computer units. It is unlikely that such load drops could be caused by noise in the data acquisition system which is usually on the order of one computer unit. This lends further credence to the technique for detecting delamination initiation.

The sensitivity of the delaminated area calculations was dependent on several factors. The load increase per unit time was dependent on the actual strain rate of the test section (which was affected by the varying amounts of tab shear in the different specimens), the actual modulus, and the actual time increment used. The load equivalent to one computer increment was obviously dependent on the load range of the testing ma-

chine that was used. The sensitivity of the method could be further increased if a way were found to decrease the relative noise of the data acquisition system.

Despite the general success of the technique, there were a number of specimens for which the determined initiation points were deemed invalid. These initiation points are divided into two types. In one type, delamination initiated from defects which were present in the untested specimen. These specimens showed delamination initiation stresses which were below the range of valid data. Thus, these are most likely initiations due to local stress concentrations around the defects. Continuation of testing for these specimens would yield only information about delamination growth and nothing definitive about the true initiation stress.

The second type of invalid initiation observed was massive delamination of the specimen. In these cases, the measured initiation stresses were above the range of valid data. Most likely these specimens exhibited a load drop due to initiation at a load just below the maximum load seen in the previous test. The fact that the initiation load could be below that of the previous maximum load may be the result of experimental scatter or may be a ramification of the loading-unloading-reloading cycle of these specimens. The computer program ignored such load drops that occurred below

the previous maximum load on the usually valid assumption that they are probably caused by system noise since replications taken at higher loads have exhibited no detectable damage. Thus, it appears that initiation occurred just below the previous maximum load and slow delamination growth continued until the delamination area reached a critical value. Steady growth could continue as long as the decrease in load per unit time due to the delamination growth did not exceed the corresponding increase in load due to regular specimen loading.

Nonetheless, the testing technique generally succeeded as indicated by the incremental tests which are a crucial check of the load drop testing method. The three specimens tested incrementally showed delamination initiation in the same general range as the specimens which were tested using the load drop method. The initiation stress range of the $[\pm 15/0]_s$ specimen showed excellent agreement with the corresponding load drop data. The initiation stress range of the $[0/\pm 15]_s$ specimen was above that of the load drop specimens. This can be attributed to experimental scatter as there is no apparent reason for the load drop method to accelerate the initiation process or the incremental test method to retard initiation. The $[\pm 15]_s$ specimen exhibited delamination slightly earlier than was seen in the specimens tested using the load drop method. However, this is within the experimental scatter.

Overall, the experimental technique proved to be an excellent method for the accurate determination of delamination initiation.

6.2 Evaluation of Delamination Models

6.2.1 The Quadratic Delamination Criterion

The Quadratic Delamination Criterion shows a great deal of potential for the prediction of delamination initiation. As evidenced in Figures 5.14 through 5.19, this criterion predicts the trend of the initiation stress data versus effective ply thickness quite well. For example, the Quadratic Delamination Criterion predicts asymptotic behavior of the initiation stress as the effective ply thickness becomes large when the interlaminar stress calculations assume finite values of the stresses at the free edge. The data does suggest that the actual behavior is asymptotic, although this cannot be conclusively determined.

The Quadratic Delamination Criterion was applied to the data in two ways. In one case, the parameters in the criterion were determined by using all the experimental data. In the second case, these parameters were determined using the data from specific laminate families. When the criterion is

applied to individual laminate families, there is excellent agreement with the delamination initiation stress data. The coefficients of variation of the actual delamination initiation stresses normalized by the predicted values are in the vicinity of 6% to 8%.

The values of interlaminar strength and averaging dimension which are used to achieve these fits are listed in Table 5.7. It can be seen that these values are similar for the $[\pm 15_n/0_n]_s$ and the $[0_n/\pm 15_n]_s$ laminate families in both the cases where thermal effects are included and the cases where they are excluded. The values for the $[\pm 15_n]_s$, however, are somewhat different. The averaging dimension is greater for this family by a factor of approximately two and the "backcalculated" interlaminar shear strength is smaller by 20% to 30%. It is important to note here that the magnitude of the average values of σ_{1z} and σ_{zz} decrease as averaging dimension increases. Thus, the increase in averaging dimension and decrease in interlaminar shear strength offset each other. Since the coefficient of variation of normalized delamination initiation stress (the parameter which was minimized to determine the best fit set of parameters) is relatively insensitive to specific values of averaging dimension and interlaminar shear strength, the actual difference in behavior between the three laminate families is well within the range of experimental

scatter. This is demonstrated by the fact that the coefficient of variation of normalized delamination initiation stress does not rise above 10% when all the data from all the laminate families are considered together. This is still excellent agreement with the data, especially since it is the correlation of data of three different laminate families with three different states of interlaminar stress.

When all the data is considered together, the best fit averaging dimensions are 0.242 mm when thermal stress effects are included and 0.178 mm when these effects are ignored. These are both of the same order of magnitude as the nominal ply thickness of the 150 g/m^2 prepreg, 0.134 mm. However, the averaging dimension did not equal the nominal ply thickness as Kim and Soni had suggested [19,20]. It is important to note that if the suggestion of Kim and Soni were taken to its logical conclusion, the laminates constructed of single plies of 190 g/m^2 would have the exact same behavior as the laminates constructed of single plies of 150 g/m^2 prepreg, as the ratio of ply thickness to averaging dimension would remain constant at one. This is definitely not what is observed. Thus, the argument that the averaging dimension can be taken as the nominal ply thickness is invalid.

The global best fit values of the interlaminar shear strength are 78 MPa for the case in which thermal effects are

included and 105 MPa for the case in which thermal effects are neglected. The second value is exactly equivalent to the in-plane shear strength of the composite as suggested by Kim and Soni [20]. Due to the uncertainty involved in determining the interlaminar shear strength, however, it is not conclusive as to which value is more accurate and whether or not thermal stress effects should be included in the analysis. Further experimentation on different specimen types will be needed to definitively determine this. Furthermore, this uncertainty points to the overwhelming need for an experiment to directly determine the interlaminar shear strength (as well as the interlaminar normal strength). These two parameters, Z^t and Z^s, should be measured directly rather than backcalculated from delamination data.

6.2.2 Strain Energy Release Rate Approach

The strain energy release rate approach appears to give good agreement with the delamination initiation stress data from the $[\pm 15_n]_s$ laminate family as shown in Figure 5.20. The coefficient of variation of the strain energy release rate values determined for the various effective ply thicknesses for this laminate family is 17.9%. The coefficient of variation of the actual delamination initiation stresses normal-

ized by the value predicted by the strain energy release rate approach is 6.5% when the average critical value of strain energy release rate of 835 Joules/m^2 for the laminate family is used.

However, this is not the case for the other two laminate families as the critical values of strain energy release rate for the $[\pm 15_n/0_n]_s$ and $[0_n/\pm 15_n]_s$ specimens are not constant with effective ply thickness. In this cases, the critical value of strain energy release rate increases consistently and substantially as effective ply thickness increases. There is a factor of more than two difference among the values of critical strain energy release rate for the $[\pm 15_n/0_n]_s$ laminate family and a factor of more than three for the $[0_n/\pm 15_n]_s$ laminate family as n varies from 1 to 5. This causes the coefficient of variation for these specimens to be on the order of twice that seen for the $[\pm 15_n]_s$ specimens. This steady increase with ply thickness can only be explained by the fact that the delamination initiation stress simply does not decay as fast as the reciprocal of the square root of effective ply thickness as predicted by the strain energy release rate model. There is no mechanism in the strain energy release rate approach that can explain this behavior.

It is important to note that the previously reported work on the strain energy release rate approach did not deal spe-

cifically with angle ply laminates such as the members of the $[\pm 15_n]_s$ laminate family. These specimens have no mode I component of strain energy release rate. Recent work [26,27,28,30] suggests that delamination initiation in statically loaded specimens with brittle matrices is sensitive primarily to mode I contributions of strain energy release rate. The argument is therefore made that, as the mode I contribution is increased, the critical value of total strain energy release rate decreases. This is what is seen for the average value of the strain energy release rate of the $[\pm 15_n/0_n]_s$ specimens. The $[\pm 15_n/0_n]_s$ specimens have a tensile value of σ_{zz} at the free edge and thus a nonzero mode I contribution to strain energy release rate. The average value of critical strain energy release rate for the $[\pm 15_n/0_n]_s$ specimens is 20% less than the average value for the $[\pm 15_n]_s$ laminate family. It is critical to note, however, that the computed strain energy release rates of individual members of the $[\pm 15_n/0_n]_s$ laminate family are on the same order of magnitude as the average value obtained for the $[\pm 15_n]_s$ laminate family. In fact, the computed value for the $[\pm 15_5/0_5]_s$ specimens is 13% higher than the average value for the $[\pm 15_n]_s$ laminate family. Thus, this trend does not hold true for individual laminates.

The average value of critical strain energy release rate for the $[0_n/\pm15_n]_s$ is approximately the same as the average value for the $[\pm15_n]_s$ specimens. However, the computed values for individual laminates range from half of the average value of critical strain energy release rate for the $[\pm15_n]_s$ laminates to more than 50% more than this value.

In summary, the strain energy release rate approach does a poor job of predicting the behavior of delamination initiation stress within individual laminate families. There is a wide variation (a factor of two to three) in the critical value of strain energy release rate for a particular laminate family and this parameter increases consistently with effective ply thickness. This would indicate that the critical value of strain energy is not a material or laminate constant, but is dependent on a number of other factors as well.

6.2.3 Comparison of the Quadratic Delamination Criterion and the Strain Energy Release Rate Approach

The Quadratic Delamination Criterion and the strain energy release rate approach both show very good agreement with the delamination initiation stress data for the $[\pm15_n]_s$ laminate family. The Quadratic Delamination Criterion, however, is able to correlate the data from the $[\pm15_n/0_n]_s$ and

$[0_n/\pm15_n]_s$ laminate families while the strain energy release rate approach exhibits wide variations in the computed values of critical strain energy release rate. When the actual values of the initiation stresses are normalized by the predicted values of the initiation stresses, the coefficients of variation for these values are 6.5%, 13.7%, and 19.8%, respectively, for the $[\pm15_n]_s$, $[\pm15_n/0_n]_s$, and $[0_n/\pm15_n]_s$ specimens when the strain energy release rate approach is used. When the Quadratic Delamination Criterion is used, the coefficients of variation for the entire data base are 9.9%, if thermal effects are considered, and 9.7%, if thermal effects are neglected.

This implies that the Quadratic Delamination Criterion is, in general, better at predicting the trends of the data than the strain energy release rate approach. It is important to note that this better performance was achieved using one set of material parameters rather than a single parameter determined experimentally for each laminate family. In addition, it should be possible to devise test methods to experimentally determine the interlaminar strength parameters. Thus, only the averaging dimension must be determined experimentally. In the strain energy release rate approach, experimentation is necessary to determine the critical strain energy release rate for each laminate family unless it is acceptable to estimate

this value from a preexisting data base and a determination of the mode I component from numerical methods. The current data suggests that this would be a poor prediction.

The character of curves predicted by the two methods are very different at higher values of effective ply thickness. The strain energy release rate approach predicts that delamination initiation stress decays as the reciprocal of the square root of the effective ply thickness. The Quadratic Delamination Criterion predicts an asymptotic behavior of delamination initiation stress as effective ply thickness is increased. Due to the experimental scatter, it is difficult to assert that the data does in fact become asymptotic although this behavior is suggested. However, the data definitely does not fit the behavior predicted using the strain energy release rate approach.

The ability of the Quadratic Delamination Criterion in conjunction with the Force Balance Method, which determines the state of interlaminar stress, to reasonably predict delamination initiation stress with only one experimentally determined value means that it can be a powerful preliminary design tool in evaluating the propensity for delamination of lamination sequences. It is, however, absolutely necessary that appropriate tests be established to measure the interlaminar

shear and normal strengths of composite materials so that this criterion can be properly evaluated and applied.

CHAPTER 7

CONCLUSIONS AND RECOMMENDATIONS

An experimental method has been developed to detect the onset of delamination initiation of graphite/epoxy laminates under uniaxial tensile loads and a criterion presented to correlate this initiation with material interlaminar strength parameters. The following conclusions are made based on the work reported herein:

1. The load drop method used in conjunction with the nondestructive evaluation technique of edge replication is an accurate technique for the detection of delamination initiation in advanced composites.

2. The strain energy release rate approach is unable to correlate delamination initiation in two of the three laminate families in this investigation, $[\pm 15_n/0_n]_s$ and $[0_n/\pm 15_n]_s$, as the critical value of strain energy release rate increases significantly (a factor of two to three) with effective ply thickness.

3. The Quadratic Delamination Criterion proposed herein, when used with the Force Balance Method for the calculation of interlaminar stresses, is able to easily and accurately correlate delamination initiation. This technique has the potential to be a powerful preliminary design tool for evaluating the propensity of general laminates to delaminate.

4. The values of the interlaminar shear strength parameter backcalculated using the Quadratic Delamination Criterion (78 MPa when the thermal effects are included, 105 MPa when the thermal effects are excluded) compare quite favorably with the estimated value of 105 MPa (the shear strength of the unidirectional composite).

5. The calculated averaging dimension for the Quadratic Delamination Criterion is 0.242 mm when thermal effects are included and 0.178 mm when thermal effects are excluded. This is on the order of the ply thickness of the composite but is definitely not equal to this value as has been previously suggested.

6. The data indicates that the value of the delamination initiation stress is asymptotic for large ply thicknesses as predicted by the Quadratic Delamination Criterion. However, inherent scatter in the data makes it impossible to be conclusive in this matter.

7. It is difficult to assert whether thermal effects should be excluded or included in the delamination initiation analysis.

The Quadratic Delamination Criterion has proved to be a useful tool in predicting delamination initiation. Further investigation will be needed to gain confidence in this approach. To acheive this goal, the following research is recommended:

1. Tests similar to those in this investigation should be conducted on specimens with larger contributions of interlaminar normal stress to isolate the effects of interlaminar normal stresses and their contribution to the initiation of delamination.

2. Specimens with very large ply thicknesses should be tested to confirm the existence of the asymptotic behavior predicted by the Quadratic Delamination Criterion.

3. The effects of thermal stresses should be investigated to determine their role in delamination initiation.

4. The interlaminar normal and shear strengths should be determined by direct experimentation. Once these values have been determined, the averaging dimension can be easily determined.

5. The growth of delamination from initiation to final failure should be studied. Growth must necessarily be monitored by nondestructive techniques such as X-rays, ultrasonic C-scan, and photoelasticity.

REFERENCES

1. Tsai, S. W., and Wu, E. M., "A Generalized Theory of Strength for Anisotropic Materials," Journal of Composite Materials, Vol. 5, 1971, pp. 58-80.

2. Lagace, P. A., Static Tensile Fracture of Graphite/Epoxy, Technology Laboratory for Advanced Composites, TELAC Report No. 82-5, Ph. D. Thesis, Department of Aeronautics and Astronautics, Massachusetts Institute of Technology, June, 1982.

3. Pipes, R. B., and Pagano, N. J., "Interlaminar Stresses in Composite Laminates under Uniform Axial Extension," Journal of Composite Materials, Vol. 4, 1970, pp. 538-548.

4. Rybicki, E. F., "Approximate Three-Dimensional Solutions for Symmetric Laminates Under Inplane Loading," Journal of Composite Materials, Vol. 5, 1971, pp. 354-360.

5. Wang, A. S. D., and Crossman, F. W., "Some New Results on Edge Effects in Symmetric Composite Laminates," Journal of Composite Materials, Vol. 11, 1977, pp. 92-106.

6. Puppo, A. H., and Evensen, H. A., "Interlaminar Shear in Laminated Composites Under Generalized Plane Stress," Journal of Composite Materials, Vol. 4, 1970, pp. 204-220.

7. Pagano, N. J., and Pipes, R. B., "The Influence of Stacking Sequence on Laminate Strength," Journal of Composite Materials, Vol. 5, 1971, pp. 50-57.

8. Whitney, J. M., "Free-Edge Effects in the Characterization of Composite Materials," Analysis of the Test Methods for High Modulus Fibers and Composites, ASTM STP 521, American Society for Testing and Materials, 1973, pp. 167-180.

9. Pipes, R. B., and Pagano, N. J., "Interlaminar Stresses in Composites - An Approximate Elasticity Solution," Transactions of the ASME, September 1974, pp. 668-672.

10. Hsu, P. W. and Herakovich, C. T., "A Perturbation Solution for Interlaminar Stresses in Bidirectional Laminates," Composite Materials: Testing and Design (Fourth Conference), ASTM STP 617, American Society for Testing and Materials, 1977, pp. 296-316.

11. Lagace, P. A., and Kassapoglou, C., "An Efficient Method for the Calculation of Interlaminar Stresses Part 1," submitted to the Journal of Applied Mechanics.

12. Kassapoglou, C., and Lagace, P. A., "An Efficient Method for the Calculation of Interlaminar Stresses Part 2," submitted to the Journal of Applied Mechanics.

13. Pipes, R. B., Kaminski, B. E., and Pagano, N. J., "Influence of the Free Edge upon the Strength of Angle-Ply Laminates," Analysis of the Test Methods for High Modulus Fibers and Composites, ASTM STP 521, American Society for Testing and Materials, 1973, pp. 218-228.

14. Herakovich, C. T., "Influence of Layer Thickness on the Strength of Angle-Ply Laminates," Journal of Composite Materials, Vol. 16, May 1982, pp. 216-226.

15. Rodini, B. T., Jr., and Eisenmann, J. R., "An Analytical and Experimental Investigation of Edge Delamination in Composite Laminates," Proceedings of the Fourth Conference on Fibrous Composites in Structural Design, 1978, San Diego, California, pp. 441-456.

16. Lagace, P. A., "Delamination Fracture under Tensile Loading," in Proceedings of the Sixth Conference on Fibrous Composites in Structural Design, AMMRC MS 83-2, Army Materials and Mechanics Research Center, November 1983.

17. Wang, S. S., and Choi, I., "Boundary-Layer Effects in Composite Laminates: Part 1 - Free Edge Stress Singularities," Journal of Applied Mechanics, Vol. 49, September 1982, pp. 541-548.

18. Whitney, J. M., and Nuismer, R. J., "Stress Fracture Criteria for Laminated Composites Containing Stress Concentrations," Journal of Composite Materials, Vol. 8, July 1974, pp. 253-265.

19. Kim, R. Y., and Soni, S. R., "Experimental and Analytical Studies On the Onset of Delamination in Laminated Composites," Journal of Composite Materials, Vol. 18, January 1984, pp. 70-80.

20. Kim, R. Y., and Soni, S. R., "Delamination of Composite Laminates Stimulated by Interlaminar Shear," University of Dayton Research Institute, unpublished.

21. Brewer, J. C., Weems, D. B., and Archard, K. A., "The Effect of Ply Thickness on Delamination Failure of Graphite/Epoxy Laminates," Technology Laboratory for Advanced Composites, TELAC Report 84-20, Massachusetts Institute of Technology, 1984.

22. Rybicki, E. F., Schmeuser, D. W., and Fox, J., "An Energy Release Rate Approach For Stable Crack Growth in the Free-Edge Delamination Problem," Journal of Composite Materials, Vol. 14 Supplement, 1980, pp. 71-87.

23. Wang, A. S. D., and Crossman, F. W., "Initiation and Growth of Transverse Cracks and Edge Delamination in Composite Laminates. Part 1. An Energy Method," Journal of Composite Materials, Vol. 14 Supplement, 1980, pp. 71-87.

24. Crossman, F. W., Warren, W. J., Wang, A. S. D., and Law, G. E., Jr., "Initiation and Growth of Transverse Cracks and Edge Delamination in Composite Laminates. Part 2. Experimental Correlation," Journal of Composite Materials, Vol. 14 Supplement, 1980, pp. 88-108.

25. O'Brien, T. K., "Characterization of Delamination and Growth in a Composite Laminate," Damage in Composite Materials, ASTM STP 775, K. L. Reifsneider, ed., American Society for Testing and Materials, 1982, pp. 140-167.

26. O'Brien, T. K., Johnston, N. J., Morris, D. H., and Simonds, R. A., "A Simple Test for the Interlaminar Fracture Toughness of Composites," SAMPE Journal, July/August 1982, pp. 8-15.

27. O'Brien, T. K., "Mixed-Mode Strain-Energy-Release Rate Effects on Edge Delamination of Composites," NASA Technical Memorandum 84592, January, 1983.

28. O'Brien, T. K., Johnston, N. J., Morris, D. H., and Simonds, R. A., "Determination of Interlaminar Fracture Toughness and Fracture Mode Dependence of Composites using the Edge Delamination Test," Proceedings of the International Conference on Testing, Evaluation, and Quality Control of Composites, University of Surrey, Guilford, England, September, 1983, pp. 223-232.

29. O'Brien, T. K., "Analysis of Local Delaminations and Their Influence on Composite Laminate Behavior," NASA Technical Memorandum 85728, January, 1984

30. O'Brien, T. K., "Interlaminar Fracture of Composites," NASA Technical Memorandum 85768, June, 1984.

31. Crossman, F. W., and Wang, A. S. D., "The Dependence of Transverse Cracking and Delamination on Ply Thickness in Graphite/Epoxy Laminates," Damage in Composite Materials, ASTM STP 775, K. L. Reifsneider, ed., American Society for Testing and Materials, 1982, pp. 118-139.

32. Reifsneider, K. L., Hennecke, E. G., II, and Stinchcomb, W. W., "Delamination in Quasi-Isotropic Graphite-Epoxy Laminates," Composite Materials: Testing and Design (Fourth Conference), ASTM STP 617, American Society for Testing and Materials, 1977, pp. 93-105.

33. Klang, E. C., and Hyer, M. W., "Damage Initiation at Curved Free Edges: Application to Uniaxially Loaded Plates Containing Holes and Notches," Proceedings of the ASTM Second United States-Japan Symposium on Composite Materials, Hampton, Virginia, June 1983.

34. Hashin, Z., "Failure Criteria for Unidirectional Fiber Composites," Journal of Apllied Mechanics, Vol. 47, 1980.

35. Kassapoglou, C., Interlaminar Stresses at Straight Free Edges of Composite Laminates, Technology Laboratory for Advanced Composites, TELAC Report No. 84-18, S. M. Thesis, Department of Aeronautics and Astronautics, Massachusetts Institute of Technology, October, 1984.

36. "Standard Test Method for Tensile Properties of Fiber-Resin Composites," ASTM Designation D 3039 - 76.

37. Lagace, P. A., and Brewer, J. C., TELAC Manufacturing Course Notes, Edition O-2, Technology Laboratory for Advanced Composites, TELAC Report 81-14, Massachusetts Institue of Technology, September 1981.

DATA TABLE 1: $[\pm 15_n]_s$ Laminate Family

Specimen	Thickness [mm]	Width [mm]	Long. Modulus [GPa]	Delamination Initiation ...		
				Type	Stress [MPa]	Strain [μstrain]
15A0-0-6	0.59	50.31	107	D	749	6666
15A0-0-7	0.60	50.49	111	C	913	8016
15A0-0-8	0.59	50.44	110	A	887	7806
15A0-0-9	0.58	50.52	110	A	---	-----
15A0-0-10	0.60	50.52	114	C	888	7578
	059 (1.4%)	50.46 (0.2%)	110 (2.3%)		859 (8.7%)	7517 (7.9%)
*15A0-0-1	0.71	50.16	107	D	693	6324
*15A0-0-2	0.70	50.21	105	D	784	7212
*15A0-0-3	0.70	50.17	103	B	588	5532
*15A0-0-4	0.72	50.20	107	A	698	6330
*15A0-0-5	0.66	50.18	100	-	---	-----
	0.70 (3.3%)	50.18 (0.6%)	104 (2.8%)		691 (11.6%)	6350 (10.8%)
215A0-0-6	1.06	50.49	97	C	599	6120
215A0-0-7	1.08	50.53	107	C	583	5484
215A0-0-8	1.06	50.47	108	C	656	5892
215A0-0-9	1.09	50.57	108	C	635	5712
215A0-0-9	1.00	50.47	91	B	382	4092
	1.06 (3.3%)	50.51 (0.9%)	102 (7.6%)		571 (19.2%)	5460 (14.6%)
315A0-0-6	1.52	49.99	102	D	568	5568
315A0-0-7	1.59	49.83	106	B	438	4116
315A0-0-8	1.60	49.93	106	D	673	6000
315A0-0-9	1.58	49.97	109	A	591	5604
315A0-0-10	1.49	49.88	92	A	434	4674
	1.56 (3.1%)	49.92 (0.1%)	103 (6.4%)		541 (19.1%)	5192 (14.9%)
415A0-0-6	2.00	49.97	101	B	326	3216
415A0-0-7	2.12	50.03	109	B	374	3366
415A0-0-8	2.16	50.00	113	A	534	4602
415A0-0-9	2.10	49.77	107	A	424	4074
415A0-0-10	2.00	49.99	96	A	259	2832
	2.08 (3.5%)	49.95 (0.2%)	105 (6.4%)		383 (27.1%)	3618 (19.6%)
515A0-0-6	2.56	49.44	102	D	472	4560
515A0-0-7	2.64	49.52	108	D	491	4554
515A0-0-8	2.72	49.77	112	A	456	4062
515A0-0-9	2.61	49.48	98	B	24	252
515A0-0-10	2.47	49.81	94	A	347	3744
	2.60 (3.6%)	49.60 (0.3%)	103 (7.1%)		358 (43.4%)	3434 (52.8%)

Numbers in parentheses are coefficients of variation
Note: "*" indicates laminate made from 190g/m^2 prepreg

DATA TABLE 2: $[\pm 15_n/0_n]_s$ Family

Specimen	Thickness [mm]	Width [mm]	Long. Modulus [GPa]	Delamination Initiation ...		
				Type	Stress [MPa]	Strain [μstrain]
15A1-0-18	0.82	50.02	117	A	663	5586
15A1-0-19	0.85	49.94	118	A	670	5352
15A1-0-20	0.82	50.01	115	A	746	6264
15A1-0-21	0.84	49.98	118	A	---	----
15A1-0-22	0.82	49.95	115	A	858	7154
	0.83 (1.7%)	49.98 (0.1%)	117 (1.3%)		734 (12.3%)	6089 (13.3%)
*15A1-0-1	0.98	50.07	113	A	624	5448
*15A1-0-2	1.01	50.15	118	A	734	6000
*15A1-0-3	1.00	50.05	115	A	622	5220
*15A1-0-4	1.02	50.12	118	A	717	5670
*15A1-0-5	0.96	50.03	106	A	507	4638
	0.99 (2.4%)	50.08 (0.1%)	114 (4.3%)		641 (14.2%)	5395 (9.5%)
215A1-0-6	1.52	50.04	106	A	645	5646
215A1-0-7	1.57	50.09	120	A	583	4848
215A1-0-8	1.59	49.99	115	A	652	5280
215A1-0-9	1.58	50.03	115	B	138	1212
215A1-0-10	1.48	49.98	105	A	618	5562
	1.55 (3.0%)	50.03 (0.1%)	112 (5.7%)		527 (41.6%)	4510 (41.5%)
315A1-0-6	2.19	49.76	108	A	569	5142
315A1-0-7	2.29	49.99	118	D	724	5940
315A1-0-8	2.35	49.96	123	B	534	4218
315A1-0-9	2.28	50.07	116	A	514	4266
315A1-0-10	2.14	49.32	100	B	424	4146
	2.25 (3.7%)	49.82 (0.6%)	113 (8.0%)		553 (19.8%)	4742 (16.5%)
415A1-0-6	2.93	49.98	104	B	484	4542
415A1-0-7	3.12	50.02	111	A	465	4002
415A1-0-8	3.15	49.98	115	A	491	4140
415A1-0-9	3.11	50.13	108	A	495	4152
415A1-0-10	2.97	50.07	104	A	471	4362
	3.06 (3.2%)	50.04 (0.1%)	108 (4.4%)		481 (2.7%)	4240 (5.0%)
515A1-0-6	3.73	50.05	109	A	457	4176
515A1-0-7	3.80	50.18	112	A	451	4008
515A1-0-8	3.82	50.04	116	D	579	4986
515A1-0-9	3.76	50.16	107	A	447	4026
515A1-0-10	3.54	50.02	99	B	430	4350
	3.73 (3.0%)	50.09 (0.1%)	109 (5.8%)		473 (12.7%)	4309 (9.3%)

Numbers in parentheses are coefficients of variation
Note: "*" indicates laminate made from 190g/m^2 prepreg

DATA TABLE 3: $[0_n/\pm15_n]_s$ Family

Specimen	Thickness [mm]	Width [mm]	Long. Modulus [GPa]	Delamination Initiation ...		
				Type	Stress [MPa]	Strain [μstrain]
15B1-0-18	0.83	50.10	114	A	---	-----
15B1-0-19	0.85	50.17	116	A	751	6246
15B1-0-20	0.84	50.12	116	A	758	6270
15B1-0-21	0.88	50.17	120	A	735	5808
15B1-0-22	0.82	49.45	111	A	783	6660
	0.84 (2.7%)	50.00 (0.6%)	115 (2.8%)		757 (2.6%)	6246 (5.6%)
215B1-0-6	1.48	49.91	102	A	583	5364
215B1-0-7	1.58	49.97	117	D	896	7500
215B1-0-8	1.64	49.88	118	B	514	4194
215B1-0-9	1.61	49.69	116	A	680	5502
215B1-0-10	1.47	49.99	106	A	673	6204
	1.56 (4.9%)	49.89 (0.2%)	112 (6.5%)		669 (21.5%)	5753 (21.1%)
315B1-0-6	2.27	49.91	110	A	534	4758
315B1-0-7	2.35	49.79	112	A	541	4686
315B1-0-8	2.37	49.86	117	A	498	4224
315B1-0-9	2.34	49.78	119	B	433	3654
315B1-0-10	2.15	49.86	101	A	413	4032
	2.30 (3.9%)	49.84 (0.1%)	112 (6.3%)		484 (12.0%)	4271 (10.8%)
415B1-0-6	3.16	49.69	101	B	490	4566
415B1-0-7	3.24	49.65	108	A	511	4596
415B1-0-8	3.24	49.59	117	A	565	4740
415B1-0-9	3.19	49.31	113	A	622	5358
415B1-0-10	3.01	49.72	94	A	368	3702
	3.16 (3.0%)	49.59 (0.3%)	107 (8.7%)		511 (18.6%)	4909 (9.1%)
515B1-0-6	4.05	49.55	107	A	576	5004
515B1-0-7	4.05	49.13	111	A	520	4608
515B1-0-8	3.99	49.24	99	A	610	5436
515B1-0-9	3.87	49.71	104	A	568	5178
515B1-0-10	3.67	49.68	98	A	420	4320
	3.93 (4.1%)	49.46 (0.5%)	104 (5.3%)		539 (13.7%)	4909 (9.1%)

Numbers in parentheses are coefficients of variation

APPENDIX A

INTERLAMINAR STRESS STATES

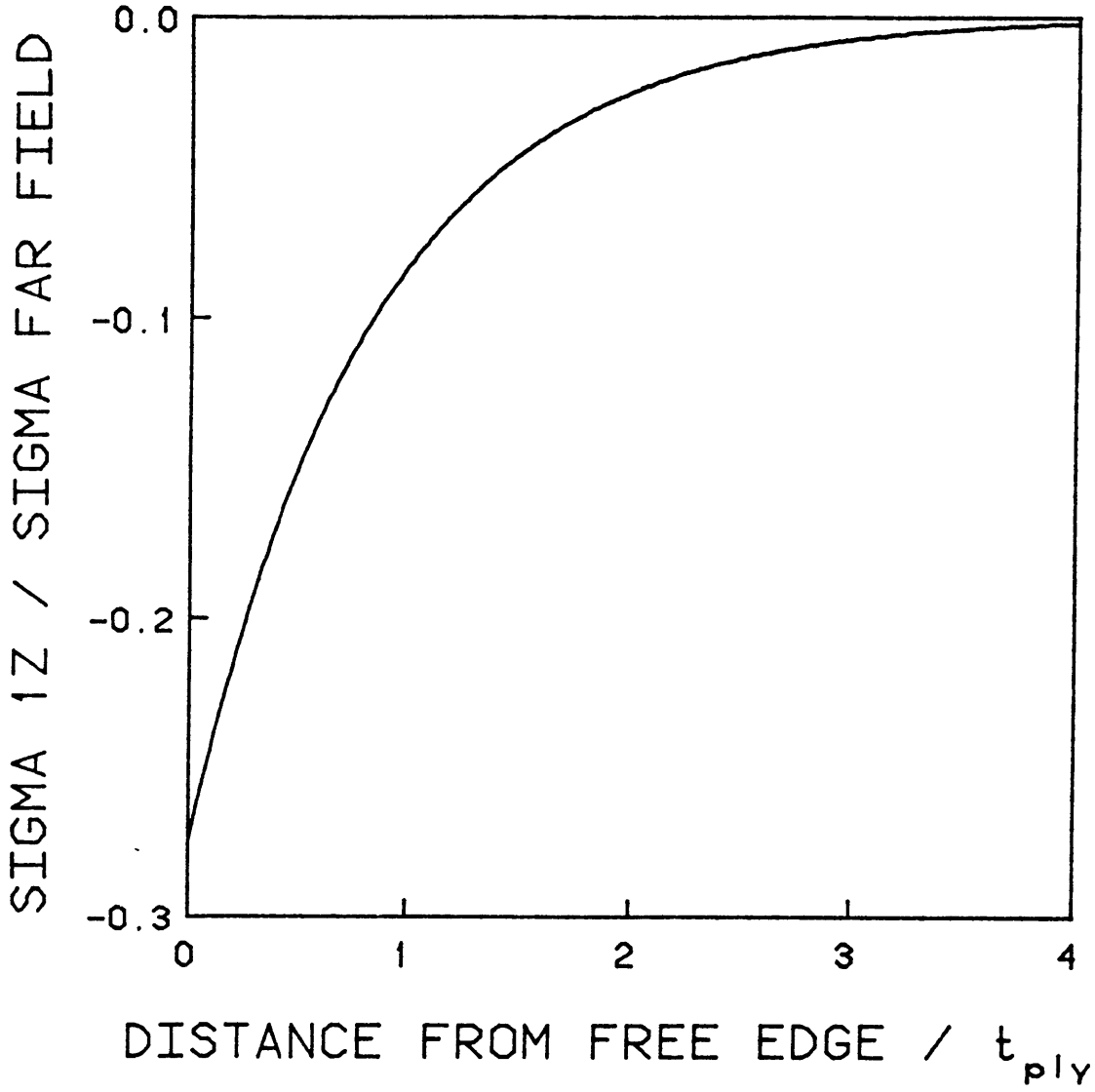

FIGURE A.1 INTERLAMINAR SHEAR STRESS DUE TO A UNIT MECHANICAL LOAD ON $[\pm 15_n]_s$ SPECIMENS

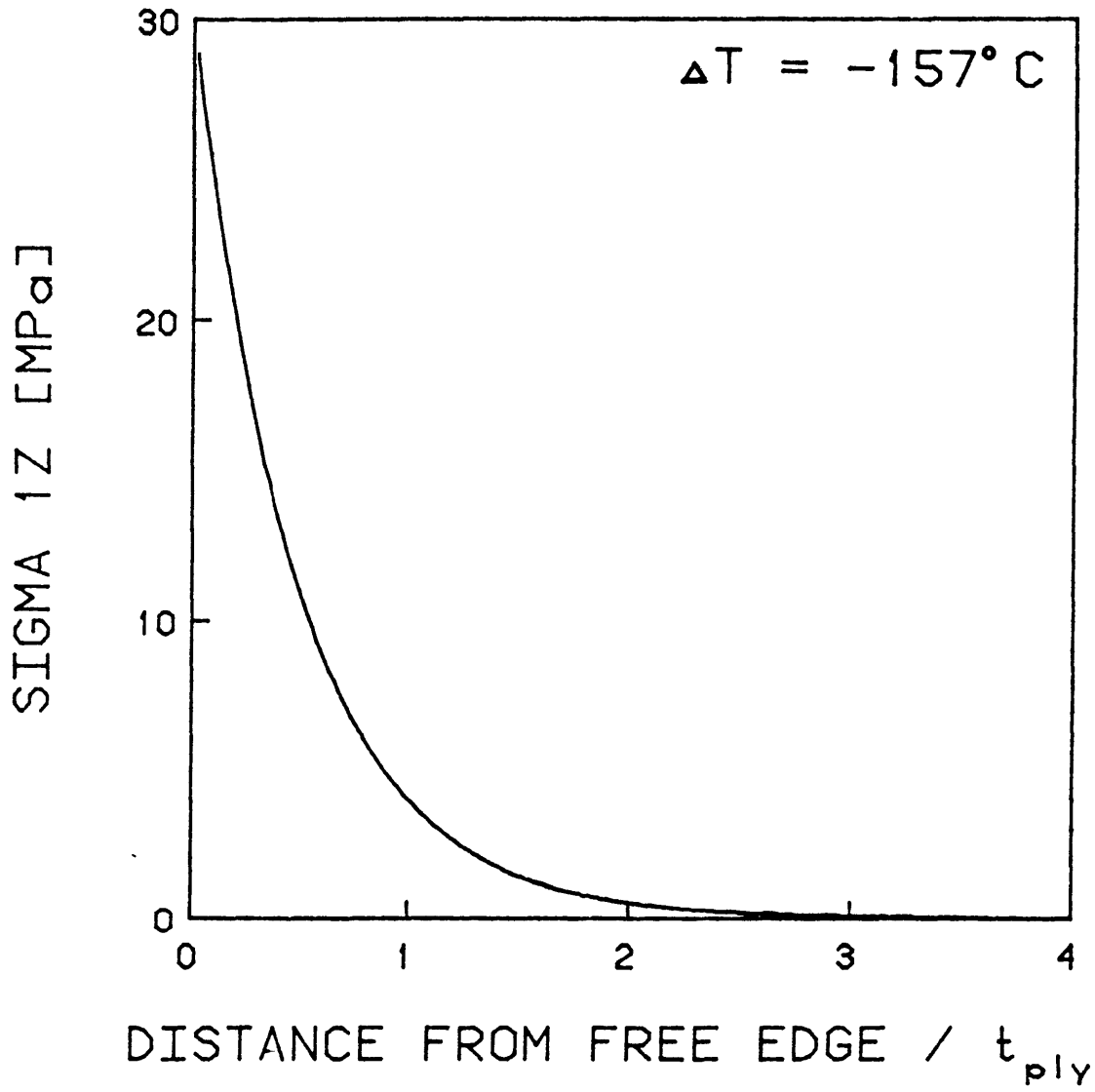

FIGURE A.2 INTERLAMINAR SHEAR STRESS DUE TO THERMAL EFFECTS ON $[\pm 15_n]_s$ SPECIMENS

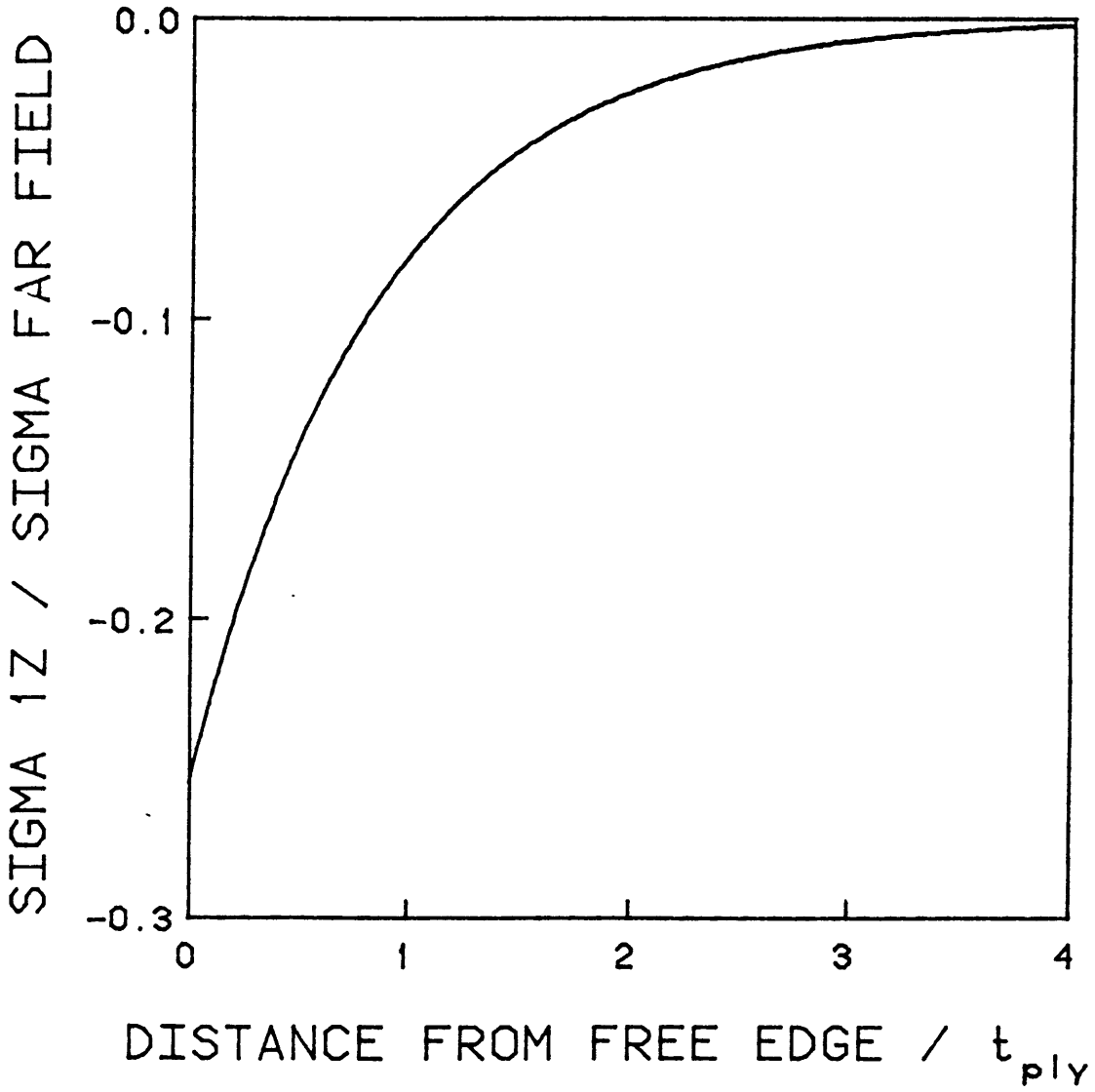

FIGURE A.3 INTERLAMINAR SHEAR STRESS DUE TO A UNIT MECHANICAL LOAD ON $[\pm 15_n/0_n]_s$ SPECIMENS

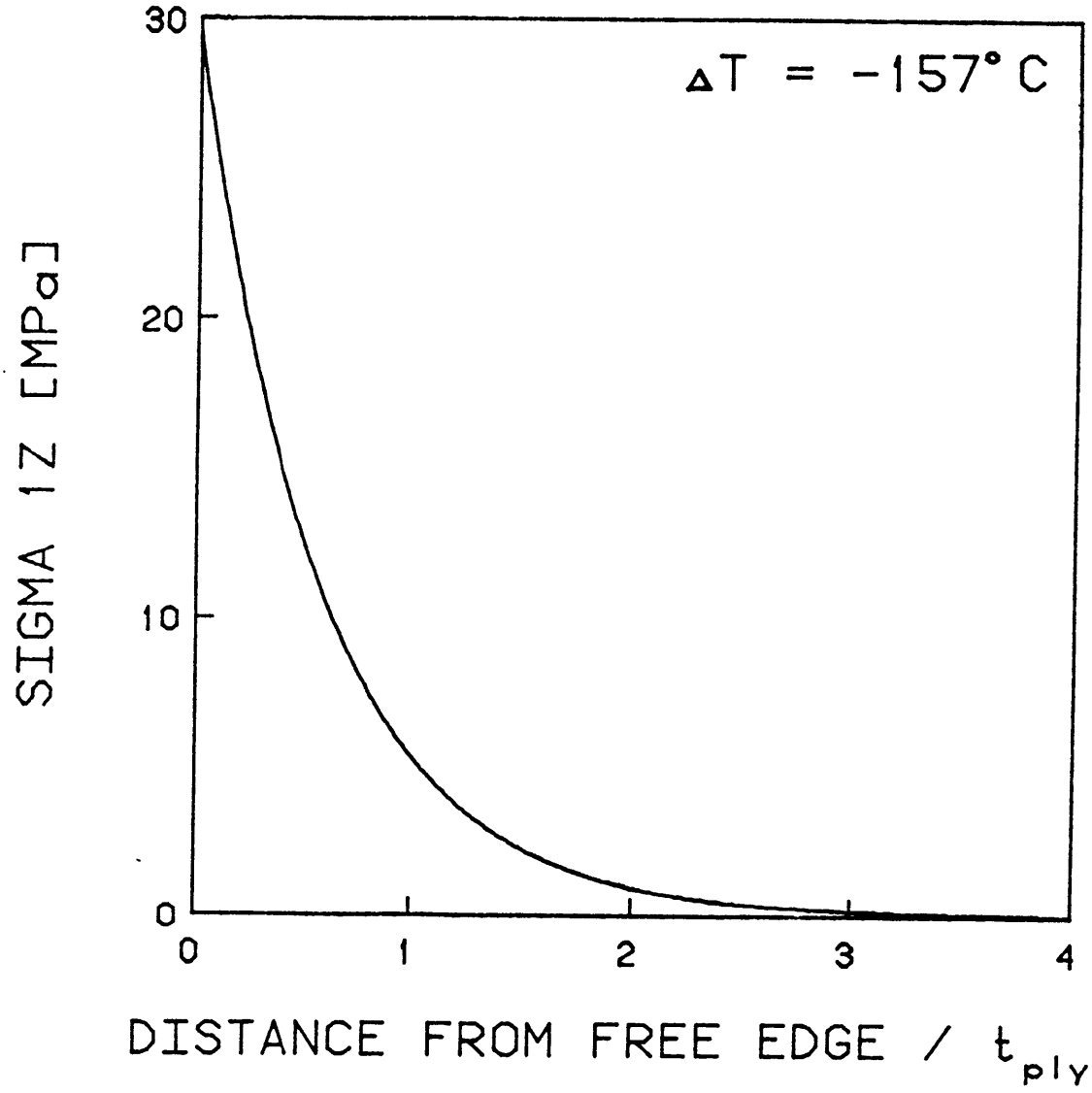

FIGURE A.4 INTERLAMINAR SHEAR STRESS DUE TO THERMAL EFFECTS ON $[\pm 15_n/0_n]_s$ SPECIMENS

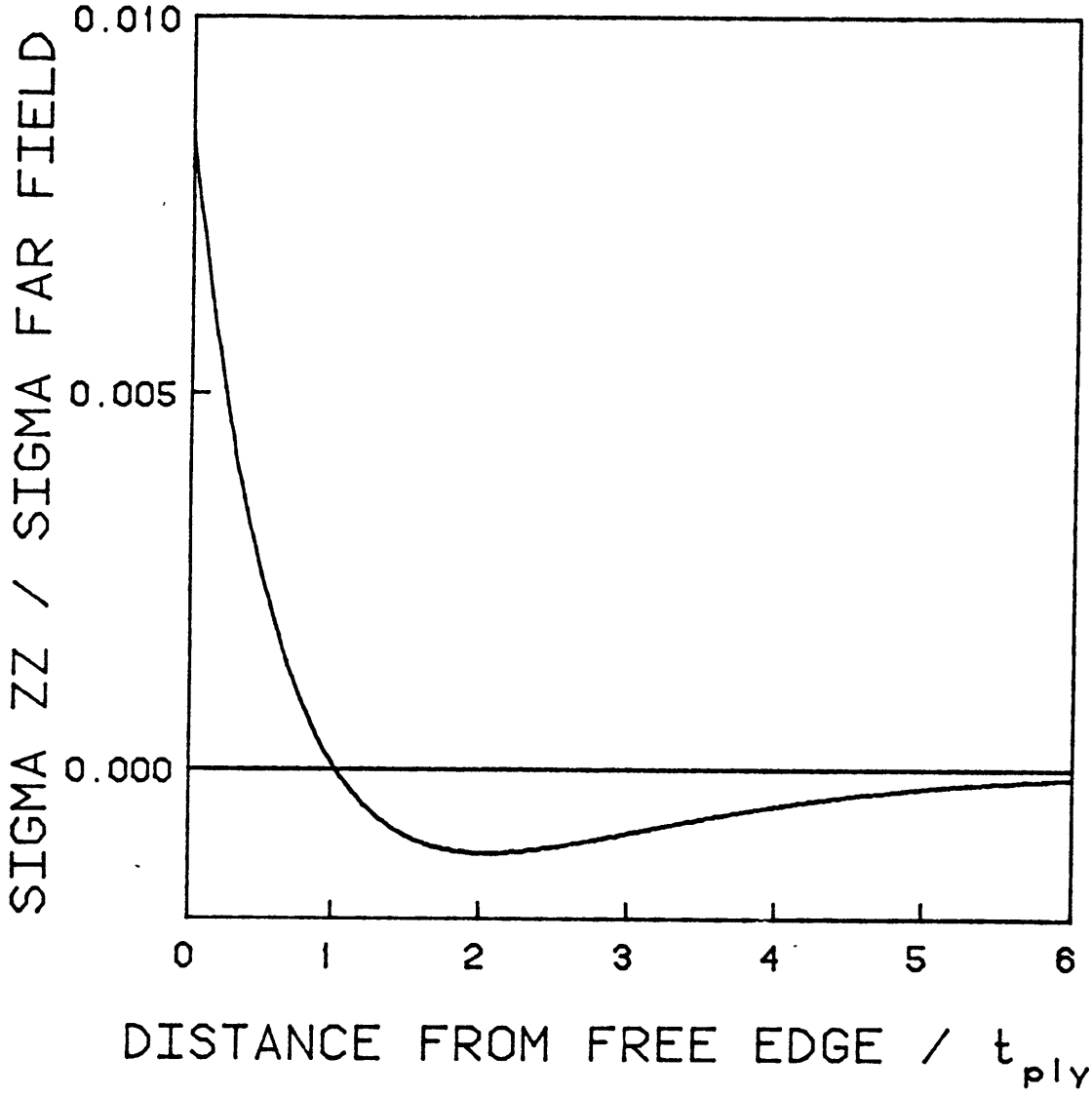

FIGURE A.5 INTERLAMINAR NORMAL STRESS DUE TO A UNIT MECHANICAL LOAD ON $[\pm 15_n/0_n]_s$ SPECIMENS

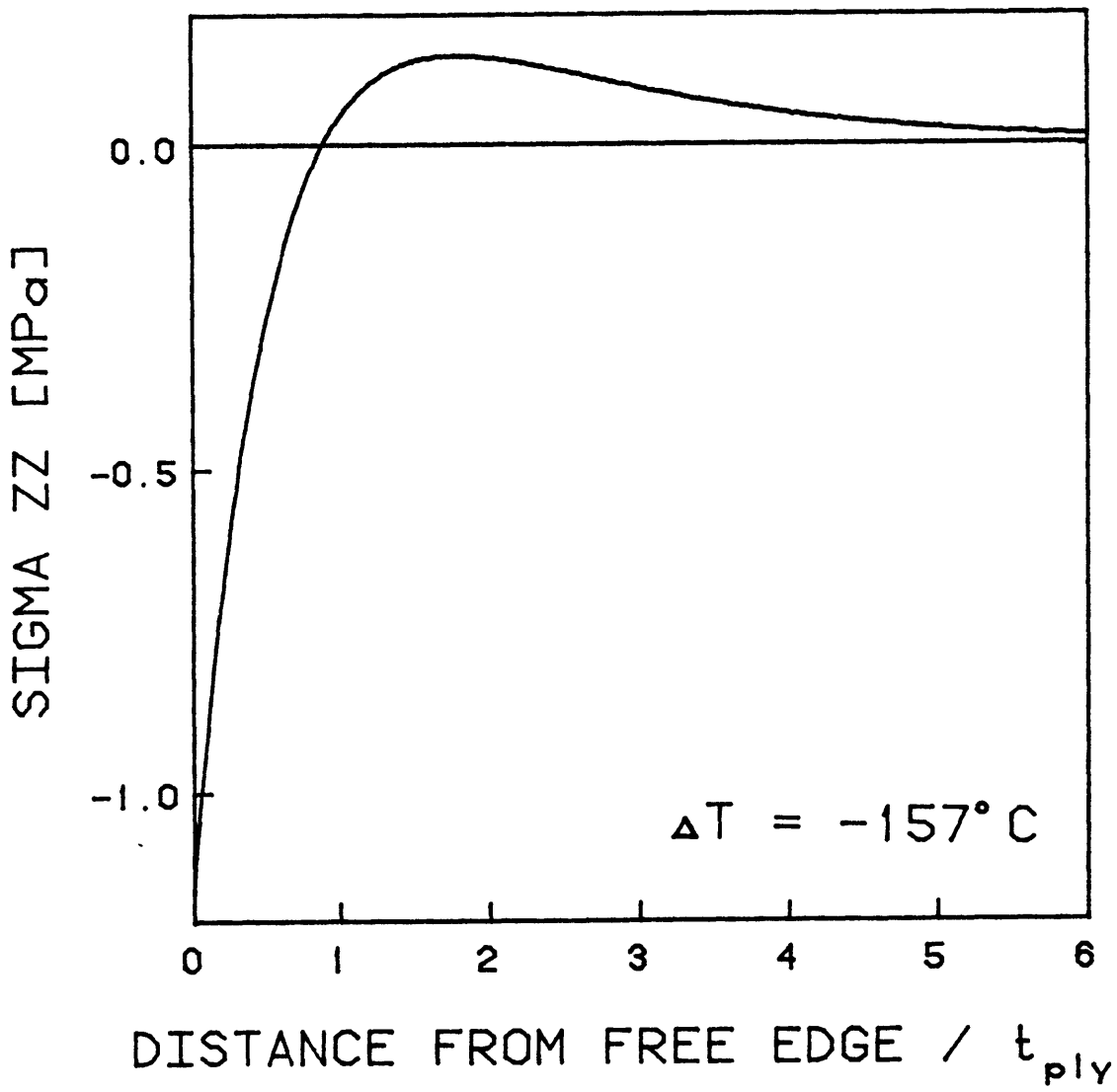

FIGURE A.6 INTERLAMINAR NORMAL STRESS DUE TO THERMAL EFFECTS ON $[\pm 15_n/0_n]_s$ SPECIMENS

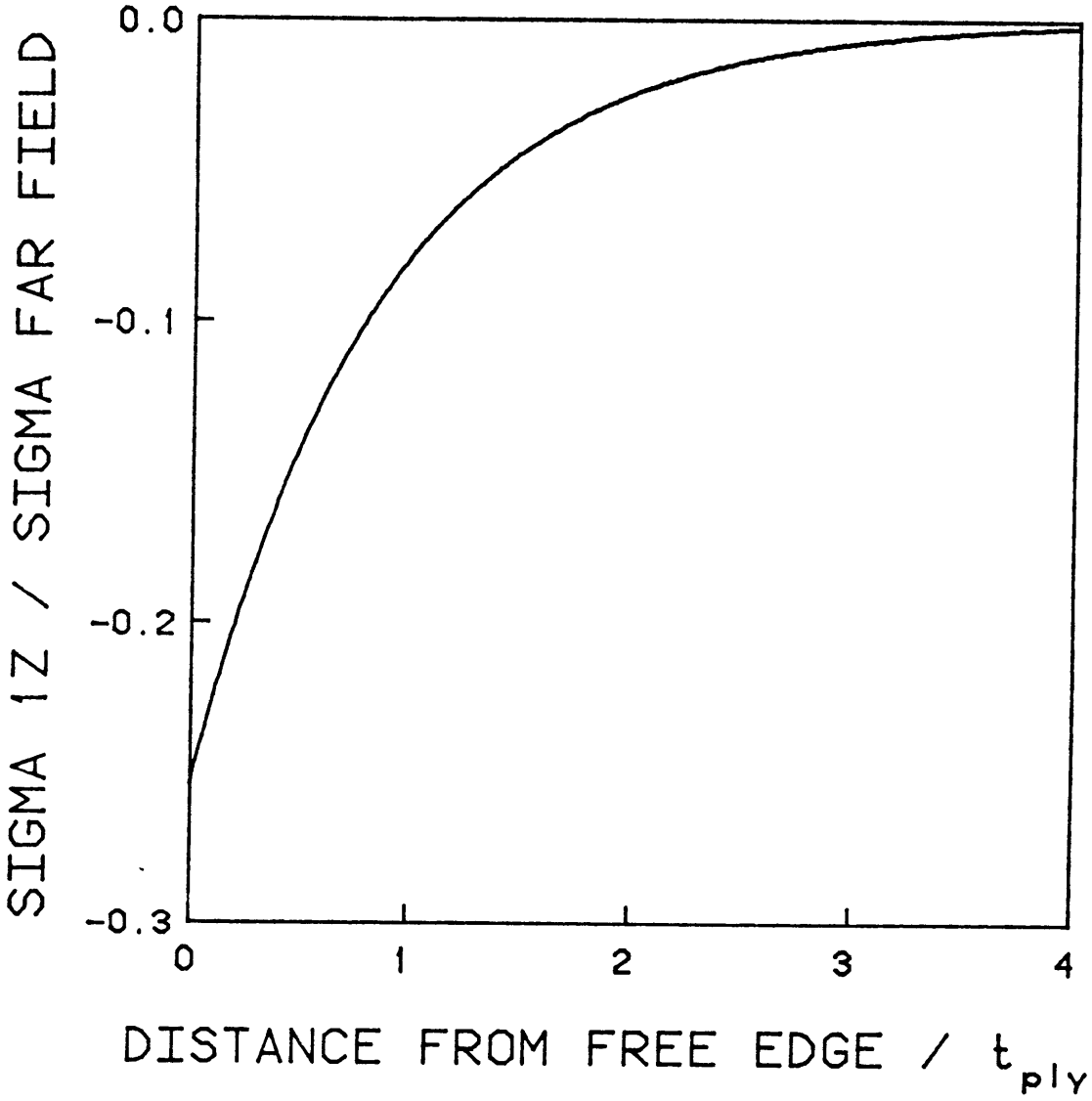

FIGURE A.7 INTERLAMINAR SHEAR STRESS DUE TO A UNIT MECHANICAL LOAD ON $[0_n/\pm 15_n]_s$ SPECIMENS

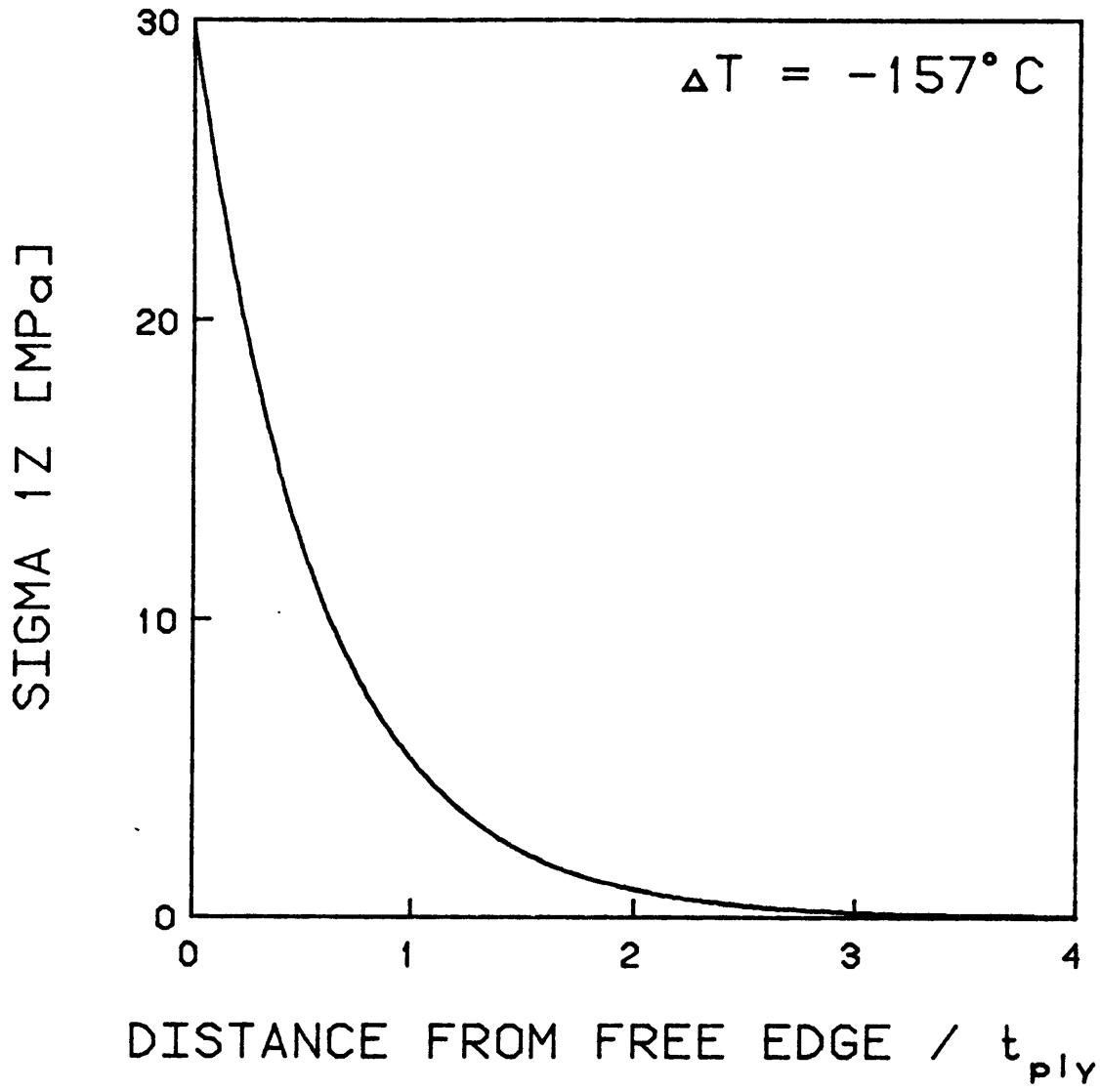

FIGURE A.8 INTERLAMINAR SHEAR STRESS DUE TO THERMAL EFFECTS ON $[0_n/\pm 15_n]_s$ SPECIMENS

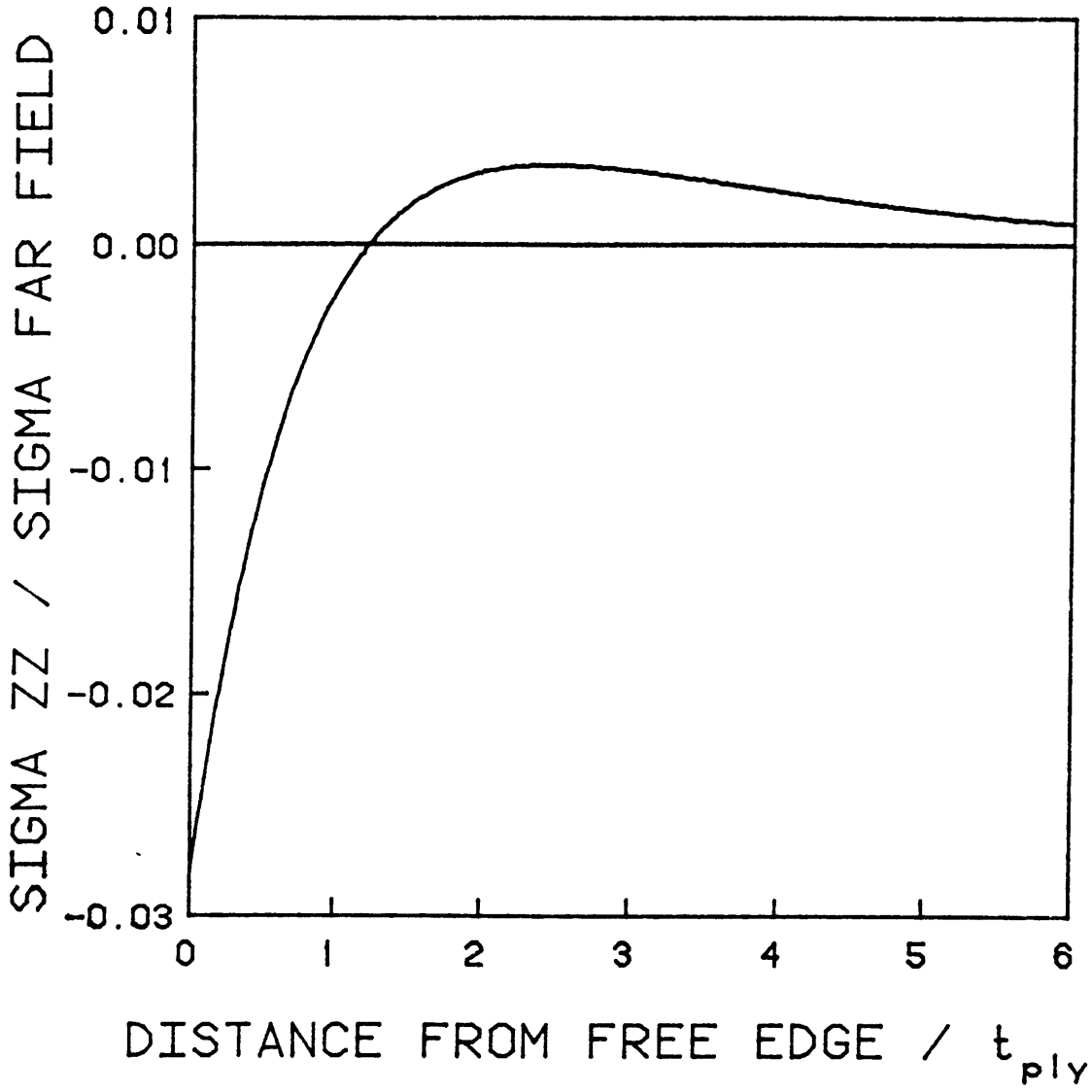

FIGURE A.9 INTERLAMINAR NORMAL STRESS DUE TO A UNIT MECHANICAL LOAD ON $[0_n/\pm 15_n]_s$ SPECIMENS

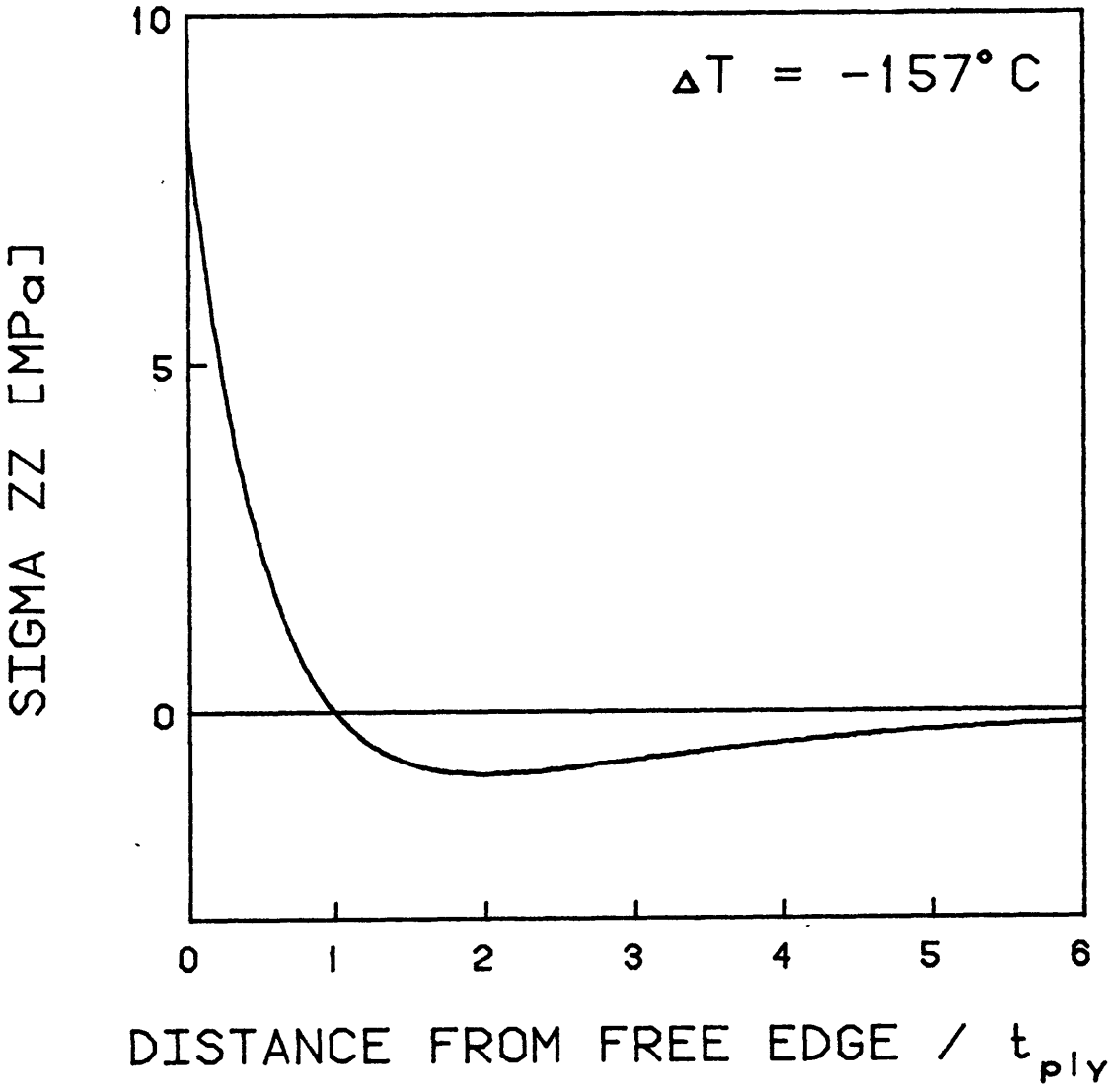

FIGURE A.10 INTERLAMINAR NORMAL STRESS DUE TO THERMAL EFFECTS ON $[0_n/\pm 15_n]_s$ SPECIMENS

APPENDIX B

CALCULATED DELAMINATION AREAS

Specimen	Computed Delamination Area [mm^2]	Difference In Computed Area Due To Error Of 1 Computer Unit [mm^2]
15A0-0-8	77	20
*15A0-0-3	81	24
*15A0-0-4	76	20
315A0-0-7	457	13
315A0-0-9	60	20
315A0-0-10	75	27
415A0-0-6	75	27
415A0-0-7	69	23
415A0-0-8	47	16
415A0-0-9	539	21
415A0-0-10	94	34
515A0-0-8	51	16
515A0-0-10	60	20

Specimen	Computed Delamination Area [mm^2]	Difference In Computed Area Due To Error of 1 Computer Unit [mm^2]
15A1-0-18	126	33
15A1-0-19	163	66
15A1-0-20	111	30
15A1-0-22	114	52
*15A1-0-1	141	56
*15A1-0-2	124	47
*15A1-0-3	144	56
*15A1-0-4	118	49
*15A1-0-5	171	69
215A1-0-6	111	34
215A1-0-7	128	38
215A1-0-8	116	34
215A1-0-10	113	36
315A1-0-6	89	26
315A1-0-8	428	28
315A1-0-10	140	72
415A1-0-6	152	57
415A1-0-7	128	59
415A1-0-8	121	56
415A1-0-9	121	58
415A1-0-10	123	59
515A1-0-6	111	48
515A1-0-7	114	49
515A1-0-9	117	49

Specimen	Computed Delamination Area [mm^2]	Difference In Computed Area Due To Error of 1 Computer Unit [mm^2]
15B1-0-19	117	30
15B1-0-20	113	29
15B1-0-21	119	30
15B1-0-22	108	29
215B1-0-6	118	38
215B1-0-9	105	33
215B1-0-10	101	33
315B1-0-6	507	28
315B1-0-7	91	27
315B1-0-8	101	30
315B1-0-9	391	34
315B1-0-10	161	91
415B1-0-7	116	54
415B1-0-8	107	49
415B1-0-9	96	44
515B1-0-6	90	38
515B1-0-7	318	43
515B1-0-8	84	36
515B1-0-10	596	53